LIBRARY
Michigan State
University

This is to certify that the
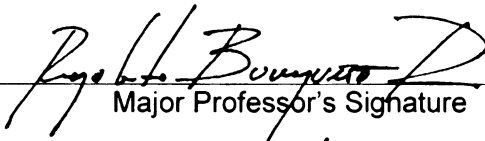dissertation entitled

Soft Computing for Damage Prediction and Cause
Identification in Civil Infrastructure Systems

presented by

Zhe Li

has been accepted towards fulfillment
of the requirements for the

___Ph.D___   degree in   ___Civil Engineering___

_____
Major Professor's Signature

___07/29/2008___
Date

PLACE IN RETURN BOX to remove this checkout from your record.
TO AVOID FINES return on or before date due.
MAY BE RECALLED with earlier due date if requested.

DATE DUE	DATE DUE	DATE DUE

Soft Computing for Damage Prediction and Cause Identification in Civil Infrastructure Systems

By

Zhe Li

A DISSERTATION

Submitted to
Michigan State University
in partial fulfillment of the requirements
for the degree of

DOCTOR OF PHILOSOPHY

In Civil Engineering

Department of Civil and Environmental Engineering

2008

ABSTRACT

Soft Computing for Damage Prediction and Cause Identification in Civil Infrastructure Systems

By

Zhe Li

The deterioration of civil infrastructures is a serious problem for society and a considerable challenge for civil engineers. To alleviate and prevent such degradation, manual inspections are carried out for continuous monitoring and records are saved in structural inventory databases. Structural damage prediction models that use an integration of statistical and artificial intelligent algorithms were developed based on an evidential database extracted and organized from a structural inventory database. Damage in the abutment walls of highway bridges was used as an example problem where the goal was to identify the sources of damage and predict their structural condition with time. Unbalance, complexity, subjectivity, and incompleteness are major deficiencies in the evidential database, which obstruct the development of prediction models. Novel data organizing schemes were thus developed to overcome these obstacles and make full use of the database in the training of an ensemble of neural networks. The damage identification performance of such an ensemble of networks reached 86%, which exceeded the performance the best-trained single networks in the ensemble by 18%. Also contributing to the development of successful prediction models were other soft computing methods, statistical analyses, field inspection and monitoring, and finite element analyses. A virtual database was created through finite element analyses to analyze the behavior of structures with different design parameters. The combination of

an evidential database and a virtual database in ensembles of neural networks was found

to be a promising innovation to improve the performance of the developed damage

prediction models.

ACKNOWLEDGMENTS

TABLE OF CONTENTS

LIST OF TABLES

xi

LIST OF FIGURES

xiii

xiv

1 INTRODUCTION

1.1 Motivation

Problems can happen in every area in the world. In the scope of medicine, a person might suffer a heart attack; in the field of meteorology, a storm might arise; in the area of the economy, inflation might happen, etc. Although they are different phenomena in diverse fields, some characteristics are common. First, something goes wrong and there are some causes behind the problem. Second, the past records and current observations of the problem are available. Third, a set of potential causes might lead to the problem. The relationship between causes and effect is highly nonlinear; and, thus, the prediction of the problem and the identification of potential causes are complex inverse problems. How to predict the problem and identify its potential causes has been the constant interest of the academic world as well as the industry in the past decades.

In the field of structural engineering, one of such problems is the degradation of civil infrastructure, such as the corrosion in bridges, cracks in concrete buildings, pavement blow-ups, etc. Degradation of civil infrastructure threatens the prosperity of the economy and the quality of life. The American Society of Civil Engineers (ASCE) assessed 15 categories of America's infrastructure in 2005 and concluded that the average condition of the country's infrastructure is poor. It has been estimated that sixteen trillion dollars are needed to address these infrastructure problems [ASCE 2005]. In an effort to monitor and alleviate these problems in a timely manner, manual inspections of transportation infrastructure are documented as Structural Inventory System Databases (SISD). For instance, in a structural inventory system database for highway bridges, an inspection

record of a bridge documents the design parameters, such as the length, width, and skew angle; the conditions of structural members, such as bridge decks and abutment walls; and operation parameters, such as average daily truck traffic.

In this research, a structural damage prediction procedure is developed through the integration of different tools, including soft computing, statistical analyses, field instrumentation, and finite element simulations. Such a procedure can be used to develop prediction models given an SISD. Civil engineers can use such a tool to predict structural damage; identify potential causes of the damage, and thus repair and maintain civil infrastructure more cost-effectively. A cornerstone in such a procedure is the advanced exploration of an SISD using an ensemble of neural networks with a novel data organizing scheme.

1.2   Specific Research Problem: Structural Damage in the Abutment Walls of Highway Bridges

An example of the degradation of civil infrastructure is the distress in the abutment walls of highway bridges in the State of Michigan. Structure and design parameters of a highway bridge are illustrated in Figure 1-1. The abutment walls of a bridge (Figure 1-2) are the two walls that provide the end supports for the bridge superstructure and contain the backfill soils. Highway bridges in the State of Michigan are suffering from distress in the form of cracks and concrete spalling in their abutment walls (Figure 1-3). The forms of abutment distress are on the front side of the abutment wall and are of the following types: U-shape concrete spalling under the girder supports (Figure 1-4), vertical cracks between girders (Figure 1-5), and vertical cracks underneath girders (Figure 1-6).

2
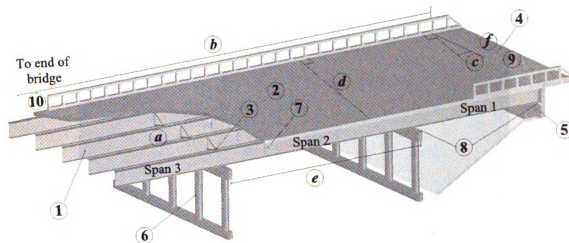
Structural components: ①steel girder, ②deck, ③cross-frame, ④approach pavement, ⑤abutment wall, ⑥pier, ⑦pin-and-hanger, ⑧bearings, ⑨expansion joint, ⑩railing.
Design parameters: (*a*)structural type, (*b*)bridge length, (*c*)skew angle, (*d*)bridge width, (*e*)span length, (*f*)approach pavement type.

Figure 1-1 Structural components and design parameters of a highway bridge
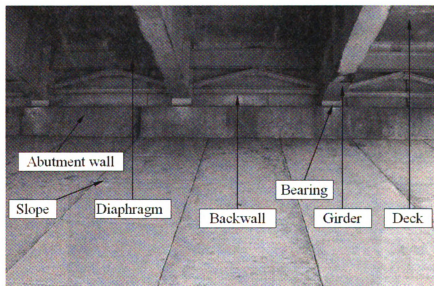
Figure 1-2 Structural members of a highway bridge (in site view)

Figure 1-3 Concrete spalling in the abutment wall

Figure 1-4 Pull-out of concrete block in the abutment wall under girder support

Vertical crack in abutment
wall (between girders,
amplified in the right figure)

(a) General view of abutment wall

Vertical
Crack
Between
Girders

(b) Detailed view of the vertical
cracks between girders
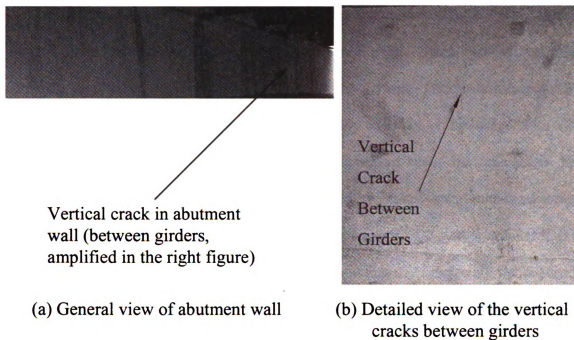
Figure 1-5 Vertical cracks between girders

Girder

Vertical cracks in
abutment wall
(underneath girder)
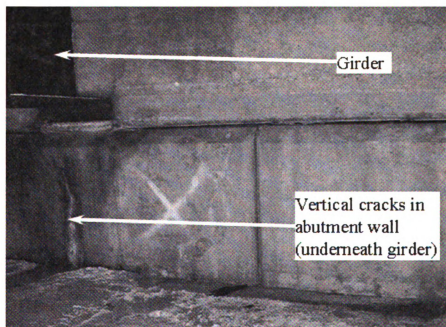
Figure 1-6 Vertical cracks underneath girders

The distress seems to be incremental, with cracks and concrete spalling growing with time as a consequence of factors not yet fully understood. Additional effects from corrosion due to leaky joints worsen or increase the damage. Thus, while initially the cracks are cosmetic, with little effect on serviceability or safety of the bridge, with time they can severely degrade the integrity of the abutment wall. In some cases, the degradation due to damage under girder supports can be extensive and thus compromise the system's structural integrity. The Michigan Department of Transportation (MDOT) has traditionally been addressing this problem by continuously monitoring the condition of this distress and then acting on repairs to restore the integrity of the abutment wall. The repair cost of damaged abutment walls is high. Figure 1-7 shows a picture of a repaired abutment wall. It is of interest to improve the understanding of the causes behind this damage, to develop strategies to alleviate it, and to create models that predict the damage in the future.

Figure 1-7 Repair of damage in abutment walls

The causes of the mentioned damage in the abutment walls are not clearly known. Possible sources include corroded, or "frozen," bearings and expansion details, e.g., pin-and-hanger assemblies (Figure 1-8), underperforming expansion joints, the pressure generated by the thermal movement of pavement approaches (or "pavement growth"), the leak of expansion joints in the superstructure, and the water and salt leaked to the abutment wall (which lead to the degradation of concrete, as shown in Figure 1-9), temperature effects, heavy vehicle traffic, design quality, construction quality, etc.

While the factors mentioned above are potential contributors for the damage in bridge abutment walls, the relative importance of these causes is not well understood. Focused and effective strategies for relieving the structural distress in the abutment walls can only be developed after a better understanding of the different causes and their relative importance. Furthermore, the ability to forecast potential problems in abutment walls and knowing how to avoid such problems will improve the management of maintenance and future design of highway bridges.

Figure 1-8 Corroded pin-hanger assembly

Figure 1-9 Water leaked to the abutment wall underneath a girder

1.3 National Bridge Inventory System Database

In order to keep bridges in good condition, the Michigan Department of Transportation (MDOT) maintains an SISD, which is a bridge inspection database in the National Bridge Inventory (NBI) system [Hartle et al. 1991]. The database is based on manual inspections of structural members at a time interval of no more than two years. A 0-9 scale rating is used to record the conditions of structural members, where the larger number means better condition and 0-4 means different distress levels in the structural member. The Michigan Structure Inventory and Appraisal Coding Guide [MDOT 2003] describes the inspection ratings and corresponding physical conditions of structural members of highway brides. BIR #12 Abutments (SI & A item 60, Substructure) of the Michigan Structure Inventory and Appraisal Coding Guide [MDOT 2003] is reproduced in Table 1-1.

Table 1-1 Bridge ratings and physical conditions of structural members

Rating	Condition	Description
9	New	No deficiencies in any of the structural components that will affect the long term performance.
8	Good	All structural components are sound and functioning as designed. There may be superficial cracking or weathering of protective coatings and/or dirt contamination on structural components.
7	Good	All members retain full section properties and function as designed. There may be minor cracking in structural components.
6	Fair	All members retain full section properties and function as designed. There may be some deterioration affecting structural members such as minor cracking, scaling, small scattered spalls, or shallow scour. Some protective coating failures.
5	Fair	Moderate deterioration affecting structural members such as cracking, scaling scattered spalls, minor settlement or shallow scour. Minor section loss in low or no stress areas. All members continue to function as designed.
4	Poor	Considerable deterioration affecting structural members such as cracking, scaling, scattered spalls, partial settlement or, scour. . All members continue to function as designed.
3	Serious	Considerable deterioration affecting structural members. Structural, hydraulic, and/or load analysis may be necessary to determine if the structure can continue to function without restricted loading or immediate repairs.
2	Critical	Deterioration has progressed to the point where the structure will not support design loads and must be posted for reduced loads.
1	Imminent failure	Bridge is closed to traffic, but corrective action may put the bridge back in service.
0	Failed	Bridge closed.

Use of the SISD poses several challenges, which need to be addressed through innovations in the development of a prediction model for structural damage. An SISD documents the condition of the infrastructure with design and operation parameters, and thus provides information for scheduling maintenance and repair. However, further exploration and the advanced use of these evidential databases are constrained by some inherent difficulties:

- The database can be highly scattered and no conspicuous trend or correlation can be extracted. For the bridge abutment problem, there is no obvious one to one relationship between cause and effect of structural damage, which means that many causes can lead to the damage of the abutment. Moreover, the relationship can be highly nonlinear and thus very hard to be extracted, if not impossible, by current methods.

- Subjectivity exists in the manual inspection methods, and there is large variance in the adopted structural evaluation ratings. For the NBI system, it has been found that for the same structural component, its ratings assigned by 49 bridge inspectors from 25 state departments were dispersed, with only 68 percent of them within ±1 (in a scale of 0 to 9) around the mean and 95 percent of them falling in ±2 around the mean [Phares et al. 2001]. Even if all the bridges with the same design and operation parameters were inspected by the same structure inspector, the ratings might still be different because construction quality can not be identical.

- The values of some variables in some observations are missing or subject to error. For instance, the approach pavement type (a parameter of importance to

the damage in highway bridge abutments) for some highway bridges in the database is missing.

- The distribution of the inspection records is unbalanced. Cases of severe damage are relatively rare in comparison to the large number of structures in relatively good condition.

1.4 Research Objective

The purpose of this research is to develop a procedure to predict structural damage in civil infrastructure and identify causes of damage within the context of structural damage in bridge abutment walls. This research was based on the research project *Identification of Causes and Development of Strategies for Relieving Structural Distress in Bridge Abutments*, which was funded by the MDOT. However, applications of the methodologies are not limited to the scope of the abutment walls or bridges. It is a generalized approach to help researchers and civil engineers alleviate the degradation of civil infrastructure. Given structural design and operation parameters, such a procedure is able to predict damage in structures and evaluate the contributions of potential damage causes through in the depth exploration of an SISD and the interaction of a series of tools. The research methods are shown in Figure 1-10. The methods in Figure 1-10 are not independent from each other or work in a sequential or linear manner. They are used interactively to help each other in the process of identifying the potential causes and developing prediction models. These methods are described in the following subsections.
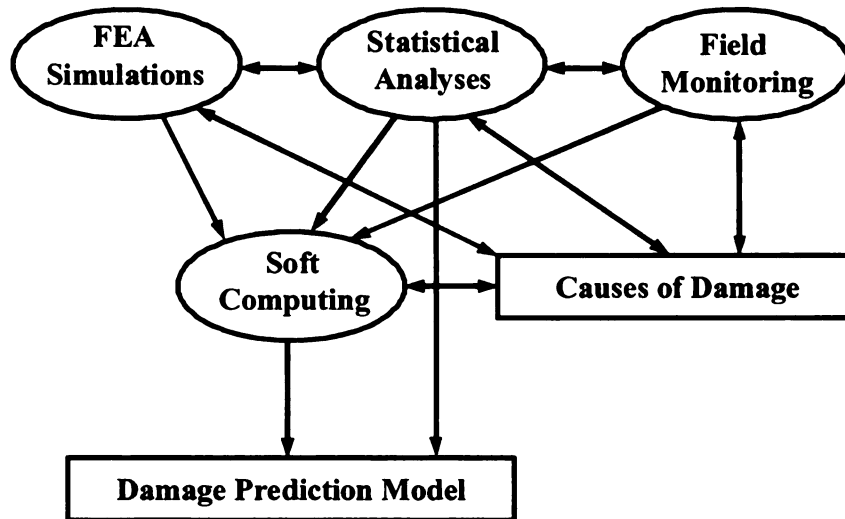
Figure 1-10 Interaction of research methods

1.4.1 Database Processing and Statistical Analyses

Generally, a structural inventory system database includes a great deal of information, and only part of it is relevant to the research goal. Thus, the database is first investigated, processed, and organized in a way that it could be analyzed. Statistical analyses were performed to identify the cause-effect association between structural damage in bridge abutment walls and bridge design and operation parameters, develop regression models to predict structural condition, and provide information and guidance for other analyses, simulations, and field instrumentation.

1.4.2 Field Instrumentation

Based on the results of the statistical analyses, a set of typical structures (bridges) were identified and inspected. Suitable ones among them were instrumented and monitored to evaluate the contribution of the identified parameters and assist the execution and validation of the analytical studies. Assuming that the number of structures

being monitored was adequate, field instrumentation also provided an additional source of information for the soft computing models.

1.4.3 Finite Element Simulation

Finite element analyses (FEA) were used to investigate the behavior of structures (bridges) with different design parameters under different damage scenarios. A virtual database created from the FEA was used in a parametric study and served as an additional information source to an ensemble of neural networks.

1.4.4 Soft Computing

Multilayer perceptron (MLP) network, radial basis function network (RBF), support vector machine (SVM), supervised self-organizing map (SSOM), and fuzzy-neural network (FNN) models were exploited interactively to overcome the difficulties with the database mentioned above and build damage-prediction models. An MLP model can "learn" from data patterns and map nonlinear relationships in the data [Haykin 1999]. It is robust to erroneous or incomplete data. MLP was applied in this research considering the difficulties mentioned in Section 1.3, especially the complexity, incompleteness, and erroneousness data. An RBF is a good tool for curve fitting. It is used to fit the relationship between explanatory variables and structural conditions in this research. An SVM model optimizes the decision boundary between data categories and avoids local minima [Taylor & Cristianini 2004]. It is a powerful tool to overcome the difficulties mentioned in Section 1.3, especially the complicated nonlinear relationship between explanatory variables and structural conditions. An SSOM is a tool for feature extraction and feature mapping. It was used in this research to identify the features of this

13

complicated problem. An FNN model is a combination of fuzzy logic and artificial neural networks. It was applied to process the discrete and highly subjective manual damage evaluation ratings as well as to overcome the subjectivity and imprecision in manual inspection and data collection.

1.4.5   Ensemble of Neural Networks and Combination of Databases

A single artificial neural network (ANN) model might suffer from local minimum and misrepresent relationships that might be correctly mapped by other ANN models [Guo and Luh 2004]. The sources behind structural damage are highly scattered; and thus it is hard for a single neural network to catch all the damage sources and derive a good prediction model. An ensemble of neural networks (ENN) is composed of a series of individual ANN models in parallel and makes predictions by collecting and combining predictions of individual neural networks through a voting process.

An ENN was used in this research to alleviate the local minima problem suffered by individual ANN models and anneal the effects of all damage sources together in the development of a prediction model. More importantly, a novel data organizing and voting scheme enabled the ensemble of neural network to overcome the unbalance of the SISD and identify the structural damage with higher accuracy. A virtual database created through finite element simulations was combined with the evidential database in an effort to improve the prediction power of an ensemble of neural network.

1.5 Causes of Structural Damage in Abutment Walls

Among the a series of potential causes for structural damage in abutment walls mentioned in Section 1.2, three of them were identified as major causes to the damage. The identification was based on the statistical analyses, field inspection, field instrumentation, and finite element simulations. As introduced in Section 1.4, these methods were used interactively, the identification of causes for structural damage also provide valuable guidance for statistical analyses, field instrumentation, and finite element simulations. Pavement pressure is identified as the most significant cause. Transverse and longitudinal temperature effects also proved to be important contributors. The evidence for the identification of these causes is presented in the following chapters.

1.5.1 Pavement Pressure

The interface between the bridge superstructure and embankments is a well-known source of large maintenance problems [Briaud et al. 1997, Long et al. 1998]. A relevant problem at this interface is the so-called "pavement growth" phenomena, which refers to the movement and expansion of pavements against the bridge deck. The causes for pavement growth are complex, encompassing pavement motions due to temperature effects, incorrect design of approach slabs, improper design of sleeper slabs, expansive soils, soil consolidation, soil embankment movement, drainage, etc. Burke [1998, 2004] found that pavement growth was generated through years of temperature variation cycles and failure of expansion joint sealing. The process is illustrated in Figure 1-11. Concrete slabs were connected with expansion joints with sealing at the end of the pavement construction process. During the winter season, temperature decreases and concrete slabs

contract, thus increasing the gap at joints. Debris falls into the expansion joint gaps if the joint sealing doesn't work well. With temperature increase during the summer period concrete slabs expand closing the expansion joint gaps and compacting the deposited debris inside of it. The compacted debris thus takes part of the space in the expansion joint gap. With the next winter cycle the pavement joints will again open allowing more debris to deposit in the joint gaps, which will later be once again compacted when the gap closes during the summer season. The repetition of this process over the years will fill and compact the space in the expansion joints. The reduction of free space in the expansion joint gaps generates compressive pressure between adjacent pavement slabs. The pressure can be large enough to mobilize the slabs or can result in upwards buckling of the pavement, or pavement blowup.

The mechanism and force flow behind the damage caused by pavement pressure are shown in Figure 1-12. In Figure 1-12, hollow arrows composed by solid lines represent forces generated by pavement growth. At the beginning the pavement slabs move towards the approaches of a bridge and the expansion joints at the pavement/ superstructure interface was not be able to accommodate the pavement movement. Then the generated pavement pressures against the bridge deck will transfer forces to the girders and these will subsequently transfer the loads to their bearing or anchorage detail on top of the abutment wall. If the bearings or anchorage detail are not designed to accommodate such a large pressure, or are locked due to corrosion, the pavement pressure will be transferred to the abutment wall. When the pressure transferred to the abutment wall is large enough, cracks underneath the girder through the position dowel

will occur in the abutment wall. In serious cases, complete concrete segments will be pulled out from the abutment wall, as shown in the in-site picture in Figure 1-12.

Sealing
Expansion joint

Concrete pavement (New)

Sealing opened
Debris fell into opened space

Contracted

In winter

Debris compacted
in the sealing
Pressure generated

Expanded

In summer

Years of cycles

Huge pressure accumulated
in concrete slabs

15 to 30 years later
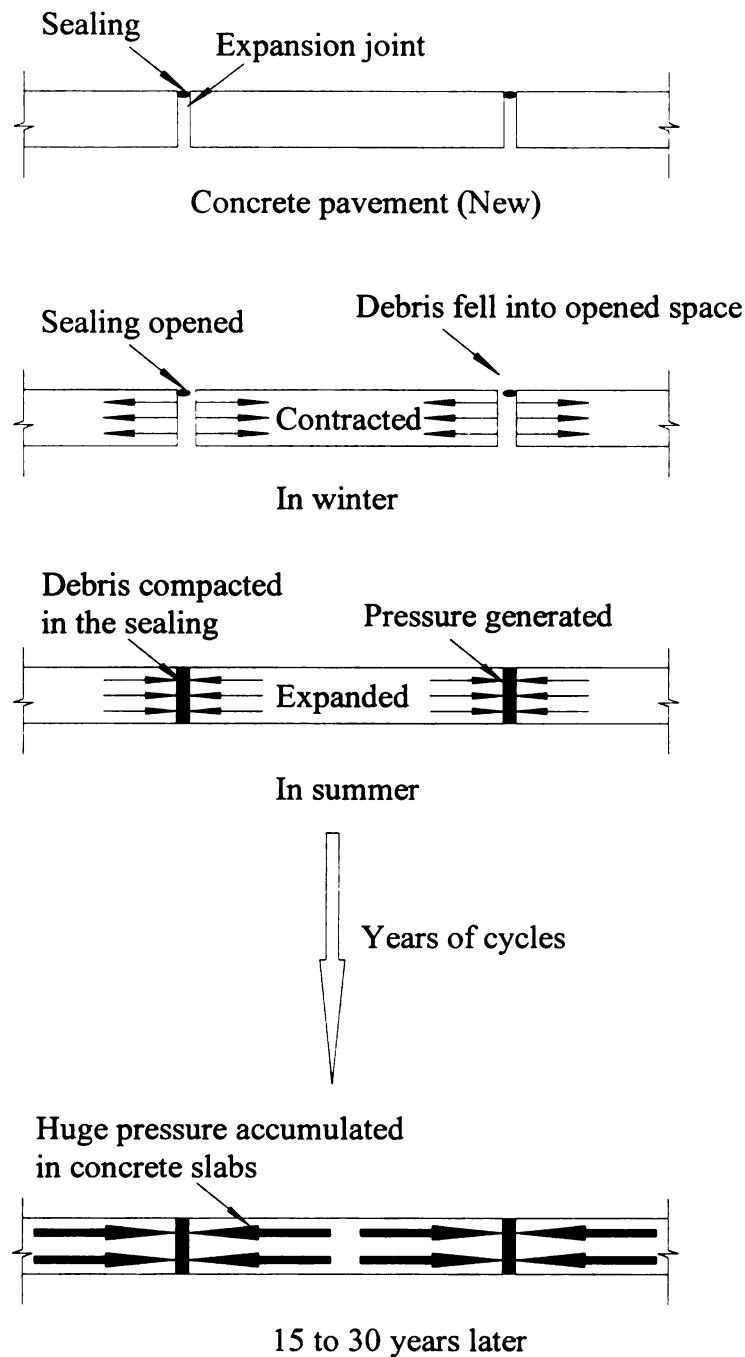
Figure 1-11 Generation of pavement pressure

Push by pavement

Deck slab

Dependent
Backwall

Forces
transmitted
from slab

Approach pavement

Bearing

Force Generation
Index:

Steel girder

Pavement growth

Contraction of
structure combined
with lock of pin and
hanger

Connection
Bolt

Forces
transmitted
from girder

Abutment wall

Concrete
pullout

In-site picture
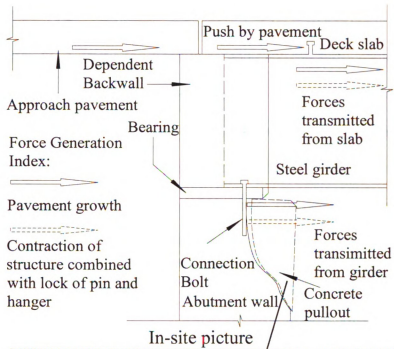
Figure 1-12 Concrete pullout caused by pavement pressure

18

1.5.2 Transverse Temperature Effect

Temperatures in bridge superstructure and substructure could be different significantly in summer and winter. The sunshine in summer time heats up the bridge deck, and thus makes the temperature of superstructure to be higher than substructure. The soil around substructure keeps them warm in winter time, and thus makes the temperature of superstructure lower than substructure. The details of temperature profile can be found in Section 5.4.2. Transverse effects of this temperature difference can lead to vertical cracks in abutment walls at locations between girder supports.

The mechanism and force flow behind the damage caused by the transverse temperature effect are shown in Figure 1-13. In summer, the temperature in the bridge superstructure is higher than substructure. Thus, the superstructure has a trend to expand relatively to the substructure. In Figure 1-13 hollow arrows represent forces generated by the transverse thermal expansion of the superstructure. At the beginning, the deck heats up and expands. The expansion of the deck will lead to an increase of the transverse distance between girders. At the same time, the abutment wall, which has less expansion than the deck, will restrain the girders from transverse movement. If the bearings, or anchorage details, are not designed to accommodate such transverse movement, or are locked due to corrosion, tensile stresses will be generated in the abutment wall. When the tensile stresses generated in the abutment wall are large enough vertical cracks will occur in the abutment wall at locations between girder supports, as shown in the in-site picture in Figure 1-13.

Thermal expansion in transverse direction

Deck slab — Connection bolt

Forces transmitted through slab

Vertical crack of concrete

Backwall

Steel girder

Bearing

Force transmitted from girder

Abutment Wall

Connection bolt

Vertical crack of concrete

In-site picture
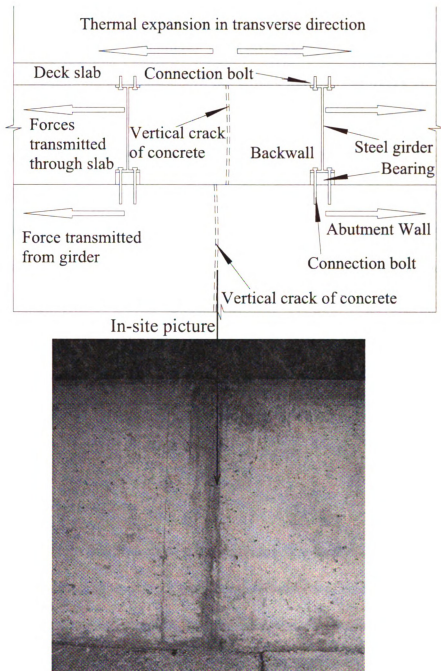
Figure 1-13 Bridge abutment damage with their possible causes

1.5.3 Longitudinal Temperature Effect

When the pin-and-hanger assemblies of a steel bridge are rusted and can not accommodate the longitudinal movement of the girders longitudinal forces are generated at the bearings and then transmitted to the abutment wall. Figure 1-12 illustrates the mechanism and force flow behind the damage caused by longitudinal temperature effects. In Figure 1-12, hollow arrows composed by dashed lines represent forces generated by longitudinal temperature effects. If the deck and girders are contracted due to a temperature decrease then girder ends will move away from their supports (bearings or anchorage). If the bearings, or anchorage details, are not designed to accommodate such a longitudinal movement or are locked due to corrosion, stresses will be generated in the abutment wall. When these stresses are large enough, damage will occur due to the pulling forces transmitted from the girder through position dowels cast inside the abutment wall.

1.6 Research Contributions

The most important contribution of this research is the innovative application of an ensemble of neural networks to overcome inherent difficulties of an SISD in developing a prediction model for structural damage. Such a contribution advanced the state-of-the-art of knowledge in diagnosing structural damage using artificial intelligence in the interdisciplinary field between civil engineering and computer science. Details of the innovation and contribution in this research are listed below:

- A comprehensive procedure to develop prediction models for damage in civil infrastructures through the integration of a series of tools.

- New data organizing and voting schemes in an ensemble of neural networks to identify the damage of structures.

- Concept and methodology for the combination of evidential and virtual databases in an ensemble of neural networks to solve a complex inverse problem.

- Identification of potential causes for the distress through the interaction of field inspections, analyses and simulations.

The procedure designed in this research can predict damage in structures and evaluate the potential causes of damage. Use of this procedure and tools for the prediction of the structural condition and the identification of potential causes of damage can allow for more efficient maintenance and repair of civil infrastructure.

1.7 Dissertation Overview

This dissertation includes eight chapters. The first chapter is an introduction, including the motivation, challenge, and objective of the research and introduction of a specific research problem: distress in abutment walls of highway bridges. The state-of-the-art research in related fields and the application and innovations of similar research methods are reviewed in Chapter 2. Chapter 3 presents the processing of a structural inventory system database, the creation of evidential database for the research, and a series of statistical analyses: frequency analysis, correlation analysis, analysis of factorial effects, and regression analysis. Chapter 4 illustrates the field monitoring plan executed for this specific research problem. The field monitoring work consisted of bridge selection, field inspection of typical bridges, field instrumentation, data collection, and data interpretation. Chapter 5 introduces the finite element analyses in this research. Seven hundred and eighty three (783) highway bridges were simulated, and the results

were used in two ways: parametric studies to identify the influence of design parameters on the behavior of bridges and the creation of a virtual database to be used in an ensemble of neural networks.

Chapter 6 documents the development of soft computing models to predict structural damage in abutment walls of highway bridges. Five models were applied: MLP, RBF, SVM, SSOM and FNN. Chapter 7 presents the development of an ensemble of neural networks in predicting structural damage. A novel data organizing scheme for ensemble of neural networks enabled it to overcome the unbalance present in the evidential database and reach good accuracy in identifying damage in civil infrastructures. The combination of an evidential and a virtual database in the context of an ensemble of neural networks could improve the performance of the prediction model; it is a bright direction for future research. Chapter 8 looks forward to future research needs on this topic and presents conclusions from this research.

2 STATE-OF-THE-ART RESEARCH

2.1 Introduction

In order to identify effective strategies to solve the problem introduced in Chapter 1, a thorough review of the state-of-the-art research is presented in this chapter. In predicting structural damage most neural network applications used simulated or tested structural dynamic characteristics to decide the location and magnitude of damage in the structure [Chen 2005, Fang 2005, Huang et al. 2003, Park et al. 2006, Song et al. 2005, Taha and Lucero 2005, Zhao et al. 1998]. The features of these problems are very different from the inverse problem in this research. Thus instead of focusing on research in structural engineering, the literature review emphasizes the similarity in the nature of the problems no matter to which fields the problems belonged. The nature of the problems is that even though the symptoms in individuals are known, the causes of those symptoms are not clear. Symptoms and parameters of individuals are recorded historically and compose an evidential database. An inverse problem thus needs to be solved in order to identify the causes of the problem and develop effective prediction models.

The relevant research on the example problem, damage in bridge abutment walls, is investigated at the beginning. Then, a literature review summarizes the application and innovation of artificial neural networks and fuzzy logic in solving inverse problems and developing prediction models based on evidential databases. Since one of the difficulties in the NBI manual inspection database is the issue of missing values, methodologies and techniques in handling missing values in the database are discussed. The state-of-the-art

research on neural networks ensembles and the organization of training data sets for ENNs are reviewed in the later part of this chapter.

2.2 Structural Damage in the Abutment Wall of Highway Bridges

Uncertainties on the causes behind the observed abutment damage motivated the need for a more extensive literature review with the attempt to learn more about this type of distress. Continuous literature review throughout the length of this research failed to identify any published document that described a problem similar to the one being addressed by this study. Attention then focused on trying to identify literature related to the causes hypothesized as the sources of damage. Yet, while some information was found on the suspected sources of damage, these did not contain information or direct correlation to the distress in abutment walls. A brief overview follows.

Several research projects focused on evaluating the negative effects of rusted or "locked" pin-hanger assemblies on steel girder bridges. Yet, little documentation exists on the distress induced by this effect on other elements of the bridge system and most of the work focuses on the potential danger of hanger fracture or pin slip (due to pushing forces from the rust buildup). Nonetheless, some analytical work has provided evidence that the reaction forces due to locked pin-hangers can be significant at the abutments. Analyses suggest values as high as 2.5 times the stress level to initiate yield when full fixity is assumed [Elewa 2004].

Recent publications [Burke 1998, 2004] indicate that pavement growth is one of the possible causes of abutment damage, which is consistent with the expectations of MDOT bridge engineers. The phenomenon consists of the gradual movement of pavement slabs

as joint gaps between them are reduced due to debris. This generates substantial pressures and, consequently, movement, upon thermal expansion of the slabs. From the information provided by Burke [1998, 2004], Richards [1979] and Shober [1997], the magnitude of the induced compressive stress on bridge deck slabs by the movement of pavement slabs towards bridge abutments is estimated to be approximately 7 MPa (1 ksi.)

While the literature review process failed to identify any published work directly addressing abutment distress, the related information on the possible sources of damage provided ideas for the systematic organization of database used in this research. It also helped to clarify the mechanisms that could lead to abutment distress. The identification of important parameters in the damage of bridge abutments was necessary in order to extract relevant data and predictive parameters from the National Bridge Inventory (NBI) database, which was to be used as an evidential database of damage for statistical analyses and diagnosis model development. While the NBI rating has provided a good mechanism to constantly evaluate the state of highway infrastructure, its use for statistical and predictive model development posed considerable problems because the data are highly scattered and clear patterns were not easily identifiable. The subjectivity and large deviation of the visual inspection for highway bridges used in the NBI database are discussed in a research report by the Federal Highway Administration [FHWA 2001] and a paper by Phares et al. [2001]. The inspection process was found to be subjective and with large deviation, which supported initial struggles in this research in interpreting the data and later provided justification to assess its variability.

2.3 Artificial Neural Networks and Fuzzy Logic

Cattan and Mohammadi [1997] applied a multilayer perceptron network to predict subjective condition ratings for railroad bridges using bridge design parameters. The subjective bridge condition rating used numerical values between 1 and 5. When applied to an MLP, the subjective bridge condition rating was transformed to four binary variables, and twelve input design parameters were transformed to 45 binary variables. An MLP network model was developed using a database containing 405 railway bridges in the Chicago metropolitan area. The input layer and output layer of the MLP included 45 and 4 neurons, respectively. Two hidden layers were deployed in the MLP with 45 hidden neurons in each layer. In the testing phase, the MLP network obtained a correct ratio of 73%. Since no operation or environmental information was incorporated in the training of the MLP, the network can not retrieve the degradation history or predict the future degradation trend of a railway bridge. An attempt was made in using analytical data as one of the input parameters to improve the performance of the MLP. However, the trial failed because the analytical data only used a few design parameters.

Shyur et al. [1996] and Luxhoj et al. [1997] applied MLP networks in predicting safety performance indicators of aircraft using operation parameters. The database used in developing prediction models is the combination of part of the service difficulty reporting database and the aircraft utilization database. The database is only for one type of aircraft monitored over a 16-year period; and thus the data is less unbalanced, less noisy, and less complicated compared to the database used in this research. Performance of the MLP networks was good in predicting safety performance indicators of aircraft.

In order to improve the performance of an MLP, Roberts and Attoh-Okine [1998] applied a quadratic function ANN model to predict the international roughness index of pavements. A quadratic function ANN uses an evolutionary mechanism to develop a near-optimal structure. The database included 105 records documented by the Kansas Department of Transportation. The output variable of the network was the international roughness index for the pavement, which uses three integer numbers for severity. The input variables were severity values for different distresses and values for loading. The quadratic function ANN model showed a better performance than a conventional MLP.

Pleune et al. [2000] predicted the fatigue life of carbon and low-alloy steels successfully using an MLP trained with test data. Researchers had more control on test data than field data and thus the test data had less noise and were easily learned by the MLP network. The fatigue life of smooth cylindrical specimens was determined through tests under fully reserved axial strain control loading. The records of 1036 fatigue tests were used as training data. The input variables of the MLP were a series of environmental, compositional, and structural parameters. The output variable of the MLP network was the fatigue life of steel component. The MLP network provided insights into the fatigue trends of steel.

Pande and Abdel-Aty [2005] applied MLP and RBF networks to classify the types of accidents on highways. The database used for developing the prediction model was collected from highway loop detectors. Four thousand crashes were included in the database; 52% of them were rear-end crashes. The response variable was binary: the crash is a rear-end collision or not. The MLP in the research had one hidden layer with 12

hidden neurons. The RBF in the research used unequal width. The performance of the MLP and RBF was reported to be worse than a decision tree.

In the paragraphs above, the applications of MLP and RBF networks are discussed. With regard to SVM networks, they have been used in the diagnosis of breast cancer based on historical clinical data with reasonable performance [Land, et al. 2003]. The database included about 2,500 samples. There are enough cases of breast cancer in the training database. Evolutionary programming was used to find the optimal structure of the SVM. It was proved that SVM could be used to develop software to assist in breast cancer detection.

In addition to MLP, RBF, and SVM, SSOM is also a promising tool in developing prediction models. Xiao et al. [2005] applied an SSOM network to classify compounds using a dihydrofolate reductase inhibition data set. The data set included 135 compounds: 80% of them were used as training data and the remaining 20% were used for testing. SSOM models were trained through two approaches: training with a k-means clustering limit with a zero neighborhood radius and training until the neighborhood radius decreased to zero. The SSOM model outperformed models using multiple linear regression, partial least squares, genetic functional algorithm, and the k-NN algorithm.

By combining a fuzzy set with one or several MLPs, an FNN is expected to have a better tolerance of imprecise and subjective data in building prediction models. Pal and Mitra [1992] applied an FNN in speech recognition. They applied the FNN to a database consisting of 871 Indian Telugu vowel sounds. Input vectors with a dimension of nine were obtained from a spectrum analysis on the speech data. The resultant variable was

the classification of vowels. The fuzzy-neural network model achieved a better result than conventional neural networks and a Bayes classifier.

Juang et al. [1999] applied an FNN to solve uncertainty in the input and output parameters in a geotechnical engineering problem and showed that the performance of the FNN was superior to that of conventional neural networks. Quantitative variable collapse potential was the target variable of the FNN. The input variables for the FNN were seven soil parameters. The database used in training the network was field recorded data.

Mitra and Hayashi [2000] conducted a survey on neuro-fuzzy algorithms and categorized various neuro-fuzzy models used for rule generation. The fuzzy neural network model was applied to diagnose hepatobiliary disorders. The database consisted 536 patient cases of various hepatobiliary disorders. Nine of the input parameters were biochemical test results and one parameter was the gender of the patients. The neuro-fuzzy model achieved more refined results.

An MLP with back propagation algorithm and an FNN were used to predict the root-mean-square pressure coefficients and the time series of wind-induced pressures on a large gymnasium roof [Fu et al. 2007]. Data from a wind tunnel test were used as training sets. Performance of both the MLP and FNN models was satisfactory for engineering applications. Nonetheless, the FNN was found to have better accuracy than the MLP.

2.4 Handling Missing Values in Data Analysis and Neural Network Application

As mentioned in section 1.3, one of the difficulties in using a structural manual inspection database is that there are missing values for some variables in some records. Two approaches are commonly used to handle missing values in a database. One approach is to delete the missing values [Little and Rubin 2002], either by deleting the records that include variables with missing values or by deleting the variables with missing values from all records. The other one is to utilize records with missing values after estimating those missing values [Chan et al. 1976, Dixon 1979, Wagstaff and Laidler 2005].

Granger et al. [2000] applied fuzzy ARTMAP [Carpenter et al. 1992], which is a neural network architecture based on Adaptive Resonance Theory, in the classification of radar pulse data. Incomplete data included a limited number of training cases, missing components, missing class labels, and missing classes. Fuzzy ARTMAP obtained a high accuracy in the classification.

Juszczak and Duin [2004] proposed an ensemble of one-class classifiers trained on each individual explanatory variable to handle missing values in the database. The ensemble could still make a prediction with the rest of classifiers when the value for a variable, by which one classifier was trained, was missing. This approach was used together with two commonly used methods to solve a missing value problem on several of UCI data sets. UCI database is a series of data sets maintained by University of California–Irvine to serve the machine learning community [Blake and Merz 1998]. At

present, UCI database is consists of 171 data sets. It was shown that an ensemble of one-class classifiers had a better performance than a classifier trained by either deleting records with missing values or estimating missing values.

Wagstaff and Laidler [2005] applied a clustering analysis algorithm, "K-means with Soft Constraints" (KSC) to handle missing data in astronomy to separate stars from galaxies based on the Sloan Digital Sky Survey database. In the KSC algorithm, fully observed features were used for clustering, and records with missing values were used to create soft constrains on the clustering algorithm. The KSC algorithm achieved up to 90% improvement in the correct separation of stars and galaxies.

Lim et al. [2005] presented a hybrid neural network to handle missing features in training data for pattern classification. The hybrid network was FAM-FCM. FAM is an acronym for fuzzy ARTMAP [Carpenter et al. 1992], which is a neural network architecture based on Adaptive Resonance Theory. FCM is an acronym for Fuzzy C-Means Clustering. Two stages were included in the training of the hybrid neural network. In the first stage, FAM was trained using data with complete features. In the second stage, a number of FCM-based strategies were applied to estimate and replace missing features. Then, data with estimated features were combined with data with complete features to retrain the FAM. The hybrid network was applied to two benchmark problems (the Iris problem and the Pima Indian Diabetes problem in the UCI database) and an acute coronary syndrome problem. In the acute coronary syndrome problem the database included 118 records of suspect heart attack patients. The performance of the hybrid neural network was found to be promising.

In this research, the features of the NBI manual inspection database were different from those used in research methods mentioned above. The NBI manual inspection database includes a large number of inspection records. About one third of the records had missing values for the qualitative variable "approach pavement type". The number of records with missing or erroneous values for other variables was relatively small. The loss would be too large if all the records with missing values for "approach pavement type" were discarded. Furthermore, estimating that large portion of missing values could hardly be reasonable and would harm the prediction model rather than improve it. Thus, the qualitative variable "approach pavement type" was transformed to three dummy variables: one code sequence of dummy variables represented those cases with missing values. Records with missing or erroneous values for the other variables were deleted from the database.

2.5 Ensemble of Neural Networks

An ensemble of neural networks can be trained separately for a problem and their predictions can be combined through a certain voting scheme. Such an ensemble of neural networks can overcome the local minima and explore the database from multiple perspectives. The concept of combining estimators to achieve better performance has been applied in a variety of fields for some time [Sharkey 1999]. Hansen and Salamon [1990] proved theoretically that an ensemble of neural networks could improve prediction accuracy. They applied an ensemble of neural networks to classify a number of regions in a 20-dimensional hypercube. The regions were defined by 10 "pure" patterns chosen randomly. Both plurality and majority voting rules were evaluated. It was proved

that an ensemble of neural networks could outperform a single neural network even though each individual neural network in the ensemble was less accurate than that single network.

Hansen et al. [1992] applied neural network ensembles in the recognition of handwritten digits. The database included 6973 handwritten digits written by 280 people. An ensemble of neural networks outperformed the best individual neural network in the ensemble by 20-25%. The authors also observed that the improvement of performance of an ensemble by adding more neural networks was not significant after more than 15 neural networks were included in the ensemble.

Zhou et al. [2002] applied neural network ensembles in lung cancer cell identification. Images of specimens were used as input, and cancer diagnoses were used as output. By using the 'bagging' approach in data organization and two stages with full voting in the first stage, the network ensembles were shown to have better performance than individual networks.

Based on traffic accident records, Sohn and Lee [2003] predicted the severity of road traffic accident using driving environmental factors as predictors. The database was composed of accident records and thus no unbalance problem existed. The accuracy of prediction was improved with the application of an ensemble of networks with a normal bagging algorithm.

Yun et al. [2003] and Lee et al. [2004] applied an ensemble of neural networks for structural health monitoring. Modal parameters were used as input for the network and

element level damage indices were used as output. The ensemble of networks was found to significantly improve the identification of damage.

In predicting market clearing prices, Guo and Luh [2004] proposed an ensemble of networks using a weighted voting scheme. The weighting coefficients of individual neural networks were decided based on their possibility to map an input-output relationship correctly. The method was applied in predicting the market clearing prices in New England power markets and was proved to outperform both individual neural network and an ensemble of networks using ensemble-averaging voting.

Yang and Browne [2004] proposed a multistage ensemble of neural networks in which another neural network was applied to collect voting and produce final results. Data sets used for developing prediction models included "breast cancer," "iris," "Pima-diabetes," etc. The training data sets were organized through distributing sample presentation sequences randomly, noise injection, bagging, boosting, etc. After the training of individual neural networks, the whole training data was applied to individual neural networks and their outputs were used as inputs to the voting neural network. Compared with majority voting, voting through another neural network improved the performance of the ensemble of neural networks.

Yu et al. [2008] applied an ensemble of neural networks with a reliability-based voting scheme in credit risk assessment. Prediction models were developed based on two databases. One involved with Japanese consumer credit card application approval, which included 653 records with 357 granted cases and 296 refused cases. The other database concerned a UK corporation credit that included 60 records: 30 of them were failed firms

while the other 30 were non-failed firms. The records in the database were balanced. However, the databases suffered from insufficient records. The bagging algorithm was applied to make full use of insufficient data. The ensemble of neural networks outperformed fuzzy-SVM, SVM, MLP, and logit regression models.

2.6 Data Organization for an Ensemble of Neural Networks

Two major approaches in organizing data sets are bagging [Breiman 1996; Duda et al. 2001; Sharkey 1999] and boosting [Duda et al. 2001; Schapire 1990]. Bagging is a procedure to produce multiple training sub-sets by drawing samples randomly from the original training set with replacement. Boosting is a procedure to produce multiple training sub-sets in a manner that the subsequent selection is focused on the samples that are not recognized well by the classifiers training on the previous training sub-sets.

Breiman [1996b] introduced bagging theory and its application in the real-world and simulated data sets. The real-world data sets included breast cancer, waveforms, letters, etc. It was shown that the bagging algorithm can significantly improve the accuracy of predictions. Bagging is effective in making full use of small data sets; and Breiman [1996a, 1996b] also proved that bagging can improve the accuracy of unstable prediction models, such as neural networks.

Opitz and Maclin [1999] evaluated these two methods using a series of data sets, which included breast cancer, credit, diabetes, iris, letters, vehicles, etc. Explanatory variables, target variables, and the number of records in each data set were all varied from one set to another. Bagging proved to be more stable than boosting even though boosting was sometimes more accurate than bagging. It was also concluded that most of

the improvements in performance was achieved when the first few classifiers were added to the ensemble.

Quinlan [1996] compared bagging with boosting by testing both techniques on a collection of representative data sets, which included letters, vote, waveforms, etc. Both algorithms improved the performance of the prediction model. Bagging proved to be more resilient to noise and more stable, which was also a major difficulty in using a structural inventory system database. Boosting had a better accuracy for some data sets, while it suffered from severe degradation on others. Boosting was modified slightly to alleviate the setbacks and a better performance was achieved.

Parasuraman et al. [2006] applied two ensembles of neural networks in predicting the saturated hydraulic conductivity of soils. Data sets from two field tests were used to build prediction models respectively. One data set included 126 records; the other data set had 78 records. The input parameters were sand content, silt content, clay content, and bulk density. The training data for neural networks in two ensembles were organized using a bagging algorithm and a boosting algorithm, respectively. It was shown that the ensembles of neural networks trained on field-scale data outperformed the general purpose neural network, which was trained on a larger-scale database. The ensemble of neural networks using training data organized through the boosting algorithm performed better than its counterpart using training data organized through the bagging algorithm.

Chen and Yu [2007] proposed a new bagging algorithm for an ensemble of neural networks. The training subsets of individual networks were distilled based on Euclidean distances between two arbitrary samples. Weighted averaging was used as the voting

scheme for the ensemble. The algorithm was applied to regression data sets and a real-world problem of measuring ethylene yield with good performance.

2.7 Discussion

No information was found on research that directly analyzed the problem of structural damage in the abutment walls of highway bridges. Literatures that discussed issues related to the damage in bridge abutment wall were reviewed. That related research provided implications in evaluating the causes of damage in bridge abutment wall even though none of them presented a direct analysis of the problem.

Only a few works were found on the use of ANNs to develop prediction models for structural damage based on a historical inspection database. In other areas, several types of ANN models were applied to solve inverse problems with good performance. The applied ANN models included MLP, RBF, SVM, SSOM, and FNN. None of that research encountered an evidential database with a highly unbalanced distribution of records. Methods used to handle missing values in data analysis and artificial neural network were evaluated. The Fuzzy ARTMAP and an ensemble of one-class classifiers showed good performance. Since the characteristics of the NBI database in this research were different from the research found in that literature, a different strategy was applied to handle missing values in this research.

An ensemble of neural networks was applied successfully in different areas to develop prediction models and solve inverse problems. However, none of them was developed based on a highly unbalanced database. Bagging and boosting are two widely used methods in organizing training data sets for an ensemble of neural networks. Both of

them have been successfully used. In this research, a novel training data organization strategy was devised through bagging within categories to overcome the unbalance in the training data. Modified majority voting, subjectivity voting, and evaluation voting schemes were applied to overcome subjectivity in the training data. An ensemble of networks was then developed using the novel data organization strategy and voting schemes.

3 DATABASE CREATION AND STATISTICAL ANALYSES

3.1 Introduction

As mentioned in Section 1.1, the design parameters and manual inspections of infrastructure are documented in Structural Inventory System Databases (SISD). SISDs should be exploited and used at an advanced level to identify the causes and develop prediction models for structural damage. By extracting raw data from an SISD, screening, preprocessing, and organizing the raw data; an evidential database can be subsequently created. This chapter shows the statistical analyses on an evidential database consisting of frequency analyses, correlation analyses, analysis of factorial effects, hypothesis tests, and regression analyses. They serve three major functions:

- Identify cause-effect associations between structural damage in bridge abutment walls and bridge design and operation parameters.

- Develop regression models to predict structural condition given design and operation parameters.

- Provide information and guidance for other analyses, simulations, and field instrumentation.

Details on each type of the statistical analyses are only partially shown in this chapter due to space considerations. A complete review of all the statistical analyses made on this example problem can be found in the final research report on this project for MDOT [Burgueño and Li 2008]. The commercial statistical software SPSS 13.0 [SPSS 2004] and SAS 9.1 [SAS 2004] were used in the analyses.

3.2 Evidential Database

An example of an SISD is the National Bridge Inventory (NBI) system database [Hartle et al. 1991], which is based on manual inspections of bridge structural members at an interval of no more than two years. For the sample bridge abutment problem, an evidential database was created to directly identify the potential causes of damage in bridge abutment walls and provide an information data bank for the other analyses and simulations. The evidential database consisted of data from the NBI bridge inspection records, which document design and operation parameters as well as abutment inspection ratings for highway bridges. The information database provided important information for the subsequent simulations and analyses, as well as for the field inspections and instrumentations in this research. The commercial software Infomaker 10.0 [Sybase Inc. 2004] was used to retrieve data from the raw bridge inventory database.

3.2.1 Definition of parameters

The definition of structural design and operation parameters in the bridge abutment problem is listed in Table 3-1. The average daily truck traffic (ADTT) is the product of the average daily traffic and the corresponding truck percentage for each bridge. The average daily traffic data was not always measured in the same year for all bridges, and direct application of average daily traffic data without accounting for the year in which it was measured would introduce additional errors. Thus, all of the ADTT retrieved for individual bridges were converted to the ADTT measured at the time of inspection by the following procedure.

Table 3-1 Definition of parameters

Parameter	Definition
*Matdiff**[1]	Annual temperature difference at the location of a bridge
*Ageinsp**[2]	Age of a bridge at the time of inspection
*Apprsurstif**[3]	Approach surface type
ADTT	Average daily truck traffic at the time of inspection
Maxspan	Maximum span (m)
Length:	Total length (m)
Deck width	Total deck width(m)
Pin type	Whether has pin-and-hanger assembly
Skew	Skew angle (°)
*Materialmain**[4]	Main structure type

*1: The difference between mean annual maximum temperature and mean annual minimum temperature for each county in Michigan, which were estimated from corresponding graphs.

*2: Obtained by subtracting built year from inspection date (months and days are converted to years after dividing by 12 and 365 respectively.)

*3: It was converted to three indicator variables in the statistical analyses and ANN models.

*4: It was transformed to four indicator variables in the artificial neural network application.

First, the ADTT increasing rate (ADTTinc) was estimated with equation (3-1) for each bridge:

$$ADTTinc = \left(\frac{ADTT_{predicted}}{ADTT_{measured}} \right)^{\lambda} - 1 \qquad (3-1)$$

42

where ADTT$_{measured}$ is the ADTT in the year in which it was measured; ADTT$_{predicted}$ is the predicted ADTT in the future; λ is calculated using equation (3-2).

$$\lambda = \frac{1}{(Year_{predicted} - Year_{measured})} \qquad (3-2)$$

Where Year$_{measured}$ is the measured year for ADTT$_{measured}$ (months and days were converted to years by dividing by 12 and 365, respectively); Year$_{predicted}$ is the year in which the ADTT is predicted. The ADTT at the time of inspection (ADTT$_{insp}$) is then calculated as:

$$ADTT_{insp} = ADTT_{measured} \cdot (ADTTinc + 1)^{\kappa} \qquad (3-3)$$

$$\kappa = (Year_{insp} - Year_{measured}) \qquad (3-4)$$

3.2.2   Initial data screening

Raw inventory data retrieved from the MDOT NBI database was initially screened to exclude outliers and erroneous observations. The criteria for this initial screening are shown in Table 3-2. Most of the MDOT highway bridges are of one of three structural/material types: simple/cantilevered steel, continuous steel, and prestressed concrete. A scatter plot matrix of abutment rating for simple/cantilevered steel bridges and five design and operation parameters is shown in Figure 3-1. Each cell in the matrix is a scatter plot and describes the distribution of observations concerning two parameters on the abscissa and ordinate. It can be seen from Figure 3-1 that the database is highly complicated and that no clear trend can be observed. Some observations had almost

43

identical predictor values but with abutment rating differing each by more than 1. Those

confusing observations could cause a problem of node proliferation, which was highly

detrimental to the development of prediction models as well as the identification of

causes for abutment damage. Thus, they were deleted from the database. The deleted

observations accounted for less than 3% of all the observations.

Table 3-2 Criteria for data extraction

#	Parameters	Criteria
1	*userbrdg_legal_cd**	1
2	*abutment rating*	0~9
3	*built year*	>0
4	*maximum span*	>0
5	*deck area*	>0
6	*deck width*	>0
7	*skew angle*	>=0
8	*average daily total traffic*	>0
9	*truck percentage*	not equal -1
10	*type of design/construction*	>=0 & not equal 18 & not equal 19
11	*inspection year*	no earlier than built year
12	*year at which daily traffic was measured*	>=0

* userbrdg_legal_cd is MDOT Legal system, 1=MDOT, 2=County Primary, 3=County Local, 4=City Major, 5=City Minor, 6=Other. Userinsp_abut_rtg_cd is abutment rating.
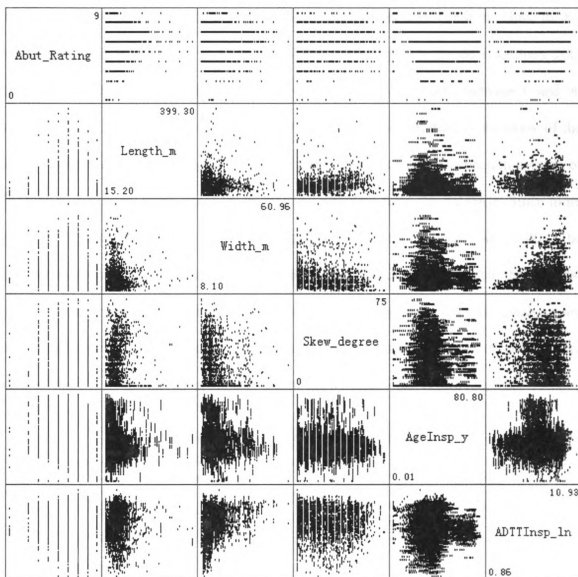
Figure 3-1 Scatter plot matrix of simple/cantilevered steel bridges

3.2.3 Database creation

Raw data extracted from MDOT's NBI database were organized into a consistent evidential database to be used in statistical analyses, field inspection and instrumentation, numerical simulation, soft computing, and an ensemble of neural networks. After examining the NBI database, it was found that the longest bridge is up to 5,866.7 m;

however, more than 99.8 % of them have their lengths less than 1,000 m. Thus, in this research bridges with lengths of more than 1,000 m have been removed as outliers from the evidential database. A skew angle of a bridge should be a value between 0 and 90 degrees. Since "99 degrees" in the record indicates a major variation in the skew of the substructure units and "90 degrees" doesn't make sense in reality, inspection records of bridges with a skew angle equal 90 or 99 were removed from the database. Since more than 99.8 % of the bridges have average daily truck traffic less than 30,000, the inspection records for the bridges with average daily truck traffic greater than 30,000 were removed from the database. The criteria for creating the evidential database are shown in Table 3-3. After filtering by the mentioned criteria, 905 inspection records were deleted and the evidential database was composed of 19,615 inspection records.

Table 3-3 Criteria to refine the data set

#	Parameters	Criteria
1	*Length*	> 0 ft and < = 1000 m
2	*Deckwidth*	> 0 ft
3	*skew angle*	>= 0° and < 90°
4	*Age at inspection*	>= 0
5	*Approachtype*	>= 0
6	*Average daily truck traffic at inspection*	> 0 and <= 30, 000

3.2.4 Deficiencies of MDOT NBI database

Further exploration and advanced use of the MDOT NBI database is constrained by these inherent difficulties:

- The database is highly complicated and no conspicuous trend or correlation can be extracted. There is no one-to-one relationship between the cause and effect of structural damage, which means many causes can lead to the damage of the abutment wall. Moreover, the relationship can be highly nonlinear and thus very difficult to be extracted if not impossible, by current means.

- Subjectivity exists in the manual inspection methods and a large variance results in the adopted structural evaluation ratings. For the NBI system, it has been found that for the same structure its ratings assigned by 49 bridge inspectors from 25 state departments were dispersed, with only 68 percent of them within ±1 (in a scale of 0 to 9) around the mean, 95 percent of them fall in ±2 around the mean [Phares et al. 2001]. Even if all the bridges with the same design parameters were inspected by the same engineer the ratings might still be different because construction quality can not be identical.

- The values of some variables in some observations are missing or subjected to error. For instance, the approach pavement type (a parameter of importance to the damage of bridge abutments) for some bridges in the database is missing.

- The distribution of inspection records is unbalanced. Cases of severe damage are relatively rare in comparison with the large number of bridge abutments in relatively good condition.

- The abutment rating is a general condition rating but the details of the damage are unknown.

- Some important factors are not available, such as soil type and pavement type.

3.3 Significance of Design and Operation Parameters

3.3.1 Frequency Analyses

Frequency analyses in this research aimed at finding out the distribution of highway bridge populations to reveal common features of highway bridges that were susceptible to damage in abutment walls. The analyses concerning approach pavement surface type is presented here as an example.

Pavement pressure was one of the susceptible causes of damage in bridge abutment walls. Its frequency analyses are shown in Figure 3-2. In Figure 3-2, each column represents one structural type, where "simstl" means inspections of simple/cantilevered steel bridges, "constl" denotes inspections of continuous steel bridges, and "prscrt" represents inspections of prestressed concrete bridges. Each row represents one type of approach surface type, where "Bimcon" means freeway designed bituminous concrete on aggregate base, and "Concret" denotes concrete pavement. The label "unknown" means that the corresponding value in the database is missing. The ratios of poor abutment for each category in Figure 3-2 are shown in Figure 3-3.
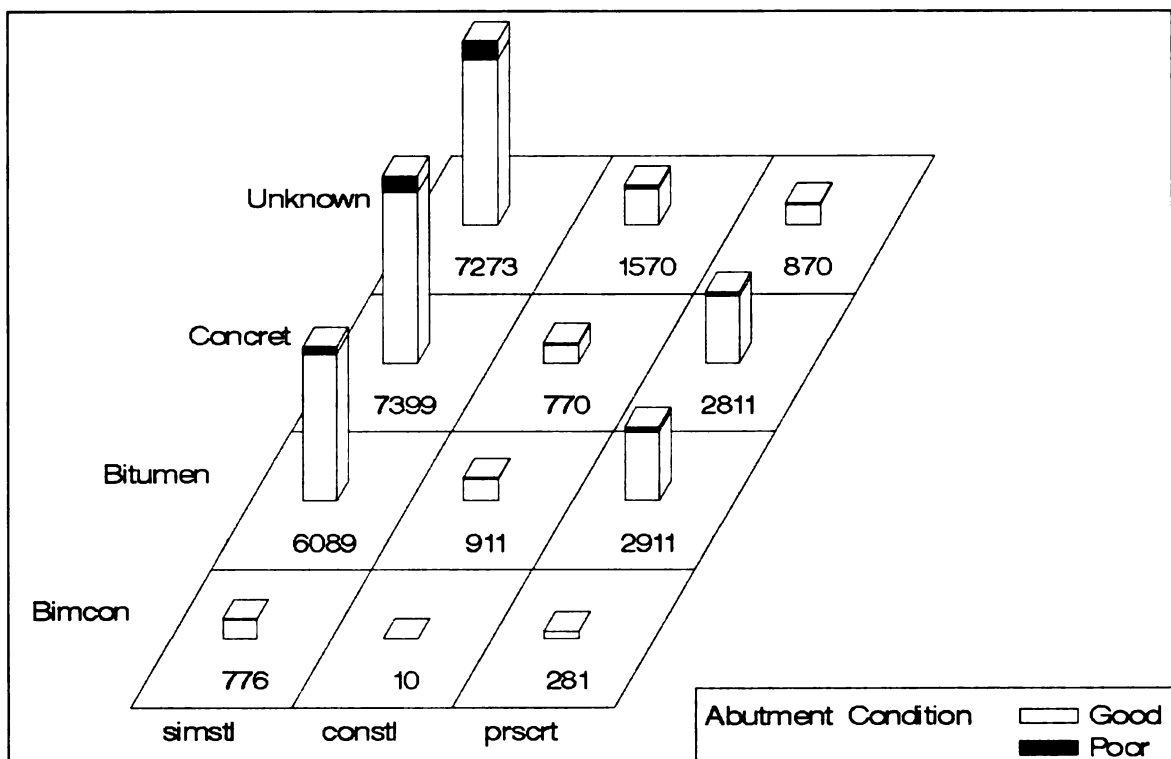
Figure 3-2 Frequency analysis of highway bridge inspections
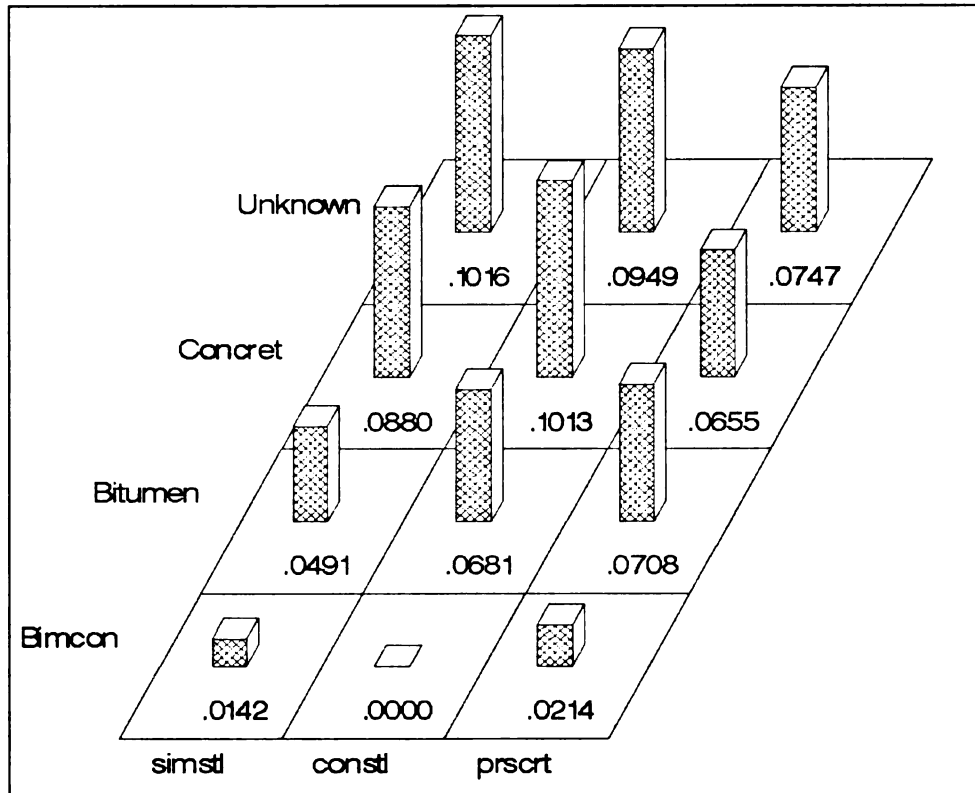
Figure 3-3 Ratio of poor abutment rating

After a detailed evaluation of Figure 3-2 and Figure 3-3 it can be concluded that steel bridges with concrete approach pavement and "unknown" approach pavement have a high percentage of poor abutment rating. For prestressed concrete bridges the ratio of poor abutment rating does not seem different for any of the approach pavement types. Frequency analyses revealed common characteristics of bridges that were susceptible to abutment damage. These common features are summarized in Table 3-4.

Table 3-4 Common characteristics of bridges with poor abutments

Structural type Design parameters	Simple or cantilevered steel	Continuous steel	Prestressed concrete
Length (m)	[76.2, 1000]	[121.9, 1000]	[45.7, 91.4]
Maximum span (m)	[24.4, 46.7]	[30.5, 54.9]	[18.3, 30.5]
Deck width (m)	[18.3, 24.4]	[9.1, 18.3]	[18.3, 21.3]
Skew angle (degree)	[0, 60]	0	[0, 45]
Approach pavement type	concrete	concrete	bitumen, concrete
ADTT	[5000, 30000]	[5000, 30000]	[5000, 30000]
Year built	before 1980	before 1980	before 1980
Age at inspection (year)	30	30	30

3.3.2 Correlation Analysis

Correlation analysis is an important statistical tool to draw inferences about the strength of the relationship between two or more variables. That is, it is a measure of the degree to which the values of these variables vary in a systematic manner. In this manner, it provides a quantitative index of the degree to which one or more variables can be used to predict the values of another variable. Correlation analyses were used for bridge

abutment problem in an attempt to reveal the association between bridge abutment rating

and explanatory parameters, such as design and operation variables.

3.3.2.1 Statistical theorem about covariance and correlation

The degree of linear association between two variables X and Y was reflected by

value of *Pearson product-moment* correlation coefficient R [Snedecor and Cochran 1989].

The conception of the Pearson correlation coefficient is to separate the variation of values

of random variable Y into two parts: linear variation with random variable X and

nonlinear variation. The correlation coefficient is defined as the ratio of linear variation to

the total variation. That is, the fraction of the total variation that is explained by the linear

relationship between Y and X. Based on the concept mentioned above, Equation (3-5) was

used to calculate the correlation coefficient R.

$$R = \frac{\sum_{i=1}^{n} x_i y_i - \frac{1}{n}\left(\sum_{i=1}^{n} x_i\right)\left(\sum_{i=1}^{n} y_i\right)}{\sqrt{\sum_{i=1}^{n} x_i^2 - \frac{1}{n}\left(\sum_{i=1}^{n} x_i\right)^2}\sqrt{\sum_{i=1}^{n} y_i^2 - \frac{1}{n}\left(\sum_{i=1}^{n} y_i\right)^2}} \tag{3-5}$$

where x_i is the ith value of random variable X, i=1, 2, ... , n; and y_i is the ith value of

random variable Y, i=1, 2, ... , n. If the linear variation of values equals the total variation,

the correlation coefficient will equal 1. If the relationship between X and Y is inverse and

the linear variation equals the total variation in magnitude, R will equal -1. These

conditions represent the extremes, but both values indicate a perfect association, with the

sign only indicating the relationship. A correlation coefficient of zero, which is

sometimes called the null correlation, indicates no linear association between the two variables X and Y [Ayyub and McCuen 1997].

The physical characteristics of the correlation coefficient are elaborated in Figure 3-4. The schematic in Figure 3-4a indicates that there is no linear relationship between the two random variables; as the value of X increases it is not certain whether Y will increase or decrease. The correlation coefficient is expected to be close to zero; and the two random variables can be considered to be uncorrelated. Figure 3-4b indicates a positive correlation between X and Y, that is, Y increases as X increases. However, the relationship is not perfectly linear, indicating that R is expected to be between 0 and 1.0. Figure 3-4c shows an example of perfectly positive correlation between the two random variables X and Y; Y increases linearly as X increases. Data points (X, Y) form a straight line with a positive slope rate in the X, Y plane; the correlation coefficient is expected to be close to one. Figure 3-4d illustrates a case of perfectly negative correlation between the two random variables; that is, Y decreases linearly as X increases. Data points (X, Y) form a straight line with a negative slope rate, indicating that R is negative one. Figure 3-4e and f indicate that there could be some nonlinear relationship between the two random variables; however, since the relationship is not linear, R is expected to be zero.

If the correlation coefficient needs to be calculated from observed sample values, it is rare to obtain values of precisely zero, +1 or -1. Two random variables can be considered to be statistically independent if the absolute value of correlation coefficient is less than 0.3; and they can be considered to be perfectly correlated if the absolute value of correlation coefficient is greater than 0.9 [Haldar and Mahadevan 2000].

(a) $R = 0$

(b) $0<R<1$

(c) $R = 1$

(d) $R = -1$

(e) $R = 0$

(f) $R = 0$
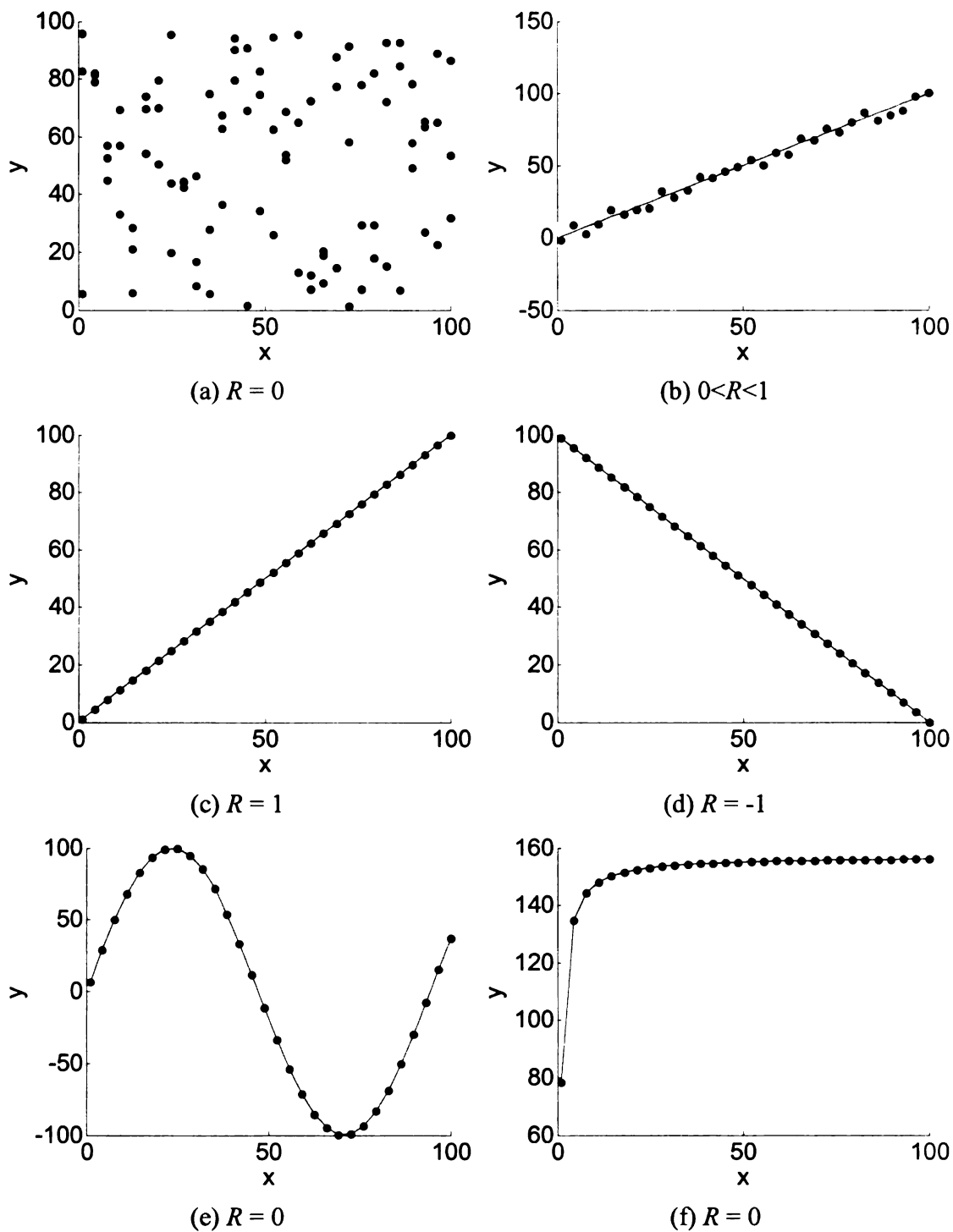
Figure 3-4 Schematic representations of the correlation of two random variables

3.3.2.2 Analysis on entire database

Efforts were made to discover a correlation between bridge abutment rating and explanatory variables by analyzing the whole database. However, the correlation coefficients were less than 0.3. Figure 3-5 is one of the scatter plots generated in these analyses. It can be seen that the data are highly scattered in the graph, which means the two random variables can be considered to be uncorrelated. A series of similar analyses showed that this kind of calculation throughout the whole database would provide very limited information about which parameters correlated with abutment rating.
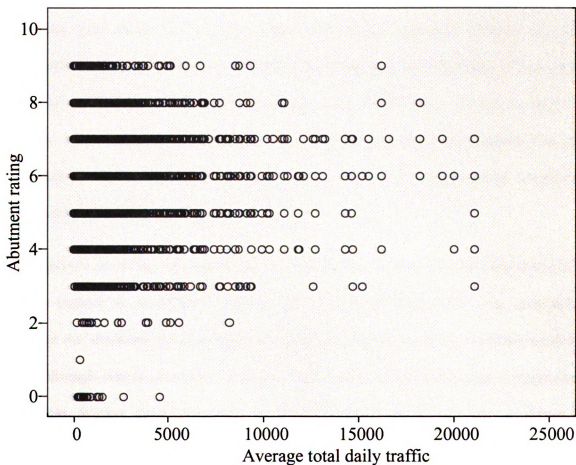
Figure 3-5 Scatter plot for abutment rating and average daily total traffic

3.3.2.3 Division by main structure type, maximum span, skew and approach type

Since the correlation obtained from the analyses on the entire database provided limited information, the database was sub-divided into categories to evaluate the correlation coefficients based on each individual data group. Data with common features were categorized in the same division (Figure 3-6). This rationale for dividing the database followed from the consideration that for bridges with common features, the mechanism that caused degradation of abutment walls would be similar.

Figure 3-7 shows the scatter plot for abutment rating and age at inspection. The abscissa and ordinate are abutment rating and age at inspection respectively. It can be seen that there seems to be some degree of negative correlation between the two parameters; with the correlation coefficient expected to be a value between -0.3 and -0.9. The analysis showed that the correlation value was –0.555. Thus, for this category of bridges, with a maximum span between 18.3 m and 30.5 m, skew angle greater than 45° and flexible surface approach, the age at inspection is, to some extent, negatively correlated with abutment rating.

Analyses on all the data sub-divisions identified in Figure 3-6 were carried out in a similar manner as described throughout this section. In general, no clear association between the abutment rating of highway bridges and the explanatory variables could be found through simple correlation analyses. Deck width, pin condition, age at inspection, built year, average daily total traffic, and average daily truck traffic were all shown to have some degree of correlation to abutment rating. The correlation coefficients varied

according to the different data categorizations and subdivisions and evidence was not strong enough to support a more general positive conclusion.
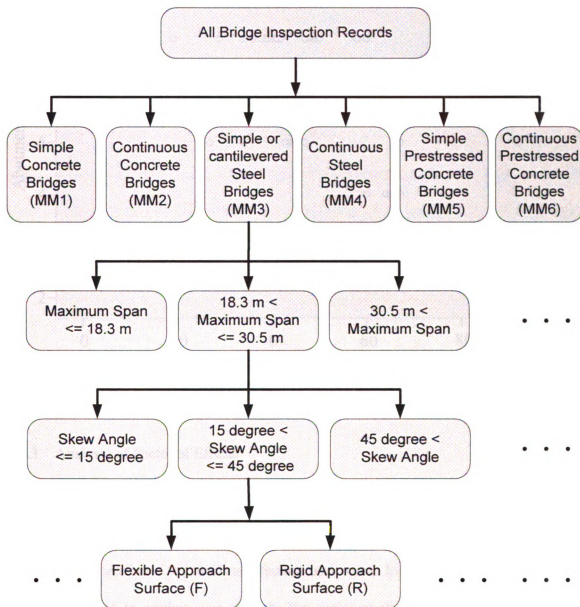
Figure 3-6 Database Sub-Division for Statistical Correlation Analyses
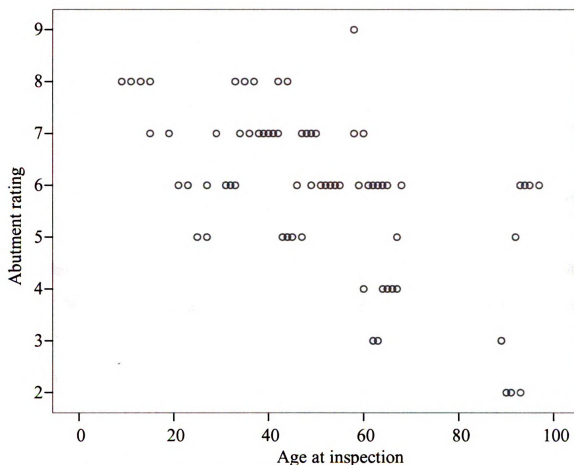
Figure 3-7 Scatter Plot for Abutment Rating and Age at Inspection

3.3.3 Analysis of Factorial Effects

Factorial effects were analyzed through a two-way analysis of variance (ANOVA). ANOVA is a statistical method to divide the variation in response variable into several components contributed by different factors and error. In ANOVA, linear regression models are used to explain and separate the variation in the response variables. The model is shown in equations (3-6)-(3-9) [Rice 1995].

$$Y_{ijk} = \mu + \alpha_i + \beta_j + \delta_{ij} + \varepsilon_{ijk} \qquad (3-6)$$

$$\sum_{i=1}^{I} \alpha_i = 0 \tag{3-7}$$

$$\sum_{j=1}^{J} \beta_j = 0 \tag{3-8}$$

$$\sum_{i=1}^{I} \delta_{ij} = \sum_{j=1}^{J} \delta_{ij} = 0 \tag{3-9}$$

In the above equations Y_{ijk} is the kth record in the group with ith level of factor A and jth level of factor B; α_i is the differential effect of ith level of factor A; β_j is the differential effect of jth level of factor B; δ_{ij} is the effect of interaction between ith level of factor A and jth level of factor B; and ε_{ijk} is the random error in the kth record for the group with ith level of factor A and jth level of factor B. The total sums of squares can be partitioned using equation (3-10):

$$SS_{TOT} = SS_A + SS_B + SS_{AB} + SS_E \tag{3-10}$$

where SS_{TOT} is the total sums of squares; SS_A, SS_B, SS_{AB}, and SS_E are sums of squares for factor A, factor B, interaction between A and B, and error, respectively. Using the sums of squares, F tests can be carried out to evaluate the significance of the factors, as shown in equation (3-11). In equation (3-11), df_A means the degree of freedom for factor A, df_E represents the degree of freedom for error. The F statistics can be calculated for the effects of the other factors and interactions between factors in a similar manner. The F

statistics can be evaluated using either a sequential sum of squares (Type I) or by fully adjusted sums of squares (Type III.)

$$F = \frac{SS_A / df_A}{SS_E / df_E}$$ (3-11)

The analyses of factorial effects was aimed at verifying the significance of the qualitative variables "pin type" and "approach type" in the development of damage in bridge abutment walls. The analyses were conducted using generalized linear regression model procedure "SAS PROC GLM" [SAS 2004]. In the factorial design, the qualitative variable "pin type" had two levels "without pin-and-hanger assembly" and "with pin-and-hanger assembly". The qualitative variable "approach type" had three levels: "rigid," "flexible," and "unknown." Six covariates were added to this model: "length," "deck width," "age at inspection," "average annual temperature difference," "ADTT at inspection," and "maximum span."

Table 3-5 shows one of the Type III analysis of variance (ANOVA) models derived in the analyses of factorial effects. It can be seen from Table 3-5 that the interaction term between "pin type" and "approach type" was significant under a type I error rate of 0.01%. Thus, the effect of the levels of one factor within the levels of another factor needed to be explored. It can also be seen that "approach type" was also significant under a type I error rate of 0.01 %. Even though "pin type" was significant under type I error rate of 5 %, the evidence was not very strong. This justifies the model selected in section 3.4, in which the dummy variable "pin type" was excluded by Mallow's C_p criterion.

Table 3-5 Type III Model ANOVA

Source	DF	Type III SS	Mean Square	F Value	Pr > F
Pin type	1	4.44	4.44	3.88	0.0487
Approach Type	2	213.36	106.68	93.28	<.0001
Pin type × Approach type	2	68.30	34.15	29.86	<.0001

The tests of difference in factorial effects were carried out based on the results shown in Table 3-5. All the covariate values in the model were set to be constant in each test. Three scenarios were considered according to covariate values "0," "-1," and "1." It can be seen from the residual plots in Section 3.4 that these three values encompassed the samples that were most frequent. The factorial effects when covariates had a value of "0" are shown in Table 3-6.

It can be seen from Table 3-6 that the effect of "pin type" was not significant for bridges with flexible approach. However, for the bridges with the rigid approach or unknown approach, the effect of "pin type" was significant. For bridges with unknown approach the abutment rating of bridges with pins was significantly higher than those without pins. However, for bridges with rigid approach pavement, the abutment rating of the bridges with pins were significantly lower than those without pins under a type I error rate of 0.01 %. The difference of the effect of approach types was always significant under the type I error rate of 0.01 % no matter whether pins were present or not. The abutment ratings of bridges with flexible approach pavement were significantly higher than those for bridges with the other two types of approach pavements, irrespective of whether pins were present or not. For bridges with pins, the abutment ratings of those with unknown approach pavement type were significantly higher than bridges with rigid

approach type. Conversely, for bridges without pins, the abutment rating of bridges with rigid approach pavement type was significantly higher than those with unknown approach pavement type.

Table 3-6 Test of factorial effects (covariates values are 0s)

Parameter	Estimate	Standard Error	t Value	Pr > |t|
Difference of pin within flexible approach	0.041	0.033	-1.24	0.2157
Difference of pin within unknown approach	0.133	0.033	4.06	<0.0001
Difference of pin within rigid approach	0.201	0.029	-6.92	<0.0001
Difference of flexible and unknown approach for bridges with pin	0.147	0.031	4.82	<0.0001
Difference of flexible and rigid approach for bridges with pin	0.335	0.029	11.52	<0.0001
Difference of unknown and rigid approach for bridges with pin	0.187	0.029	6.43	<0.0001
Difference of flexible and unknown approach for bridges without pin	0.322	0.033	9.83	<0.0001
Difference of flexible and rigid approach for bridges without pin	0.175	0.031	5.66	<0.0001
Difference of unknown and rigid approach for bridges without pin	0.147	0.031	-4.81	<0.0001

3.3.4 Hypothesis Test

Hypothesis test is a statistical algorithm to evaluate the possibility of an assumption to be untrue based on the gathered data. The assumption under consideration is called null hypothesis, H_0. A test statistic needs to be defined in a hypothesis test. Assuming H_0

is true, the distribution of test statistic can be derived. The result of a test is expressed in the possibility of obtaining a statistic if the null hypothesis is true. The values of a test statistics can be calculated based on the gathered data, and the possibility to get that value if H_0 is true can be compared with a significance level, α. If the possibility is less than α, H_0 can be rejected. Otherwise, H_0 can not be rejected.

A series of statistics can be used in hypothesis test, such as z, t, χ^2, etc. In this research, χ^2 test of goodness of fit [Snedecor and Cochran 1989] was applied. Chi-square distribution is the sum of squares of independent standard normal variables. The value of χ^2 statistics can be calculated by equation (3-12). In equation (3-12) f_i means the observed frequency in a class; F_i represents the expected frequency from theoretical distribution; and k signifies the number of classes in consideration.

$$\chi^2 = \frac{\sum_{i=1}^{k}(f_i - F_i)^2}{F_i} \tag{3-12}$$

Hypothesis tests were applied to investigate the contribution of beam type and approach pavement type in the development of abutment damage of prestressed concrete bridges. Specifically, chi-square hypothesis tests were applied. At first, the abutment conditions were divided into 10 classes: 0-9. Four beam types were considered in the analyses: adjacent box girder, spread box girder, I-girder, and others. The inspection records of prestressed concrete bridges were categorized into 40 cell groups considering all combinations of beam types and abutment conditions. It should be pointed out that 53 % of the cells had expected counts less than 5; and thus, the chi-square test was not a valid test. Similarly, for associations between the approach pavement type and abutment

condition, four approach pavement types were considered: bitumen concrete mixed, bitumen, concrete, and unknown. Again, 47.5 % of the 40 cells had expected counts less than 5 and thus the chi-square test was not valid.

In further analyses, abutment conditions of prestressed concrete bridges were categorized in two groups: "with abutment distress" (abutment rating less than 5) and "no abutment distress" (abutment rating larger than 4). Two reasons accounted for the regrouping of the inspection records. First, of primary concern was whether the bridge had abutment distress instead of differentiating between a rating of 7 or 8. Thus, frequency analyses and hypothesis tests on whether the bridge had abutment distress were more rational. Second, after converting the 10-category abutment ratings to 2-category abutment conditions each cell would have enough counts to facilitate the hypothesis tests.

Results of the frequency analyses concerning abutment condition and beam type are shown in Table 3-7. Results of the corresponding chi-square hypothesis test are shown in Table 3-8. The null hypothesis H_0 is: "no association between abutment condition and beam type." It can be seen from Table 3-8 that the null hypothesis test can be rejected under a type I error rate of less than 0.01 %. The conclusion was that for prestressed concrete bridges there is association between abutment condition and beam type.

Table 3-7 Frequency analysis by girder type and abutment condition

Beam	Abutment Condition	Good	Poor	Total
Adjacent Box	Frequency	184	39	223
	Percentage	19.93	4.23	24.16
	Row Percentage	82.51	17.49	
Spread Box	Frequency	41	17	58
	Percentage	4.44	1.84	6.28
	Row Percentage	70.69	29.31	
I-Girder	Frequency	569	70	639
	Percentage	61.65	7.58	69.23
	Row Percentage	89.05	10.95	
Total	Frequency	794	126	920
	Percentage	86.3	13.7	100

Table 3-8 Chi-square Test for H_0: no association between abutment condition and beam type

Statistic	Degree of Freedom	Value	Probability
Chi-Square	2	18.7403	<.0001

Similarly, for approach surface type, the frequency analysis is shown in Table 3-9. Results of the corresponding chi-square hypothesis test are shown in Table 3-10. The null hypothesis H_0 is: "No association between abutment condition and approach surface type." It can be seen from Figure 3-10 that the null hypothesis can not be rejected even under type I error rate of 50 %.

Table 3-9 Frequency analysis by approach surface type and abutment condition

Approach Surface / Abutment Condition		Good	Poor	Total
Bitumen and concrete mixed	Frequency	29	3	32
	Percentage	3.17	0.33	3.49
	Row Percentage	90.63	9.38	
Bitumen	Frequency	340	57	397
	Percentage	37.12	6.22	43.34
	Row Percentage	85.64	14.36	
Concrete	Frequency	322	53	375
	Percentage	35.15	5.79	40.94
	Row Percentage	85.87	14.13	
Unknown	Frequency	99	13	112
	Percentage	10.81	1.42	12.23
	Row Percentage	88.39	11.61	
Total	Frequency	790	126	916
	Percentage	86.24	13.76	100

Table 3-10 Chi-square Test for H_0: no association between abutment condition and approach surface type

Statistic	Degree of Freedom	Value	Probability
Chi-Square	3	1.1198	0.7723

3.4 Regression Analysis

Regression analysis is an area of statistics that deals with methods for investigating the association, and, if present, the characteristics of the associations among various observable quantities [Graybill and Iyer 1994]. These associations can further be expressed in the form of mathematical expressions, which may allow the prediction of the

unobservable value of a variable based on the observed value of one, or more, associated or related variables. These models may also help to determine how to manipulate a given variable to control the value of an associated or related variable. Thus, regression analysis offers a sensible and sound approach for examining associations among variables and for obtaining good rules for prediction. Regression models are widely used in engineering analysis and have been successfully applied in a project to evaluate the causes behind precast I-girder end cracking [Myers et. al. 2001].

The linear regression models are linear combination of first order of the regression coefficients, no higher order or cross product of coefficients is involved in the model [Montgomery et. al. 2006, Myers et. al. 2002, Weisberg 2005]. A linear regression model can use the first order of the explanatory variables or a higher order of the explanatory variables. While multiple linear regressions with the first order of explanatory variables are adequate for modeling a wide variety of relationships between response variables and predictor variables, many situations require terms of higher order to be considered. Equations (3-13)-(3-17) [Montgomery et al. 2006] define a multiple linear regression model. In these equations, y is a vector of values of a response variable, X is a matrix of levels of explanatory variables; β is a vector of regression coefficients; and ε is a vector of residuals. The underlying assumption in the process of fitting a regression model is that the residuals are NIID, which means the residuals are normally, independently and identically distributed.

$$y = X\beta + \varepsilon \tag{3-13}$$

$$y = \begin{bmatrix} y_1 \\ y_2 \\ \vdots \\ y_n \end{bmatrix} \quad (3\text{-}14)$$

$$X = \begin{bmatrix} 1 & x_{11} & x_{12} & \cdots & x_{1k} \\ 1 & x_{21} & x_{22} & \cdots & x_{2k} \\ \vdots & \vdots & \vdots & & \vdots \\ 1 & x_{n1} & x_{n2} & \cdots & x_{nk} \end{bmatrix} \quad (3\text{-}15)$$

$$\beta = \begin{bmatrix} \beta_1 \\ \beta_2 \\ \vdots \\ \beta_k \end{bmatrix} \quad (3\text{-}16)$$

$$\varepsilon = \begin{bmatrix} \varepsilon_1 \\ \varepsilon_2 \\ \vdots \\ \varepsilon_n \end{bmatrix} \quad (3\text{-}17)$$

3.4.1 Linear regression using first order of explanatory variables

3.4.1.1 Selection of explanatory variables

(a) Automatic search Procedures

Stepwise regression based on an iterative procedure was applied in this research. The procedure considers a sequence of t-tests on the explanatory variables at each stage. It can be classified as forward stepwise regression, backward stepwise regression, etc, depending on the iteration scheme. It may be initiated with no variables in the model and variables can be added later on; or it could be started with all the variables in the model and variables can be later deleted from it [Kutner et. al. 2005]. A forward stepwise procedure was used to search for a proper subset of explanatory variables to build a model to predict abutment condition in highway bridges.

The subset of explanatory variables for simple/cantilevered steel bridges selected by the forward stepwise procedure is shown in Table 3-11. It can be seen from Table 3-11 that eight variables were included in the subset, each of them with a significance value of less than 0.0015. Even though this can not ensure that the subset is optimal, it can still provide a valuable reference for the identification of key parameters, especially after the models were verified.

Table 3-11 Subset of explanatory variables for simple/cantilevered steel bridges

Step	Variable Entered	Partial R-Square	Model R-Square	F Value	Pr > F
1	Matdiff	0.0343	0.0343	729.06	<.0001
2	Ageinsp	0.0282	0.0625	615.94	<.0001
3	Deckwidth	0.0301	0.0925	679.06	<.0001
4	Apprsurstif	0.0054	0.0979	121.93	<.0001
5	ADTTinsp	0.0015	0.0994	34.22	<.0001
6	Maxspan	0.0014	0.1008	31.22	<.0001
7	Pin type	0.0005	0.1013	12.05	0.0005
8	Skew	0.0004	0.1018	10.08	0.0015

(b) Criterion based on all combinations

There are many criteria for the selection of proper models from all combinations, such as R_p^2, $R_{a,p}^2$, C_p, AIC_p, SBC_p and $PRESS_p$ [Kutner et. al. 2005]. Mallow's C_p [Kutner et. al. 2005] criterion was used in this research. Mallow's C_p is computed as

$$C_p = \frac{SSE_p}{MSE(X_1, X_2, ..., X_{P-1})} - (n - 2p)$$

(3-18)

where SSE_p is the sum of the square error of the model in consideration, and MSE is the mean squared error of the full model that included all the explanatory variables. SSE_p is the summation of two terms. One error is that due to bias; that is, the model does not properly reflect the relationship between dependent and independent variables. The second component is due to variation, which is a sampling error. Thus, when C_p is plotted against p and a line $C_p = p$ is drawn on the plot, the $C_p s$ of models with little bias will fall

in the vicinity of the line, the C_ps of models with significant bias will fall high above the line, and the C_ps of models without bias will fall below the line. The assumption underlining the calculation of Mallow's C_p factor is that the full model, including all the explanatory variables, has no bias. That is, MSE is an unbiased estimator of the variation σ^2.

In the application of Mallow's C_p criterion, a Mallow's C_p that is small and close to the p value is sought. A small C_p value means a small total square error. A C_p value close to p ensures the bias term to be small. A small C_p value itself can not ensure a small bias, so the model with a larger subset of explanatory variables with only a slightly larger C_p value is preferable in comparison with models with slightly smaller C_p values and smaller p values. The C_p value for the full model (including all the explanatory variables) is p [Kutner et. al. 2005].

The subsets of explanatory variables for simple/cantilevered steel bridges seem to be good as tested by Mallow's C_p criterion and shown in Table 3-12. It can be seen from Table 3-12 that the most suitable subset is the first one, since its C_p value is small and close to the number of variables p. It is reassuring to find out that the first subset exactly matches the subset obtained by the stepwise automatic selection, as seen by comparing with Table 3-11. Thus, the first subset was selected and tested.

Table 3-12 Explanatory variable subsets of simple/cantilevered steel bridges and their Mallow's C_ps

Number of variables p	C_p	Variables in Model
8	7.812	Deckwidth Skew Matdiff Apprsurstif Maxspan Pin Ageinsp ADTTinsp
9	9.291	Length Deckwidth Skew Matdiff Apprsurstif Maxspan Pin Ageinsp ADTTinsp
9	9.588	Deckwidth Skew Matdiff Apprsurstif Maxspan Pin Designload Ageinsp ADTTinsp
10	11	Length Deckwidth Skew Matdiff Apprsurstif Maxspan Pin Designload Ageinsp ADTTinsp

3.4.1.2 Regression analysis and validation

A regression model developed for the abutment degradation of simple/cantilevered steel bridges is presented in this section. The first order of the variables listed in Table 3-11 were used as predictors and the abutment rating was the response variable. The plot of predicted values versus residuals is shown in Figure 3-8. It can be seen from Figure 3-8 that the variance of the residuals is not constant and the magnitude of the residual is large. The stem-and-leaf plot and box plot are shown in Figure 3-9. It can be seen from Figure 3-9 that the distribution of the residuals is not normal and that the distribution is skewed. The normal probability plot is shown in Figure 3-10. Again, it can be seen from Figure 3-10 that the plot is close to the reference line, but the distribution is skewed. Based on the evaluation of Figure 3-8, Figure 3-9 and Figure 3-10, it can be concluded that the residuals of the regression model for simple/cantilevered steel bridges are not

NIID. Thus, the regression model is not valid. It follows that linear regression models using the first order of explanatory variables can not reflect the relationship between explanatory variables and the abutment ratings for this research problem.
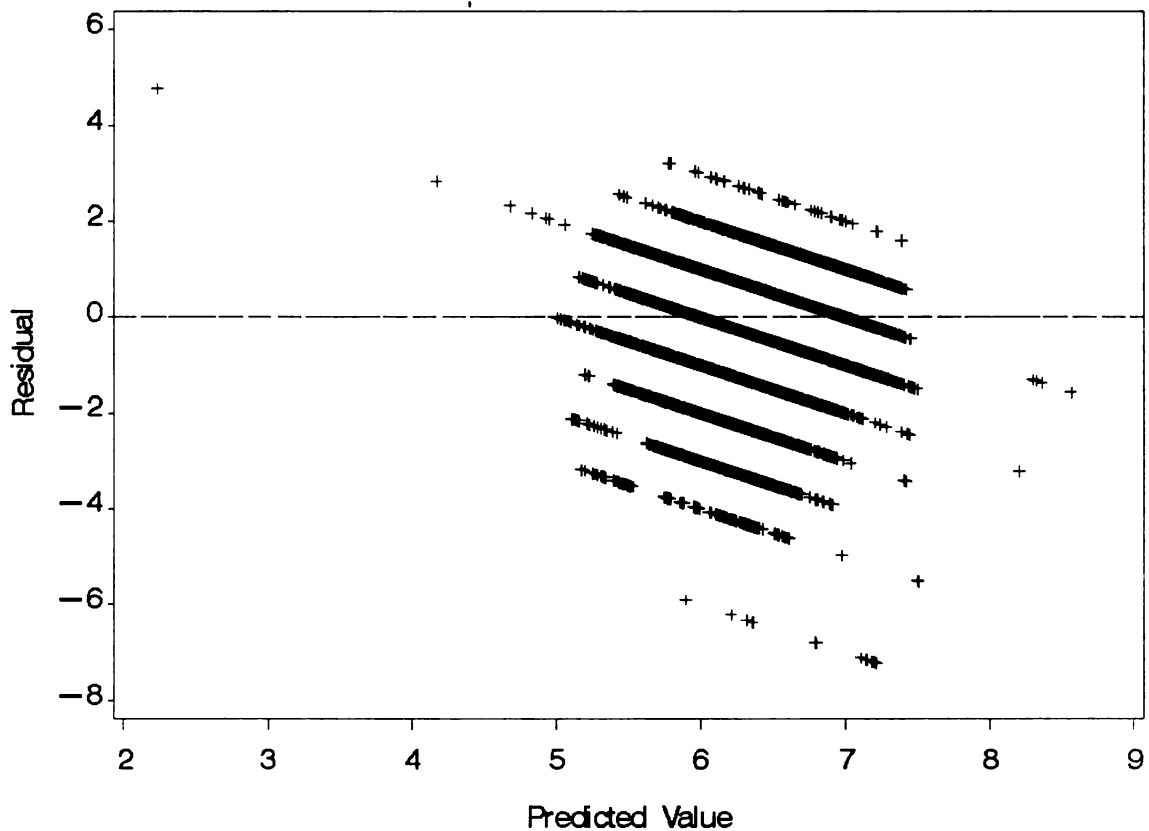
Figure 3-8 Residual plot for the model of simple/cantilevered steel bridges

3.4.2 Linear regression analysis using first and second order of explanatory variables

Multivariate linear regression models were developed considering quadratic and cross interaction terms of explanatory variables. In general, multivariate linear regression models were also found not to be adequate for predicting abutment damage.

```
                    Hstogram                      #        Boxplot
    4.75+*                                        1           *
         .
         .
         .*                                       4           0
         .*                                      18           0
         .*                                      57           0
         .******                                565           |
         .****************                      1845          |
         .*********************************************       4845       +----+
         .****************************************************  5307     *--+-*
         .**************************                          3061       +----+
         .***************                                    1679          |
   -1.25+**********                                          1168          |
         .******                                              569          |
         .*****                                               529          0
         .***                                                 297          0
         .****                                                371          0
         .**                                                  113          0
         .*                                                    53          *
         .*                                                    10          *
         .
         .*                                                     3          *
         .*                                                     4          *
         .*                                                     3          *
   -7.25+*                                                      7          *
        ----+----+----+----+----+----+----+----+----+--
        * may represent up to 111 counts
```

Figure 3-9 Leaf and stem plot and box plot of residuals for simple/cantilevered steel bridge

3.4.2.1   Data preparation

In order to avoid a possible multi-colinearity problem, and the severe round off error caused by it, the seven quantitative variables were normalized using equation (3-19) before quadratic and cross interaction terms were added. The corresponding mean and standard deviation of the variables are shown in Table 3-13.

Figure 3-10 Normal probability plot for the model of simple/cantilevered steel bridges

$$x_i^* = \frac{x_i - \overline{x_i}}{\sigma_i}$$

(3-19)

The qualitative variable "approach type" was coded by two dummy variables: "app1" and "app2," where app1 = 0 and app2 = 0 for bitumen approach pavement; app1 = 1, app2 = 0 for bitumen and concrete mixed approach pavement; and app1 = 0, app2 = 1 for

concrete pavement. The qualitative variable "pin type" can be defined as a dummy variable itself, so no recoding was needed for it.

Table 3-13 Mean and standard deviation of the quantitative variables

Parameter	Mean (μ)	standard deviation (σ)
Length (m)	64.796	38.001
deckwidth (m)	15.394	6.957
Skew (°)	19.265	18.078
Ageinsp	36.46	12.127
Matdiff (°C)	10.8	0.79
ADTTinsp	2762.1	3388.200
Maxspan (m)	24.977	9.241

Quadratic and cross interaction terms were added after the covariates were recoded. No quadratic term for the dummy variables was added. No interaction term was added between dummy variables "app1" and "app2" since they are derived from the same qualitative variables. After adding quadratic and interaction terms, the explanatory variables included 7 covariates, 3 dummy variables, 7 quadratic terms of the covariates, and 44 cross interaction terms; that is, 61 explanatory variables in all. The response variable was the abutment rating.

3.4.2.2 Selection of the optimal explanatory variables subset

The commercial statistical software SAS [SAS 2004] was used to search for the optimal subset of explanatory variables using Mallow's C_p criterion. The regression analysis module "SAS PROC REG" [SAS 2004] procedure evaluated 4151 regression models developed with different combinations of explanatory variables. Figure 3-11

shows a plot of "p" versus "Mallow's C_p". It can be seen that most of the points fall under the $C_p = p$ line in this plot. The top seven models are shown in Table 3-14 ordered by the C_p value. Considering parsimony, the subset that contained 40 explanatory variables with the smallest C_p value (the last row in Table 3-14) was chosen.
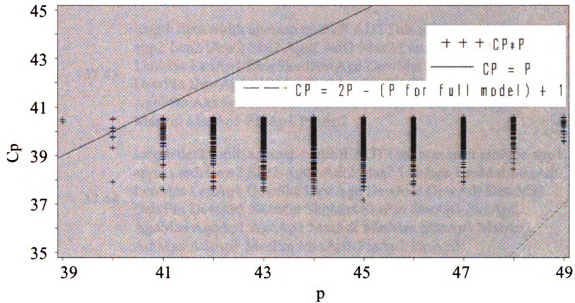
Figure 3-11 Mallow's Cp against p

3.4.2.3 Regression analysis and validation

A regression model considering the first and second order of explanatory variables was developed for abutment degradation of simple/cantilevered steel bridges and is presented in this section. The explanatory variables were listed in the last row of Table 3-14 and abutment rating was used as the response variable. In order to verify the model, residuals are plotted against predicted values and explanatory variable "deck width" in Figure 3-12 and Figure 3-13, respectively. Both plots feature fan-shape patterns and the variances of the residuals are not constant. There are also some outliers in both plots.

Table 3-14 Results of Mallow's Cp Selection Method (Top 7 rows)

p	Cp	Variables in the model
44	37.18	length deckwidth ageinsp matdiff ADTTins maxspan pintype app1 app2 Len2 Dew2 Ske2 Age2 Adt2 Mas2 LenAge LenMat LenAdt LenMas LenAp1 DewSke DewAge DewMat DewAdt DewMas DewPin DewAp1 SkeMat SkeMas SkePin SkeAp1 SkeAp2 AgeMas AgeAp1 AgeAp2 MatAdt MatMas MatAp1 MatAp2 AdtMas MasPin MasAp1 PinAp1 PinAp2
43	37.43	length deckwidth ageinsp matdiff ADTTins maxspan pintype app1 app2 Len2 Dew2 Ske2 Age2 Adt2 Mas2 LenAge LenMat LenAdt LenMas LenAp1 DewSke DewAge DewMat DewAdt DewMas DewPin DewAp1 SkeMat SkeMas SkePin SkeAp1 SkeAp2 AgeMas AgeAp2 MatAdt MatMas MatAp1 MatAp2 AdtMas MasPin MasAp1 PinAp1 PinAp2
45	37.44	length deckwidth ageinsp matdiff ADTTins maxspan pintype app1 app2 Len2 Dew2 Ske2 Age2 Adt2 Mas2 LenAge LenMat LenAdt LenMas LenAp1 DewSke DewAge DewMat DewAdt DewMas DewPin DewAp1 SkeMat SkeMas SkePin SkeAp1 SkeAp2 AgeMas AgeAp1 AgeAp2 MatAdt MatMas MatAp1 MatAp2 AdtMas AdtAp1 MasPin MasAp1 PinAp1 PinAp2
43	37.52	length deckwidth ageinsp matdiff ADTTins maxspan pintype app1 app2 Len2 Dew2 Ske2 Age2 Adt2 LenAge LenMat LenAdt LenMas LenAp1 DewSke DewAge DewMat DewAdt DewMas DewPin DewAp1 SkeMat SkeMas SkePin SkeAp1 SkeAp2 AgeMas AgeAp1 AgeAp2 MatAdt MatMas MatAp1 MatAp2 AdtMas MasPin MasAp1 PinAp1 PinAp2
42	37.56	length deckwidth ageinsp matdiff ADTTins maxspan app1 app2 Len2 Dew2 Ske2 Age2 Adt2 Mas2 LenAge LenMat LenAdt LenMas LenAp1 DewSke DewAge DewMat DewAdt DewMas DewPin DewAp1 SkeMat SkeMas SkePin SkeAp1 SkeAp2 AgeMas AgeAp2 MatAdt MatMas MatAp1 MatAp2 AdtMas MasPin MasAp1 PinAp1 PinAp2
40	37.6	length deckwidth ageinsp matdiff ADTTins maxspan app1 app2 Len2 Dew2 Ske2 Age2 Adt2 LenAge LenMat LenAdt LenMas LenAp1 DewSke DewAge DewMat DewAdt DewMas DewPin DewAp1 SkeMat SkeMas SkePin SkeAp1 SkeAp2 AgeAp2 MatAdt MatMas MatAp1 MatAp2 AdtMas MasPin MasAp1 PinAp1 PinAp2
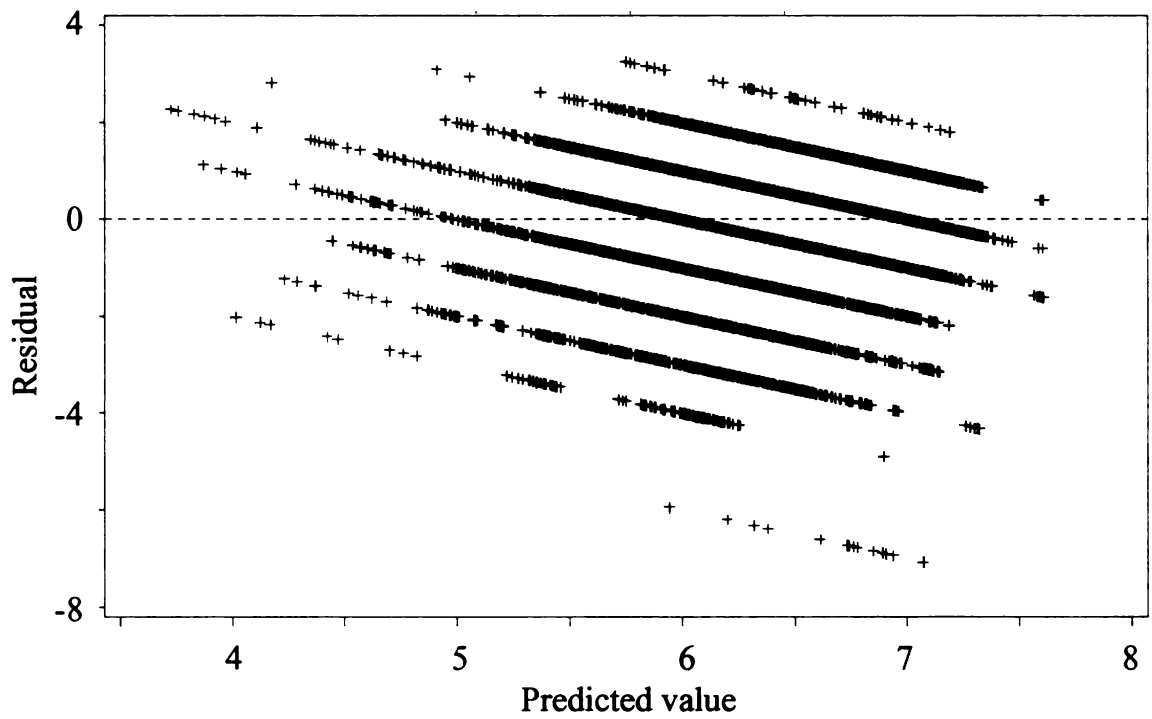
Figure 3-12 Plot of Residual against predicted values
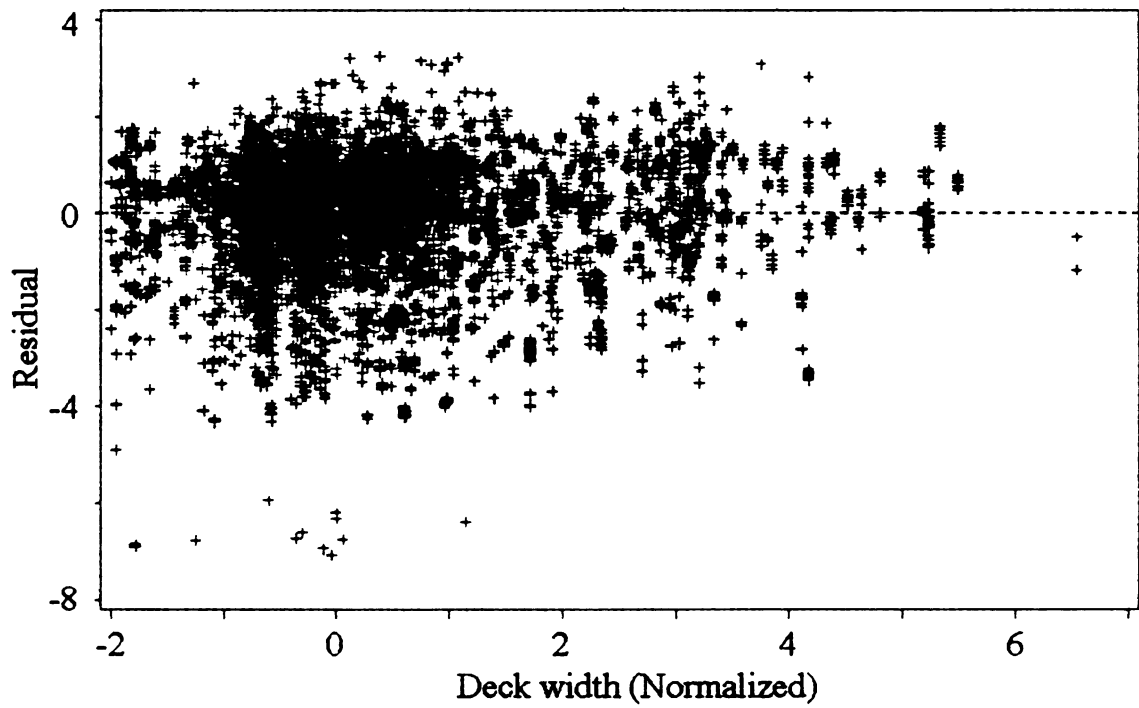
Figure 3-13 Plot of Residual against "deck width"

A check of the residual distribution is also an important procedure to validate the regression model. The stem-and-leaf plot and the box plot of residuals are shown in Figure 3-14. It can be seen from the stem-and-leaf plot on the left that the distribution of the residuals is skewed. After observing the box plot on the right, some outliers are detected in addition to the skew. The normal probability plot of the residuals is shown in Figure 3-15. The skew problem stands out again.

```
            H st ogr am                          #        Boxpl ot
 3. 25+*                                          8         0
     .*                                          18         0
     .*                                         102         0
     .****                                      438         |
     .****************                         1901         |
     .*******************************          3737       +----+
     .****************************************** 5762     *--+-*
-0. 25+****************************              3103       +----+
     .****************                         1844         |
     .********                                  968         |
     .*****                                     581         |
     .****                                      416         0
     .***                                       316         0
     .***                                       251         0
-3. 75+*                                        104         0
     .*                                          50         *
     .*                                           1         *
     .
     .*                                           1         *
     .*                                           3         *
     .*                                          10         *
-7. 25+*                                          1         *
    ---+---+---+---+---+---+---+---+---+---
     * nay repr esent  up t o 121 count s
```

Figure 3-14 Stem and leaf plot and box plot of residuals

```
    3. 25+                                                      *
         |                                                    +*
         |                                             ++++ *
         |                                          ++++*******
         |                                      +*********
         |                                 *******
         |                           *********
   -0. 25+                      *****++
         |                  *****++
         |               ****+
         |           ++***
         |        ++++*****
         | ++   ***
         | *****
   -3. 75+**
         | *
         | *
         |
         | *
         | *
         | *
   -7. 25+*
         +---+---+---+---+---+---+---+---+---+---+
           -2     -1      0     +1     +2
```

Figure 3-15 Normal Probability Plot of the residuals

Based on the residual diagnosis discussed above, it can be concluded that the NIID

distribution of residuals could not be confirmed, and thus the regression models were not

valid. Furthermore, none of the regression models developed in this research could be

proved to be adequate after a model checking process. Thus, regression analyses are not

suitable tools to develop prediction models based on a complicated and unbalanced

database as is the case in this research.

3.5 Discussion

An evidential database was created from the SISD (NBI database for the sample problem.) Statistical analyses based on the evidential database were carried out for the example problem to evaluate the significance of design and operation variables in the development of structural damage and provided valuable information for the subsequent analyses and simulations in this research.

As expected, frequency analyses revealed that older bridges have higher incidences of poor abutment performance. The higher number of bridges with poor abutment for stiff approaches (asphalt on concrete base or concrete) supports the assumption of pavement growth on abutment damage. Finally, poor performance of expansion joints was also clearly related to abutment performance. This could be indicative of abutment forces due to restrained temperature movements, poor bearing performance, and pavement growth problems.

Exploration of correlation coefficients between abutment rating and different parameters was performed. The search for the key parameters by different paths was represented by sorting the bridge population in the database in sub-divisions or sub-categories. Generally, deck width, pin condition, age at inspection, built year, average daily total traffic, and average daily truck traffic are all shown to have some degree of correlation to abutment rating. The correlation coefficients differ according to the different data categorization and subdivision.

In the analysis of factorial effects of simple/cantilevered steel bridges, two factors (pin type and approach surface type) were considered. The factorial effects were

evaluated for the different levels of factors. Since the interaction term between them was significant, the difference between the effects of levels of one factor is considered within certain levels of the other factor. It was found that when the covariates were zero, the effect of pin type was not significant for flexible approaches; while for the other approach types, the effect was significant. The effects of different levels of approach type were always significant regardless of whether the bridge had a pin or not. Some of the factorial effects also changed with the variation of covariates.

Hypothesis tests concerning the association between design parameters and abutment condition for prestressed concrete bridges showed that there was an association between beam type and abutment condition. Proper linear regression models can not be developed by only considering the first order of explanatory variables. The linear regression model using 40 covariates was a relatively good regression model for the current research problem. Covariates consist of the design parameters of the bridge and their quadratic and cross interaction terms. However, it was still not appropriate to reflect the complex problem of abutment distress. Evaluation of the residual plots shows that most of them have fan-shaped patterns and outliers. The NIID assumption concerning the distribution of residuals can not be satisfied by regression models, and thus the models are not valid.

Another generalized linear regression model that can be developed is a multivariate logistic regression model. A multilayer perceptron using sigmoid activation function without hidden layer is equivalent to a logistic regression model [Bishop 1995, Dreiseitl and Ohno-Machado 2002, Hastie et al.2001]. The multivariate logistic regression model can not be expected to have a better performance than the multilayer perceptron using

sigmoid activation function with two hidden layers developed in section 6.2. Thus, the

logistic regression model was not further explored in this research.

4 FIELD MONITORING

4.1 Introduction

Chapter 3 presented an approach to the structural damage problem from a statistical point of view, which was very helpful for evaluating the significance of different design parameters. However, it was shown that mechanisms for the development of damage and specific damage patterns can not be obtained through statistical analyses on the evidential database. Field monitoring in this research aims at evaluating the contribution of the identified parameters and to assist the execution and validation of the analytical studies.

This chapter introduces field monitoring for the example research problem, which includes the bridge selection process, the field inspection of typical bridges, field instrumentation, data collection, and interpretation of the field data. Key processes and important observations of field monitoring are presented in this chapter; a complete description of the field monitoring and analyses of the field data in the example problem are provided in the final research report for MDOT [Burgueño and Li 2008].

4.2 Bridges Selection

Typical bridges inspected in this research were chosen based on the common features of those susceptible to abutment distress identified through statistical analyses. Table 4-1, Table 4-2, and Table 4-3 list the selection criteria in inspection Phase 1 for simple/cantilevered steel bridges, continuous steel bridges, and prestressed concrete bridges, respectively. In order to solve the issues remaining from the Phase 1 inspection, and to make the field evaluation representative and effective, inspection Phase 2 was carried out. The selection criteria for simple/cantilevered steel bridges were not changed, as shown in Table 4-1. Since

unrepaired continuous steel bridges were not enough according to the original criteria, the criteria for selection of continuous steel bridges were changed to that shown in Table 4-4 in inspection phase 2. For prestressed concrete bridges, Phase 2 focused on bridges with I-girder beams or spread box beams, whose population was small, thus no additional criterion was applied except for the beam type. The selection of bridges to be inspected focused on the counties less than 240 kilometers away from Lansing, MI.

Table 4-1 Criteria for simple/cantilevered steel bridge selection (in both phases)

#	Parameters	Criteria
1	*Length*	>=76.2 m
2	*deck area*	>=1393.6 m^2
3	*average daily total traffic*	>30,000
4	*deck width*	>18.3 m
5	*approach surface type*	"Concrete" or "Unknown"

Table 4-2 Criteria for continuous steel bridge selection (Phase 1)

#	Parameters	Criteria
1	*Length*	>=121.9 m
2	*deck area*	>=1393.6 m^2
3	*Skew*	<20°
4	*skew multply deck width*	<182.9 °m
5	*approach surface type*	"Concrete" or "Unknown"

Table 4-3 Criteria for simple prestressed concrete bridge selection (Phase 1)

#	Parameters	Criteria
1	*Length*	45.7 m – 91.4 m
2	*deck area*	929.0 m^2 - 1393.6 m^2
3	*deck width*	<6.1 m or 18.3 m – 24.4 m

Table 4-4 Criteria for continuous steel bridge selection (Phase 2)

#	Parameters	Criteria
1	*Length*	>=121.9 m
2	*deck area*	>=1393.6 m^2
3	*Skew*	<20°
4	*approach surface type*	"Concrete" or "Unknown"

Bridges were assigned simple ID labels for easy identification in the inspection planning as well as in field evaluation. The ID nomenclature was in the form "Xm.n", where X is a capitalized letter indicating the structural type of the bridge, "A" means simple/cantilevered steel bridges, "B" represents continuous steel bridges, and "C" signifies prestressed concrete bridges. The "m" is a number identifying the inspection phase, where "1" means Phase 1 and "2" means Phase 2. The "n" represents the number of the bridge within list selected for inspection in each phase.

Forty-four highway bridges were selected for field inspection. Nine simple/cantilevered steel bridges, eight continuous steel bridges, and nine prestressed concrete bridges were selected for inspection Phase 1. Two simple/cantilevered steel bridges, six continuous steel bridges, and ten prestressed concrete bridges were inspected in Phase 2. Table 4-5 shows the list of simple/cantilever steel bridges inspected in Phase 1.

Table 4-5 Simple/cantilevered Steel Bridges Field Assessment Result (Phase 1)

ID	Bridge Key	Abutment rating	Approach pavement	Length (m)	Built year	ADT total	Skew (°)	Location
A1.1	82182123 000S120	4 (R)*	Hot mix asphalt (HMA) +shared with A1.2	85.6	1970	143000	20	IN DETROIT
A1.2	82182123 000S130	4 (R)*	Concrete+shared with A1.1	100.9	1970	15300	45	IN DETROIT
A1.3	82182102 000S060	7(6-7)*	Concrete	76.8	1976	38500	7	1.2 MI W OF PLYMOUTH
A1.4	82182292 000S050	7(6 &7)*	HMA (strait cracks concrete)	82.0	1974	32000	5	3/4 MI W OF W OF LI WAYNE
A1.5	82182293 000R030	7 (3-4 & 5)*	Asphalt (some degradation, connector w/brige)	62.8	1972	48500	41	IN LIVONIA
A1.6	82182292 000S110	7 (7)*	concrete+HMA (strait cracks)	82.0	1974	32000	0	3/4 MI W OF WAYNE C LTS
A1.7	82182291 000S110	4 (3 & 4- 5)*	Concrete	109.7	1972	49000	0	IN ROMULUS
A1.8	25125132 000S230	7 (7)*	Unknown in database, no comment in inspection	134.1	1976	63000	4	IN FLINT
A1.9	82182293 000R020	8 (7 & 5- 6)*	Concrete & Asphalt over Concrete	86.8	1971	55500	5	IN LIVONIA

* Value in parentheses represents the rating assigned to the bridge during the field inspection. "R" means that the bridge had been repaired, "_" meant different ratings were assigned to two abutments. For example, 6-7 represented rating "6" for abutment A and rating "7" for abutment B.

4.3   Field Inspection

Three major damage patterns in abutment walls of highway bridges were observed: U-shape pull out, vertical cracks between girders, and vertical cracks underneath girders through the positioning dowels.

4.3.1   U-shape pull out

The abutment of bridge A1.7 with U-shape pull out damage is shown in Figure 4-1a. Figure 4-1b shows the concrete approach pavement of the bridge, which would generate much larger compression pressure due to "pavement growth" with time. The inspection process provided compelling evidence that this type of damage was induced by the compression forces generated by pavement expansion, or pavement growth. Pressure seems to be transferred from the integral backwall through the girder anchor bolts down to the abutment wall.

(a) U – shape pull out underneath girder   (b) Concrete approach pavement
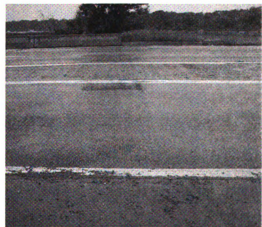
Figure 4-1 Abutment Distress and Pavement for Bridge A1.7

4.3.2 Vertical cracks between girders

Another typical damage pattern observed were vertical cracks in the abutment wall located between girders, as shown in Figure 1-5. Figure 1-5a shows a general view of the abutment wall and part of the superstructure of bridge A1.4. The vertical cracks in the abutment wall can be seen in the close-up view in Figure 1-5b. The inspections provided compelling evidence that this type of damage pattern is mainly caused by the restrained support forces generated due to transverse thermal expansion of the superstructure system.

4.3.3 Vertical cracks underneath girder through the dowel

The third important observed damage pattern was in the form of vertical cracks in the abutment wall located underneath the girder, such as the damage was observed in abutment wall of bridge B1.1 (Figure 1-6.) It can be seen from Figure 1-6 that the bearing of this bridge has been seriously corroded, thus, providing unintended fixity at the girder supports. Displacements or rotations of the superstructure will cause additional stress in the abutment due to the increased stiffness of the bearing.

Bridges visited during both phases of the field inspections were representative for major types of MDOT highway bridges and were selected with parameters that categorized them to be susceptible to abutment distress. The field inspection and assessment was very helpful in identifying typical damage patterns and their possible causes. Detailed inspection records and photographs for each inspected bridge were documented as part of the information database and served as a basis for the selection of bridges for field instrumentation.

4.4 Field Instrumentation

Field instrumentation in this research focused on the deployment of a strategic field monitoring scheme on four bridges with and without signs of abutment distress. Of the 44 inspected bridges (Section 4.3), four bridges were selected for field instrumentation as shown in Table 4-6. In addition to the factors already considered in the selection of bridges for field inspection and the additional information from damage patterns and observations noticed during the inspections, the accessibility to the bridge abutment and the overall bridge site were also taken into account. Two bridges were selected for each superstructure type for comparison; one of them already showed abutment distress and the other one showed minor abutment distress but with the potential, since they shared parameters, to develop damage.

4.4.1 Instrumentation Strategy and Implementation

The objective of the field instrumentation is to obtain the strain distribution on the abutment walls and backwalls, relative movements of the superstructure to substructure, and the temperature field on bridge structures. Since the instrumented bridges can be considered approximately symmetric about the traffic centerline, only one-half of one of the abutment walls for each bridge was provided with measuring points (see "shaded area" in Figure 4-2.) In this way, the number of instrumented bridges was doubled with the available resources. As shown in Figure 4-2, traffic direction was toward the instrumented part of the abutment wall. This abutment side was selected for monitoring because it might be able to capture any effects caused by truck braking. The location of the instrumented bridges and information on the instrumented abutment is given in Table 4-6.

Table 4-6 Final instrumentation list

ID	Bridge key	Abutment rating	Girder	Pavement	Year built	Width (ft)	Road A	Road B	Direction
A1.7	82182291000S110	4 (3 & 4-5)[3 & 5]*	I or W	Concrete**	1972	19.4	I-94	I-275	West
A2.1	25125031000S110	7 (6) [7]*	I or W	Asphalt over Concrete**	1954	20.7	Miller Rd	I-75	East
C2.1	63163174000S061	4 (4) [6 & 4]*	I	Asphalt over Concrete**	1964	18.2	I-75	Rochester Rd W	East
C2.4	25125132000S060	6 (7) [5 & 7]*	I	Concrete**	1971	37.1	I-475	Atherton Rd	South

*The value in the parenthesis is field inspection abutment rating by Dr. Burgueño, the value in square brackets is the field inspection abutment rating by a certified bridge inspector (CTE engineers, Lansing, MI.)

**Information updated according to field inspection.
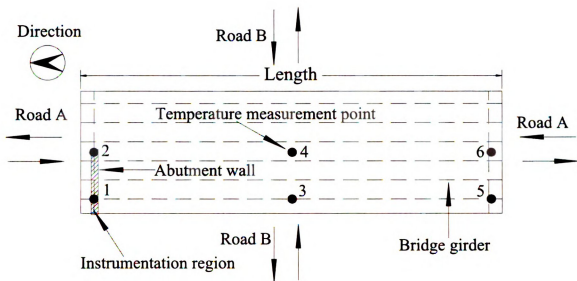
Figure 4-2 Location of bridge and instrumentation region

4.4.2 Deployment of measuring points

The measuring points consisted of brass cylinders (Figure 4-3) embedded into the abutment wall. The brass cylinders have a threaded end where a screw-in seat that can be attached (Figure 4-4). For the girder ends, target discs were glued to the beam surface using an epoxy adhesive. The deployment of measuring points on bridge A1.7 is shown in Figure 4-5.

Figure 4-3 Brass cylinders installed on the abutment wall

Figure 4-4 Measuring points with contact seats screwed on brass cylinders

4.4.3 Variables Measured

Variables measured in the field monitoring plan are listed as follows:

- The deformation of the backwall and the abutment wall: determined from the distance between the measuring points deployed on the backwall and the abutment wall (Figure 4-5.)

- The longitudinal displacement of the girder end: the location of measuring points to measure displacements of girder ends is shown in Figure 4-6.

- Temperature of the bridge: temperatures of the bridge deck as well as on the abutment wall were recorded at the start of the measurement process for each bridge. Temperatures at fifteen locations were taken using a Raynger ST non-contact thermometer. Six of the locations were on the deck (Figure 4-2) and nine of them were on the abutment wall (Figure 4-7).
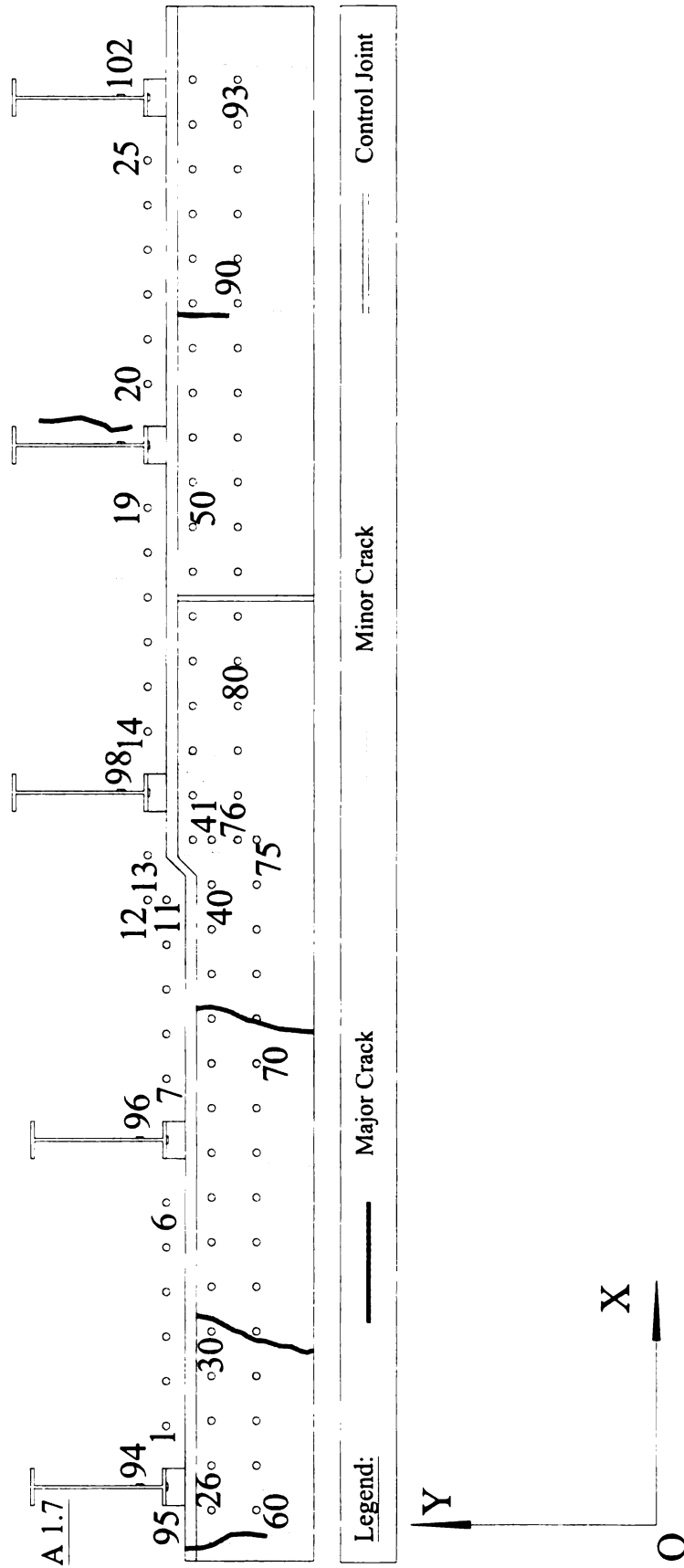
Figure 4-5 Deployment of measuring points on half of the abutment wall of bridge A1.7

Legend:

—— Major Crack

········· Minor Crack

—=— Control Joint
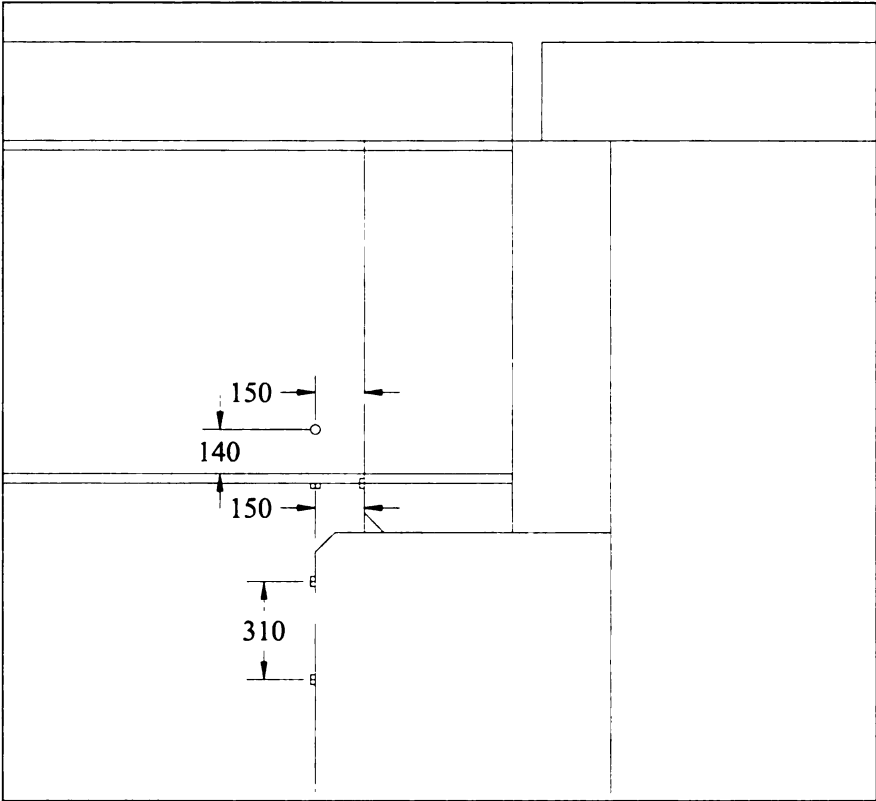
Figure 4-6 Measurement of girder end displacement (unit: mm)
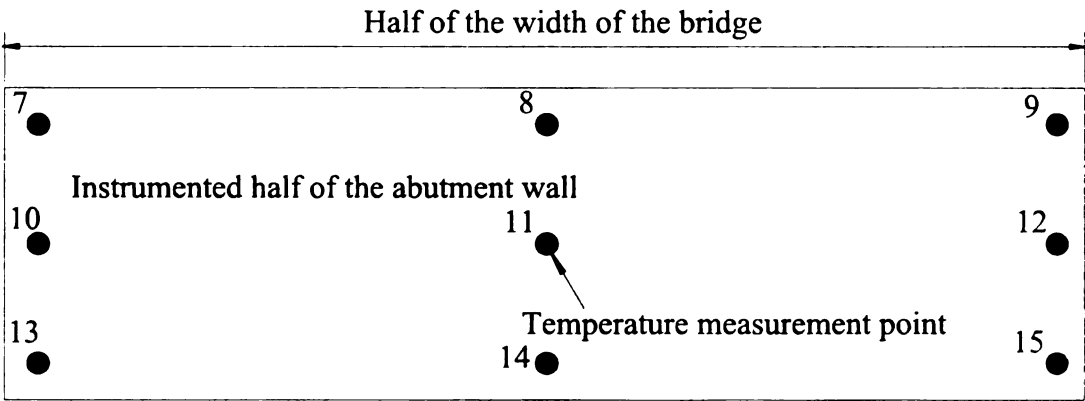
Figure 4-7 Temperature measuring points on bridge abutment wall

Two approaches were applied in calculating the strain distribution along the abutment

wall. One approach was to calculate strain value as the ratio of variation of the distance

between measuring points to its initial value, as given by equation (4-1):

$$\varepsilon_{ijk} = \frac{d_{ijk} - d_{ij0}}{d_{ij0}} \tag{4-1}$$

where ε_{ijk} means the jth strain in the ith line under the top of the abutment wall calculated

for the kth month; d_{ijk} is the jth distance between adjacent measuring points in the ith line

calculated for the kth month; and d_{ij0} is the jth distance between adjacent measuring

points in the ith line calculated for the initial measurement (in December 2006.)

The position of the calculated strain is in the middle of two adjacent measuring points.

The second approach is a moving average method that calculates the strain value in the

middle of four consecutive measuring points using the sum of variations of the distance

between those points divided by the sum of the initial distances, as given in equation

(4-2):

$$\varepsilon_{i,j+1,k} = \frac{d_{i,j-1,k} - d_{i,j-1,0} + d_{i,j,k} - d_{i,j,0} + d_{i,j+1,k} - d_{i,j+1,0}}{d_{i,j-1,0} + d_{i,j,0} + d_{i,j+1,0}} \tag{4-2}$$

4.4.4   Measurement schedule

The field monitoring data was collected over a period of one year at one-month

intervals. Continuous monitoring or more frequent measurements was not required

because the effects leading to abutment distress occur slowly over a long period. A major

cause of the abutment distress was believed to be thermal movements, which can be

assessed by measuring extreme temperatures. Furthermore, the field monitoring was not intended to provide precise measure of bridge response but to reveal the overall behavior of bridges under different circumstances over time. During the first eight months of measurements, two sets of readings were made in each round for the backwall and the abutment wall of each bridge. One set of the readings was taken directly on the anchored brass cylinders (Figure 4-3.) The other was done on the contact seats (Figure 4-4) screwed on the brass cylinders. It was found that the data collected directly from the brass cylinders were more reliable. Thus, measurements were taken only on the brass cylinders for the remaining five rounds.

4.5   Data Interpretation

Data from the field measurements were plotted in three different perspectives to help identify the relations among horizontal strain (target variables), longitudinal and horizontal girder end movements (bridge behavior), and temperature at the deck and the abutment wall (environmental variables.) The calculated variations were determined by using values measured in December 2006 as reference.

4.5.1   Distribution of Strains

The distributions of strains along the abutment wall and backwall together with girder end movements were plotted. Examples are shown in Figure 4-8 and Figure 4-9. The legend "A1" represents the horizontal line 152 mm below the top of the abutment wall. Similarly, "A2" represents the horizontal line 457 mm below the top of the abutment wall. "GM" means girder end movement, which is the average of the values measured at the side of the girder and the bottom of the girder. A positive value means that the girder end

moved away from the abutment wall and vice versa. "MiC" signifies minor cracks in the abutment wall, "MaC" signifies major cracks, and "CJ" means control joints. "Mic," "MaC," or "CJ" plotted on the upper level means that they are at the level of "A1," while when plotted on the lower level means they are at the level of "A2".

From the strain profiles in Figure 4-8 and Figure 4-9, it can be observed that wall face in the vicinity of girder pull-out was subjected to tension, while the region in the vicinity of girder inward motion was subjected to compression (Figure 4-8.) Similar trends can be observed in the backwall (Figure 4-9.) In general, cracks and control joints induced local peak horizontal strains in the abutment wall (Figure 4-8,) which is to be expected. It can be seen from Figure 4-8 that the data are noisy. Reasons include the accuracy of the digital caliper, the errors of measurements taken in a difficult environment, the large gage length used. To help filter this noise, the moving average method was used to interpret the data (Figure 4-10.) Average strain values were calculated at three point intervals. It can be seen from Figure 4-10 that variation trends of horizontal strains are clearer.

4.5.2 Peak strain vs. time and temperature in region around girders

The second approach to explore the field instrumentation data is to divide the instrumented abutment wall into regions around girders. The division of the abutment wall of bridge A1.7 is shown in Figure 4-11 as an example. The regions for the other three bridges were divided in the same manner. The maximum and minimum horizontal strains in each region were plotted together with changes of average temperatures in decks and abutment walls.
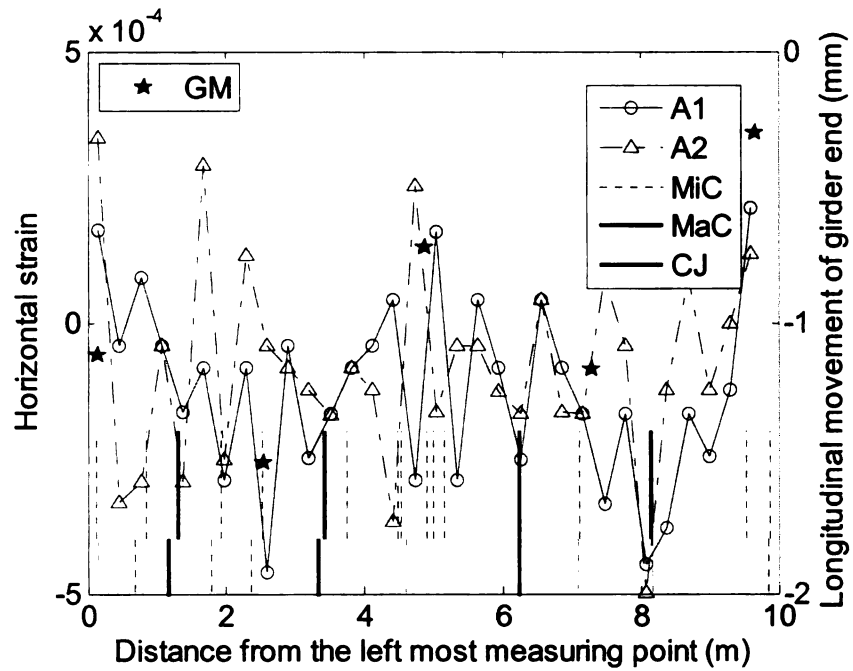
Figure 4-8 Horizontal strains, control joints and cracks on abutment wall of bridge A1.7
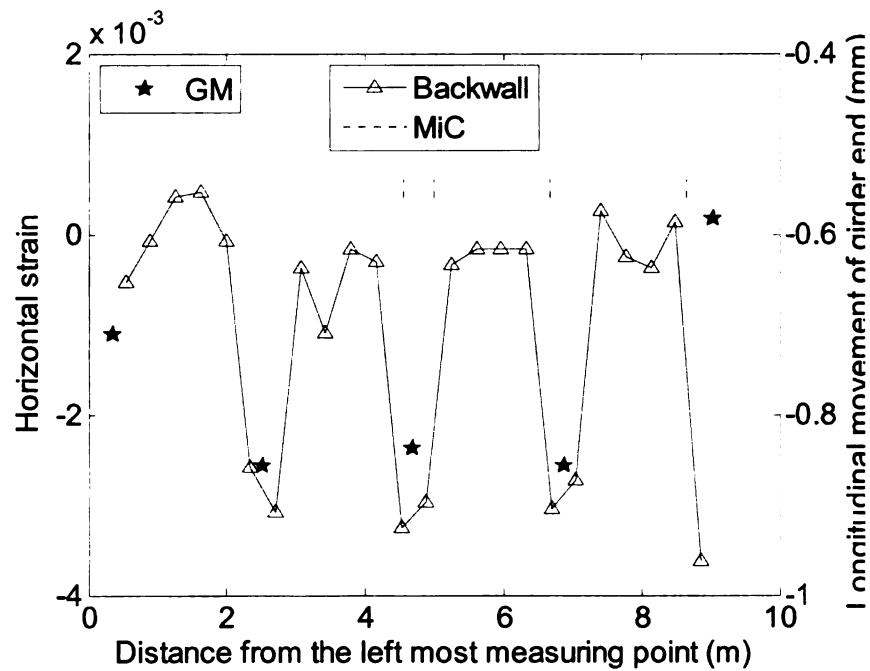
Figure 4-9 Distribution of horizontal strains and cracks on backwall of bridge C2.1
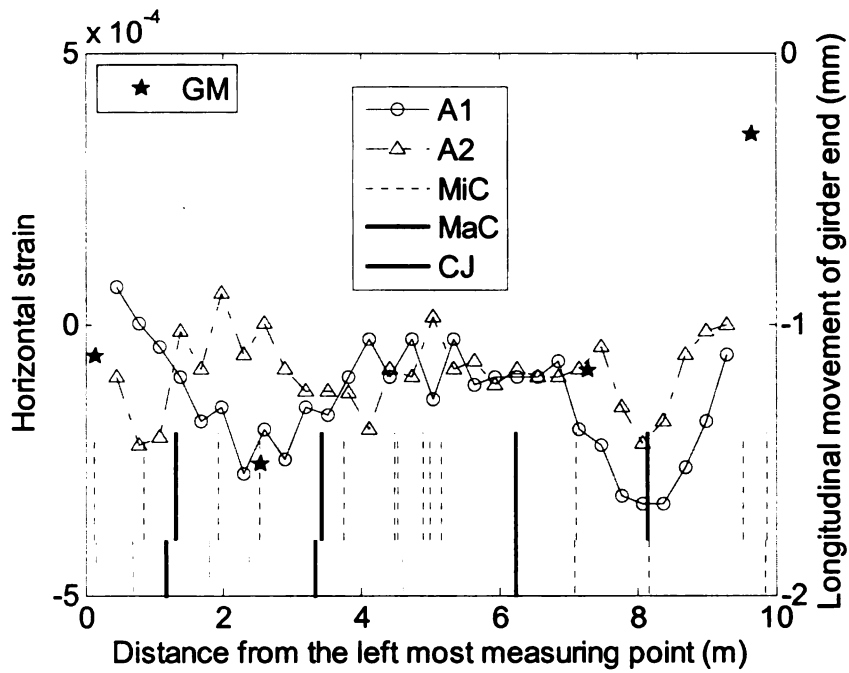
Figure 4-10 Horizontal strains on abutment wall of bridge A1.7 using moving average method

Peak strains in region 2 of bridge A1.7 is shown in Figure 4-12. Peak strains in region 5 of bridge A2.1 is shown in Figure 4-13. In Figure 4-12 and Figure 4-13 "TK" indicates the change of average temperature (°C) in the deck; "TA" means the change of average temperature (°C) in the abutment wall. "Max Str" represents the maximum horizontal strain in the region; similarly; and "Min Str" represents the minimum horizontal strain in the region.
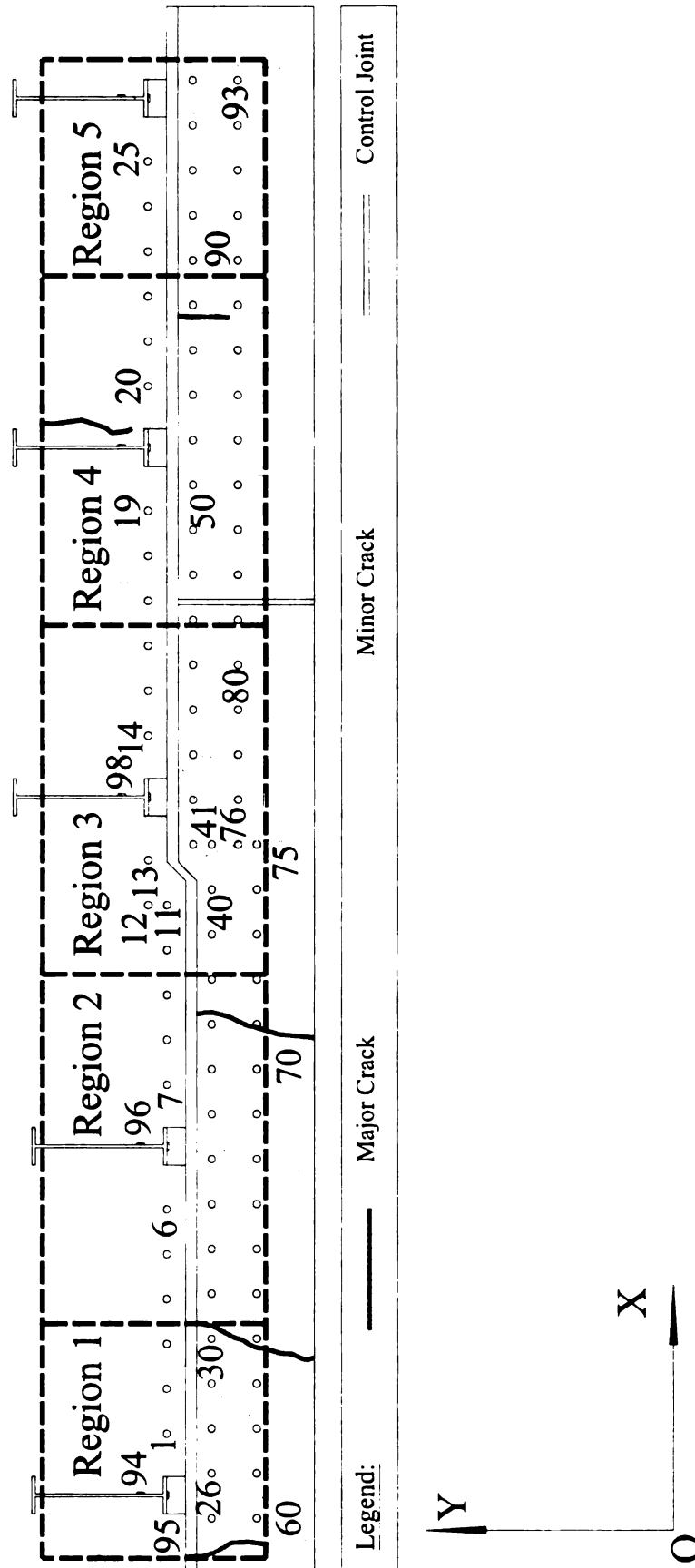
Figure 4-11 Division of measuring points on bridge A1.7 by regions
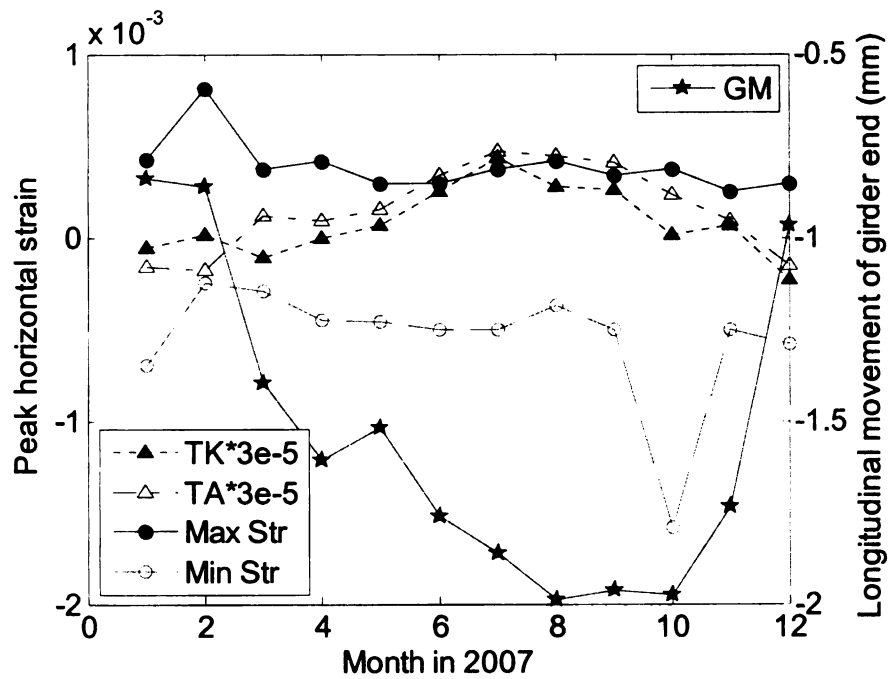
Figure 4-12 Peak strains in region 2 of bridge A1.7
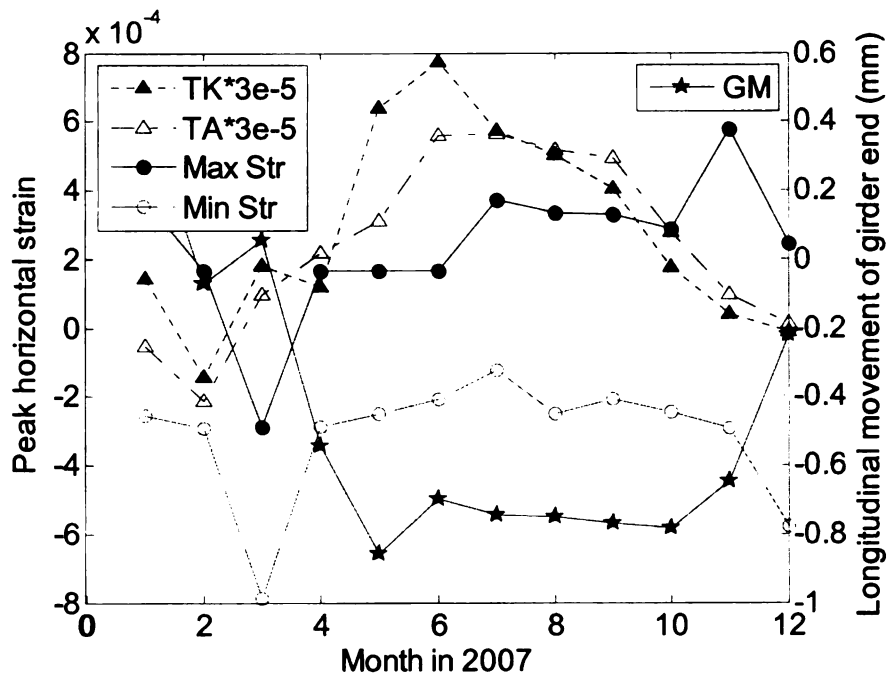
Figure 4-13 Peak strains in region 5 of bridge A2.1

It can be seen from Figure 4-12 that the girder end movement varies in an opposite way to the change of average deck temperature. The trend is reasonable since the expansion of the deck tends to push girders toward the abutment wall and vice versa. This trend only exists for part of the regions, so there must be some other reasons, such as pavement growth, that contribute to the longitudinal movement of girder ends. It can be seen from Figure 4-13 that the maximum and minimum horizontal strains in the region have their biggest change with the longitudinal movement of the girder ends. Only part of the bridges showed this matched pattern between peak strains and longitudinal movements of the girder ends. Some other bridges showed this matched pattern for a few months, and others showed cases in which value changes in these two variables didn't match at all. Longitudinal movements of girder ends can explain part of the strains in the abutment wall. No obvious relationship between temperature and horizontal strains in the abutment wall could be observed.

4.5.3 Peak strain vs. time and temperature in spans between girders

The third approach to explore the field instrumentation data was dividing the instrumented abutment wall into spans between girders. These spans for the abutment wall of bridge A1.7 are shown in Figure 4-14 as an example. The spans for the other three bridges were divided in the same manner. The maximum and minimum horizontal strains in each span were plotted together with the changes of average temperatures in the decks and abutment walls.
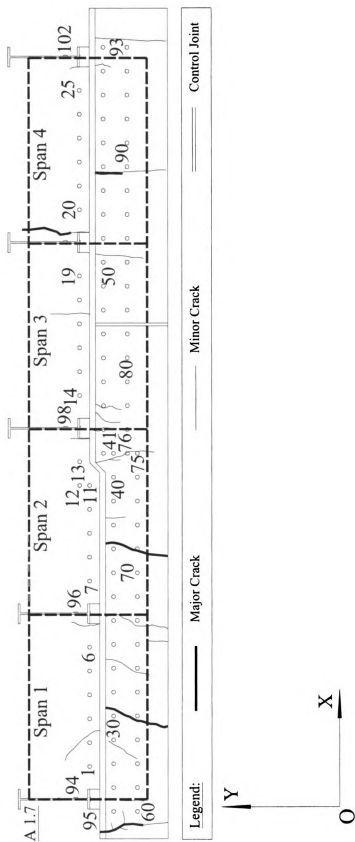
Figure 4-14 Division of measuring points on bridge A1.7 by spans

Legend:

Major Crack   Minor Crack   Control Joint

104

In some spans the variation of peak horizontal strains approximately matched the change of transverse distances between girder ends, as shown in Figure 4-15. "SC" in the figure represents the change of transverse distance between girder ends (unit: millimeter.) In other cases, the match between variation trends was not so good. For a few bridges, the transverse distance between girder ends varied with the change of average temperature in the deck (Figure 4-16). However, contrary to the expectation, this trend was not true for the majority of cases. Thus, no direct association between average temperature variation and peak strain in the spans could be observed.
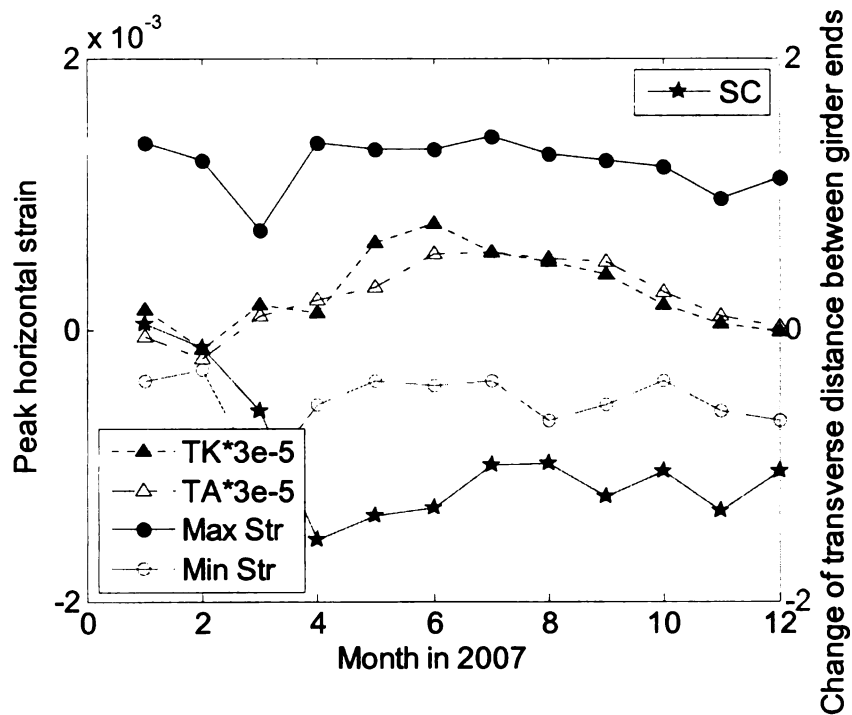
Figure 4-15 Peak strains in span 2 of bridge A2.1
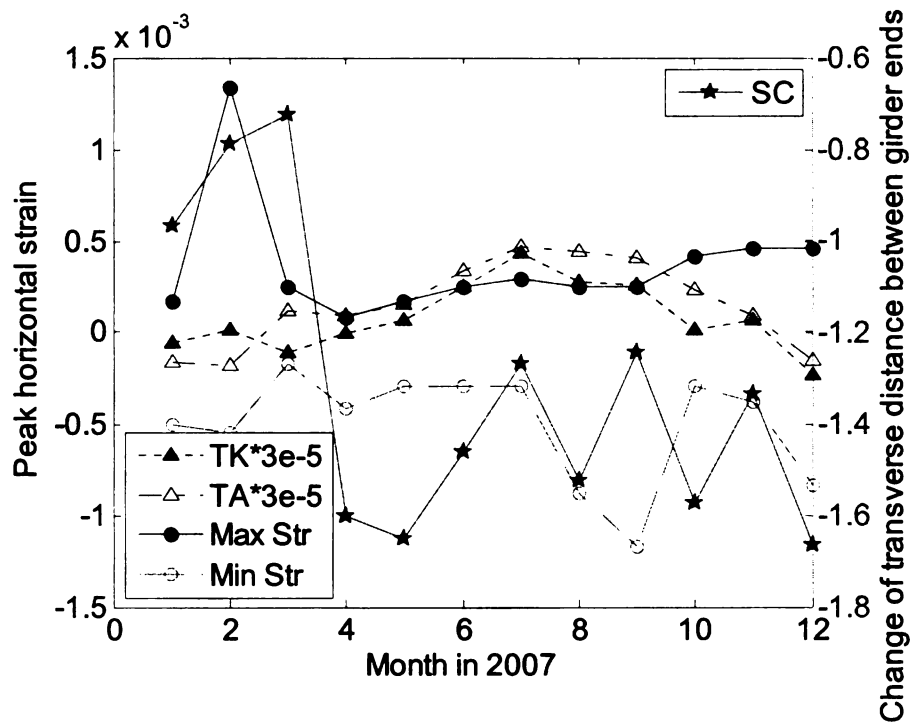
Figure 4-16 Peak strains in span 3 of bridge A1.7

4.6 Evaluation of Potential Damage Causes

4.6.1 Pavement pressure

- Evidence A: comparison of different bridges

The conditions of two abutment walls of bridge B2.1 were found to be different from each other significantly during the field inspections in the summer of 2006. The west abutment was rated as "7" (see Figure 4-17 and [Burgueño and Li 2008].) It can be seen from Figure 4-17 that its approach ended by a "T" intersection nearby (Figure 4-18) and that consequently little pavement pressure can be accumulated. The east abutment was rated as "3 or 4" (see Figure 4-19 and [Burgueño and Li 2008].) Its approach extended to a road (see Figure 4-20) and consequently very large pavement pressure can be generated along the approach of the road.

106

Figure 4-17 West abutment of bridge B2.1
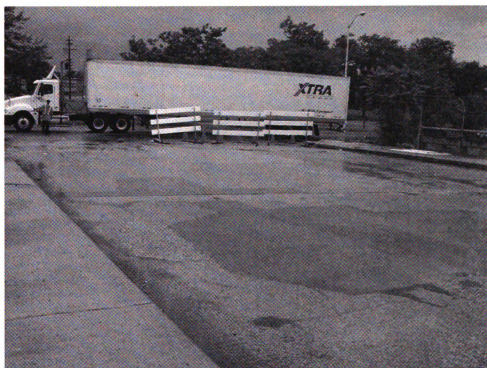
Figure 4-18 West approach pavement of bridge B2.1

Figure 4-19 East abutment of bridge B2.1

Figure 4-20 East approach pavement of bridge B2.1

- Evidence B: investigation of different structural members of the same bridge

Bridge 82182291000S110 had distress in the abutment walls as shown in Figure 4-21. The approach pavement of the bridge was concrete (Figure 4-22.) A large pavement pressure could thus be accumulated. The pin-and-hanger assembly is in good working condition (Figure 4-23) and thus only small forces can be transferred to the abutment wall through longitudinal temperature effects on the bridge superstructure.

Figure 4-21 Abutment distress in bridge A1.7

Figure 4-22 Approach pavement of bridge A1.7
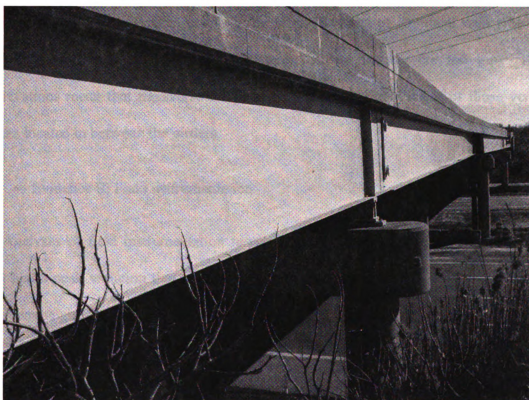
Figure 4-23 Pin-and-hanger assembly of bridge A1.7

- Evidence C: Analyses of field instrumentation

The analyses of field instrumentation results (Section 4.5) indicate that the horizontal strain in the bridge abutment wall is related to the longitudinal movements of the girders. However, temperature effects can only explain these movements for some of bridges. Thus, pavement pressure must be a high contributor to the longitudinal movement of the girders together with temperature effects.

4.6.2 Transverse temperature effect

- Evidence A: In-site observation

Many of the vertical cracks in the abutment walls were consistently located in between the girders (Figure 1-5). Furthermore, it was noticed from the field measurements that the vertical cracks occurred in the parts of abutment wall where no control joint existed or the intervals between control joints were too long. These observations mean that transverse temperature effect is a direct cause of those vertical cracks located in between the girders.

- Evidence B: Field instrumentation

Analyses of field instrumentation results indicated that the strains on the abutment wall had a peak variation that approximately matches the change of transverse distance between the girder ends.

4.6.3 Longitudinal temperature effect

Data from field instrumentation support for longitudinal temperature fields as a source of damage in the following ways:

- The outer face of the abutment wall and backwall in the vicinity of girder pull-out was subjected to tension while that in the vicinity of girder inward movement was subjected to compression.

- For some bridges, regions around girders showed that the girder end movement varied opposite to the change of average deck temperature.

- Maximum and minimum horizontal strains in the region around girders changed with the longitudinal movement of the girder ends for some cases.

4.7 Discussion

Field monitoring in this research focused on revealing the mechanisms behind the development of structural damage. For this example research problem, four MDOT highway bridges were instrumented during a one-year period. Two of them were simple/cantilevered steel bridges; the other two were prestressed concrete bridges. They were selected based on the result of statistical analyses of the NBI manual inspection database in the State of Michigan and the field inspection of forty-four bridges. All of the instrumented bridges had features that were found to be common to bridges with abutment damage. One steel bridge and one concrete bridge had poor abutment, the rest two bridges had good abutments.

Variables measured for each bridge were deformations of the abutment wall and backwall, longitudinal displacements of the girder ends, and temperatures on the bridge deck and abutment wall. Analyses of the collected data can be summarized as follows:

- On the abutment wall and backwall, concrete in the vicinity of girder pull-out was subjected to tension and the concrete in the vicinity of girder inward movement was subjected to compression.

- Cracks and control joints in the abutment wall and backwall induced local peak horizontal strains.

- In some regions around girders, the girder end movement was found to vary opposite to the change of average deck temperature. For the cases where this trend didn't exist, pavement pressure might play an important role in the girder movement.

- Maximum and minimum horizontal strains in the regions around girders changed with the longitudinal movement of girder ends for some cases.

- In some areas between girder spans the peak horizontal strains varied in the same trend with the change of transverse distance between girder ends.

- Some distances between adjacent girder ends varied in the same trend with the change of the average temperature in the deck.

- No direct association between average temperature variation and peak strain in areas between girder spans could be observed.

5 FINITE ELEMENT SIMULATIONS

5.1 Introduction

Field monitoring was very helpful in recording the behavior of structures and understanding mechanisms in the development of structural damage. Due to limitations of funding, human resources, time, traffic conditions, environmental conditions, etc., it was difficult for a field monitoring program to cover a large number of structures and thus create a database that is representative of major structures in the system. Simulation of virtual structures using finite element analysis (FEA) on high performance computer servers is relatively free from these limitations. Nonetheless, finite element simulations also have disadvantages, such as the simplification inherent in the modeling process and that its results are not easily of the same type as what can be measured in the field. Thus, finite element simulation and field monitoring should complement each other to evaluate structural behavior and the mechanisms behind structural damage.

Finite element simulations served three principal purposes in this research: predicting the effects of different assumed damage scenarios, performing parametric analyses to investigate the behavior of structures with different design parameters, and creating a virtual database for soft computing models. In the example problem, bridges of three structural types were simulated: simple/cantilevered steel bridges, continuous steel bridges, and prestressed concrete bridges with I-girders. The finite element program ABAQUS 6.6.1 [ABAQUS 2006] was used in the simulations. The number of models simulated for simple/cantilevered steel bridges, continuous steel bridges, and prestressed concrete bridges were 450, 225, and 108, respectively. This chapter presents the major

steps and representative results of the finite element analyses for the example research problem. More details on the finite element simulation studies can be found in the final research report for MDOT [Burgueño and Li 2008].

5.2 Finite Element Simulation Strategy

Highway bridges are complicated 3-dimensional structures. The effects of damage scenarios, such as temperature field, are also phenomena in 3-dimensional spaces. Thus, three-dimensional finite element models were developed in this research to simulate the behaviors of bridge structures under different damage scenarios. The elements and mesh details used in the FE simulations are summarized in Table 5-1. The material properties used in the FEA models are given in Table 5-2.

The girders are critical members for the finite element models in this research because they directly connect to the bridge abutment wall. All forces from superstructure needed to be transferred to the substructure through the girders. Geometrically, girders could be modeled using 3-dimensional beam elements since its length is much larger than cross-sectional dimensions. In this research, shear lag and cross-sectional deformation of the girders are very important for correct simulation of forces transformed to the abutment wall. However, a 3-dimentional beam element can not simulate these two phenomena. Thus, shell elements were used to simulate the steel girders and solid elements were used to simulate the concrete girders. The abutment walls are members from which the response variables were extracted and thus the foci of the finite element analyses. They were simulated using solid elements to model the bending and shear behavior under different damage scenarios.

Table 5-1 Element details used to simulate the structural members

Structural member	Material	Element type	Average element size (mm)	Geometry (mm)
Slab	Concrete	S4R: 4-node doubly curved thin or thick shell, with reduced integration, hourglass control, and finite membrane strains.	508	229 (thickness)
Girder top flange	Steel	S4R: 4-node doubly curved thin or thick shell, with reduced integration, hourglass control, and finite membrane strains.	127	19 (thickness)
Girder web	Steel	S4R: 4-node doubly curved thin or thick shell, with reduced integration, hourglass control, and finite membrane strains.	127	13 (thickness)
Girder bottom flange	Steel	S4R: 4-node doubly curved thin or thick shell, with reduced integration, hourglass control, and finite membrane strains.	127	22 (thickness)
Backwall	Concrete	S4R: 4-node doubly curved thin or thick shell, with reduced integration, hourglass control, and finite membrane strains.	127	610 (thickness)
Abutment wall	Concrete	C3D8: 8-node linear brick	127	762 (thickness)
Pier cap	Concrete	B31: 2-node linear beam in space	153	1067 (width) 991 (height)
Link plate	steel	Springs: "point to point" spring element	height of web minus 203 mm	229 (width) 13 (thickness)
Prestressed concrete I girder	Prestressed concrete	C3D8: 8-node linear brick	127	Type III or Type IV*

* Refer to prestressed concrete I-beam details in [MDOT 1999].

Table 5-2 Material properties

Material	Modulus of elasticity E (GPa)	Poisson's ratio	Coefficient of thermal expansion (1/°C)
Concrete	24	0.2	11.7×10^{-6}
Prestressed concrete	33.9	0.2	11.7×10^{-6}
Steel	200	0.3	11.7×10^{-6}

5.2.1   Steel bridges

A two-span simple/cantilevered steel bridge was used as an example to describe the models. The geometry of the bridge was the combination of the first values of each of the design variables in Table 5-3. The plan and side views of the bridge are shown in Figure 5-1 and Figure 5-2, respectively.
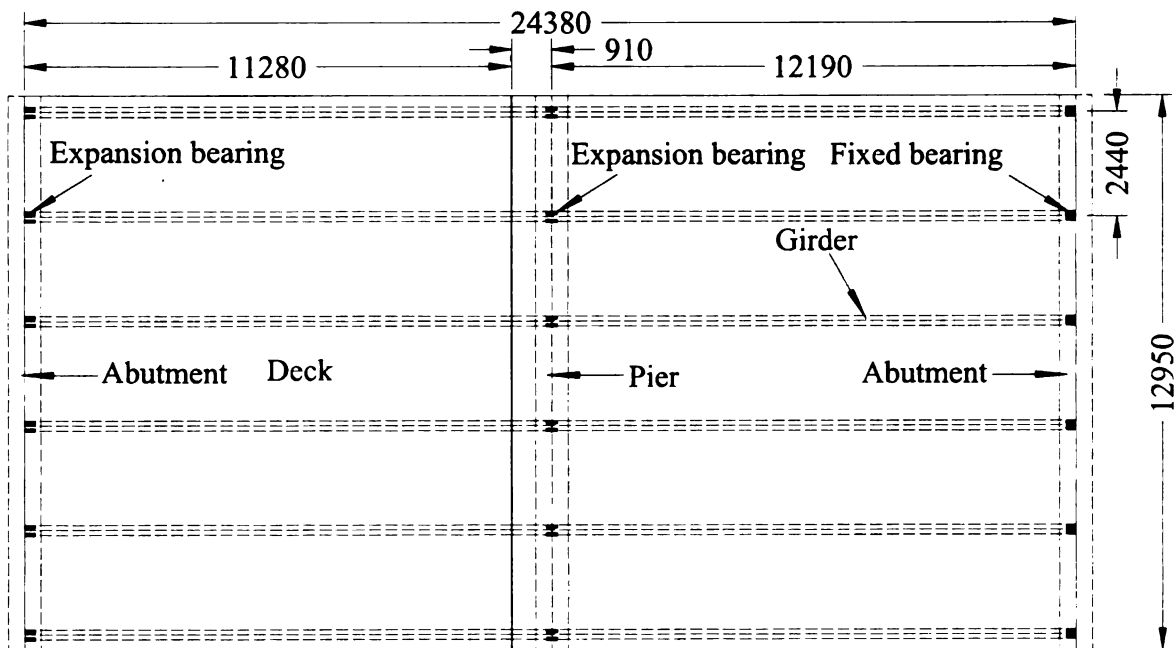
Figure 5-1 Bridge plan (unit: mm)
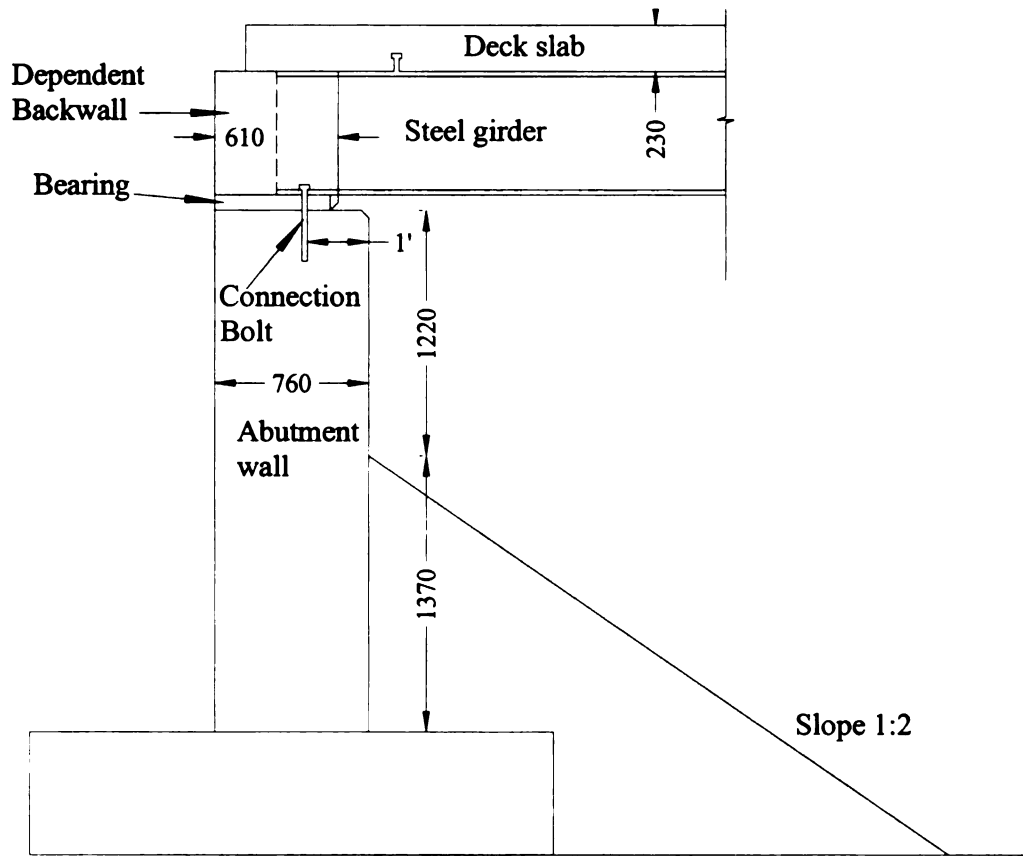
Figure 5-2 Bridge side view (unit: mm)

Three-dimensional finite element (FE) models (see Figure 5-3) were built using the general-purpose finite element program ABAQUS 6.6.1 [ABAQUS 2006] with an attempt to simulate the behavior of different bridges under possible damage-inducing demands. The concrete deck and the backwall were modeled by shell elements, and the cross frames were modeled by beam elements (Figure 5-4). The girders were modeled based on a baseline design provided by the MDOT. For steel bridges, the flanges and webs were modeled using shell elements.
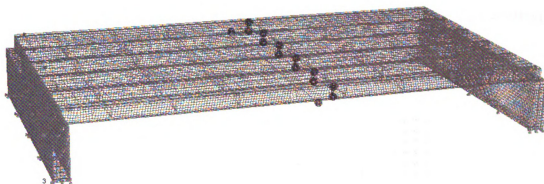
Figure 5-3 Bridge Model
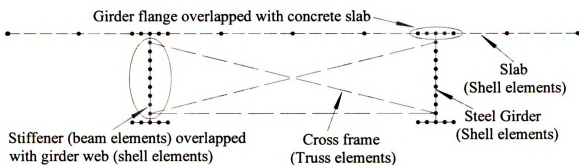
Figure 5-4 Modeling details of one transverse span of bridge

The abutment walls were simulated by eight-node linear solid elements (Figure 5-5). The height of the abutment wall was taken to be 2.6 m. The girders were tied to the backwall by the web end and constrained to the top of the abutment wall by a single point (the center node of the bottom flange). The pin-and-hanger assembly was simulated by a "point to point" spring element (Figure 5-6 and Figure 5-7). The spring element only has stiffness in the direction of the two linked points, so the girders connected by it can move or rotate freely in other directions. The stiffness of the spring element was taken to be the elastic modulus of the steel times cross-sectional area of two link-plates. The cross section of two vertical plates in the cross frame was taken to be 89.2mm × 10.2 mm to

simulate the stiffeners. A standard shape L 4×4×5/16 defined by the Steel Construction

Manual (AISC 2006) was used for other members of the cross frame.

Node of girder connected with abutment wall (Solid elements)

Girder web (Shell elements)

The region from which to extract the maximum horizontal strain along transverse direction

Vertical and longitudinal displacement fixed

Vertical displacement fixed
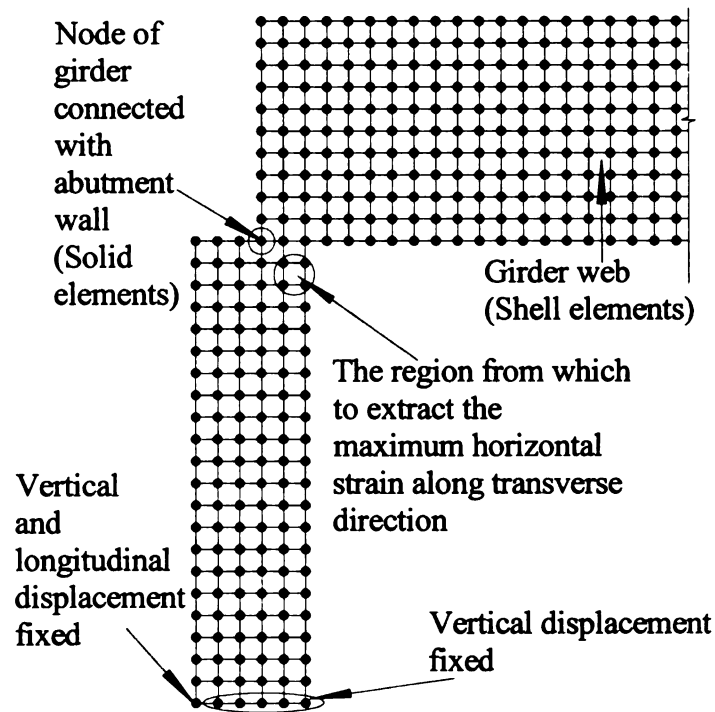
Figure 5-5 Modeling of back wall and abutment wall

Girder flange connected with concrete slab

Girder web (Shell elements)

Pin and Hanger (Spring Connection)
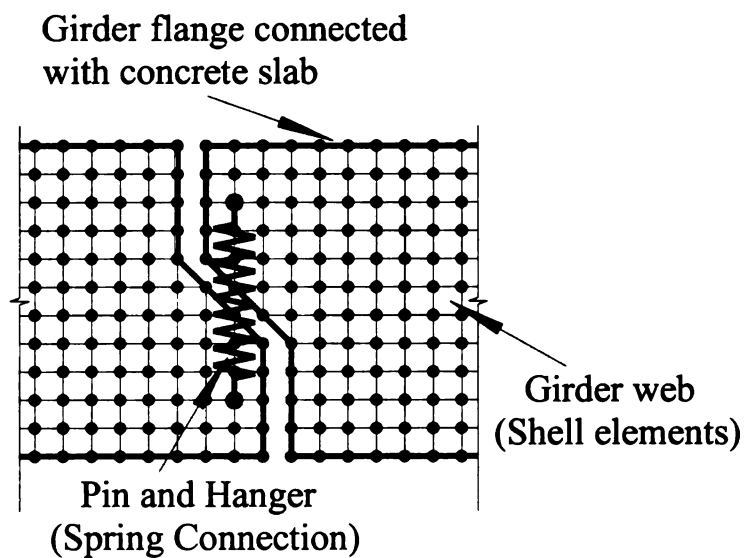
Figure 5-6 Modeling of pin-and-hanger assembly
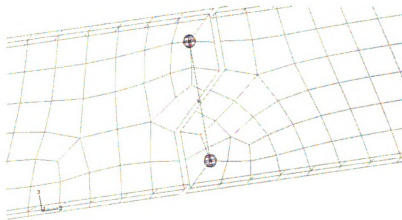
Figure 5-7 Pin-and-hanger detail in model built in ABAQUS

5.2.2   Concrete bridges

The concrete compression strength for the prestressed concrete bridges was assumed to be 48 MPa. The unit weight of concrete was taken as 2355 kg/m^3. The modulus of elasticity for the prestressed concrete I-girder can be estimated by equation (5-1) [AASHTO 2007]. Eight node linear solid elements were used to model the prestressed concrete I-girder. A typical mesh of a prestressed concrete I-girder is shown in Figure 5-8. A prestressed concrete bridge model is shown in Figure 5-9.

$$E_c = 0.043 w_c^{1.5} \sqrt{f_c'} = 33900 MPa = 33.9 GPa \qquad (5\text{-}1)$$
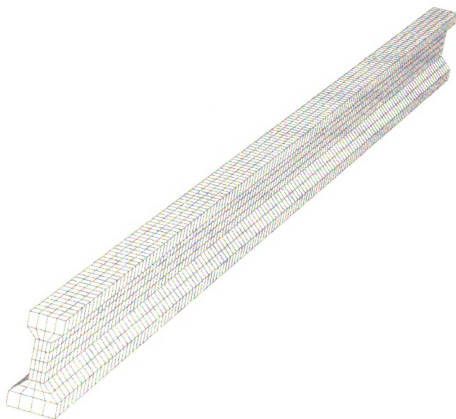
Figure 5-8 Mesh of prestressed concrete I girder
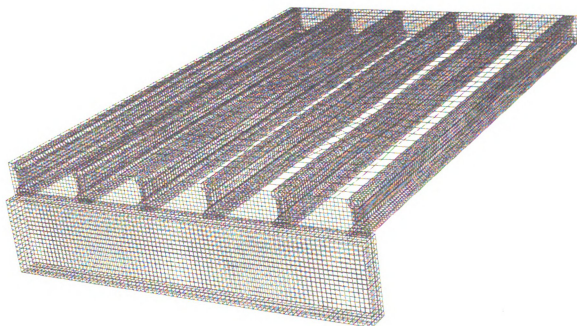
Figure 5-9 Prestressed concrete bridge model

5.2.3 Boundary conditions

The vertical displacements at the bottom of the abutment walls and pier cap were set to be zero. The horizontal boundary condition at the bottom surface of the abutment wall is shown in Figure 5-10. The boundary condition at the pier cap is shown in Figure 5-11.

Bottom surface of the abutment wall $u = 0$

v (longitudinal direction)

$v = 0$

u (transverse direction)
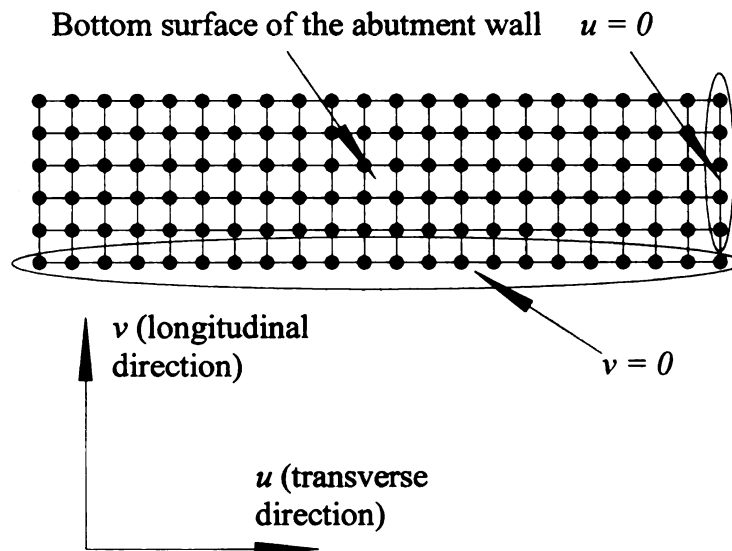
Figure 5-10 Boundary condition at the bottom surface of the abutment wall

v (longitudinal direction)

$u = 0$

u (transverse direction)
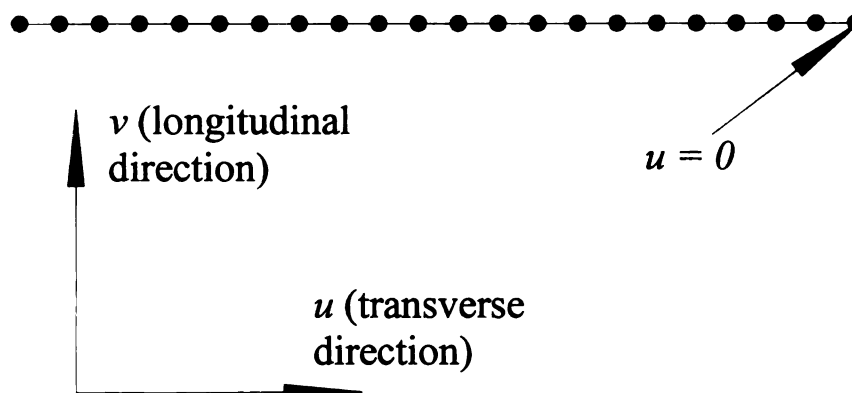
Figure 5-11 Boundary condition at the pier cap

5.3 Case Matrices and Analytical Models

Case matrices for FE simulations were defined for three types of superstructures representative of MDOT highway bridges. The bridge models covered the most frequent range of the primary design parameters. The simulation cases were further refined in the range of the parameters within which the bridges were more susceptible to abutment distress according to the results of statistical analyses.

5.3.1 Simple/cantilevered steel bridge

For simple/cantilevered steel bridges, the simulation cases were the combination of the values in the last column of Table 5-3. Seventy-five structural models were created. The damage scenarios were pavement pressure, summer temperature increase and gradient, and winter temperature drop and gradient. The conditions of a pin-and-hanger assembly in good condition and the rusted (locked) pin-and-hanger assembly were simulated under each damage scenario. Thus, there were six simulations for each geometric bridge model and 450 simulations for this structural type. The analytical diagram for the simple/cantilevered steel bridge model depicting the assumed boundary conditions is shown in Figure 5-12.

5.3.2 Continuous steel bridge

For continuous steel bridges, the simulation cases were the combination of the values in the last column of Table 5-4. The pin-and-hanger assembly were modeled as "new" for pavement pressure and modeled as "rusted" (locked) for the temperature effects. Seventy-five structural models and 225 simulations were done for this structural type. The analytical diagram for continuous steel bridges is shown in Figure 5-13.

124

Table 5-3 FEA case matrix for simple/cantilevered steel bridges

Design parameters	Most frequent interval	Features indicate potential distress	Values taken in the simulation
number of spans	<=4	>=2 and <=4	[2]
Maximum span (m)	>=12.2 and <=36.6	>=24.4 and <=42.7	[12.2, 24.4, 30.5, 36.6, 42.7]
deck width (m)	>=6.1 and <=30.5	>=18.3 and <=24.4	[13.0, 17.9, 22.7]
skew (degree)	<= 60	<= 60	[0, 15, 30, 45, 60]
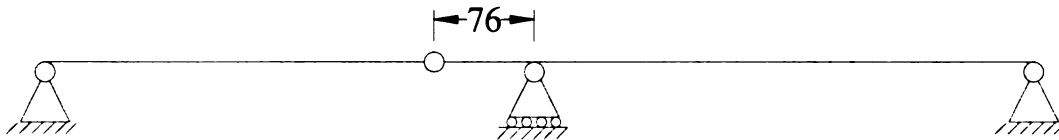
Figure 5-12 Diagram for simple/cantilevered steel bridges with 2 spans (unit: mm)

Table 5-4 FEA case matrix continuous steel bridges

Design parameters	Most frequent interval	Features indicate potential distress	Values taken in the simulation
number of spans	<=4	>=4 and <=7	[4]
maximum span (m)	>=12.2 and <=36.6	>=30.5 and <=54.9	[30.5, 36.6, 42.7, 48.8, 54.9]
deck width (m)	>=6.1 and <=36.6	>=9.1 and <=18.3	[13.0, 15.4, 17.9]
Skew (degree)	<= 60	0	[0, 15, 30, 45, 60]
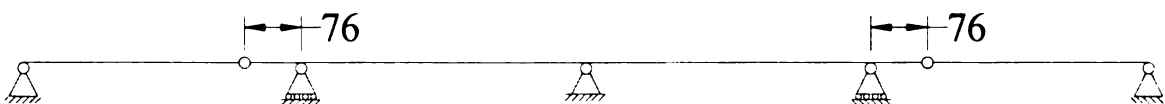
Figure 5-13 Diagram for continuous steel bridges with 4 spans (unit: mm)

5.3.3 Prestressed concrete bridge

All of the prestressed concrete bridges with I-girders inspected in the summer of 2006 were simple supported. Thus, the number of spans in the case matrix was taken to be one, as shown in Table 5-5. The damage scenarios were pavement pressure, summer temperature increase and gradient, and winter temperature drop and gradient. Thirty-six structural models and 108 simulations were done for this structural type.

Table 5-5 FEA case matrix for prestressed concrete bridges

Design parameters	Most frequent interval	Features indicate potential distress	Values taken in the simulation
number of spans	<=4	>=2 and <=4	[1]
Maximum span (m)	>=12.2 and <=36.6	>= 18.3 and <= 30.5	[18.3, 24.4, 30.5]
deck width (m)	>= 6.1 and <= 30.5	>= 18.3 and <=21.3	[13.0, 17.9, 20.3]
skew (degree)	<= 60	>= 0 and <= 45	[0, 15, 30, 45]

5.4 Damage scenarios

After evaluating possible damage scenarios and the feasibility of simulating them through FEA, three scenarios were simulated: pavement growth, temperature field during summer, and temperature field during winter.

5.4.1 Pavement growth

While pavement growth is a physical phenomenon that seems to be well accepted, a quantifiable measure of the pressure generated by pavement growth is an elusive issue. Richards [1979] conducted field testing to determine the stresses in concrete pavements

and instrumented six sites (three of them adjacent to a bridge). A stress level of 7 MPa was observed. Burke [1998, 2004] estimated the pavement pressure to be greater than 7 MPa. Shober [1997] estimated the pavement pressure to be 7-14 MPa. Richards and Burke did their studies in Ohio, while Shober performed his evaluation in Wisconsin. Since both states neighbor Michigan and have similar climatic conditions, it was reasonable to assume that the pavements of Michigan may behave in a similar manner. Thus, their results provide a valuable reference in defining a magnitude for the pressure due to pavement growth. Based on the noted research studies, the pavement growth pressure was set at 7 MPa for these simulations.

5.4.2 Temperature field

Two other damage scenarios simulated in the FEA were temperature fields in the summer and winter seasons. The temperature variation specified in the AASHTO LRFD Bridge Design Specifications [AASHTO 2007] is a piecewise linear temperature profile. Use of this profile in the simulation is too complicated especially considering the large number of models needed to be simulated. After evaluating different simplification approaches, a linear temperature gradient through the bridge deck was found to be a good approximation to the piecewise linear temperature field.

5.4.2.1 Temperature variation

Temperature ranges for bridge design purposes are given in the AASHTO LRFD Bridge Design Specifications [AASHTO 2007]. Data from this source is reproduced in Table 5-6. Here, the temperature range was taken to be -34.4 to 48.9 °C for steel bridges and -17.8 to 37.8 °C for concrete bridges.

Table 5-6 Temperature Ranges (Part of Table 3.12.2.1-1 of AASHTO Specification)

CLIMATE	STEEL OR ALUMINUM (° C)	CONCRETE (° C)
Cold	-34.4 to 48.9	-17.8 to 37.8

The temperature gradient defined by the AASHTO LRFD Bridge Design Specifications [2007] is reproduced in Figure 5-14. In Michigan, T_1, T_2 and T_3 can be taken to be 5.0 °C, -11.7 °C, and -17.8 °C, respectively for concrete pavement surfaces. The value of "A" is taken to be 305 mm.
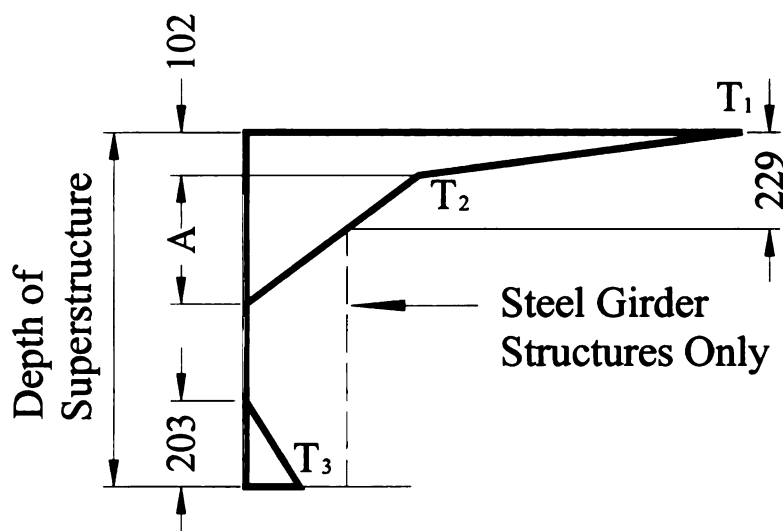
Figure 5-14 Positive vertical temperature gradient in concrete and steel structures (units: mm, Figure 3.12.3-2 of AASHTO Specification)

5.4.2.2 Simplification approach

The temperature distribution in the deck was simplified as linear, and the temperature field in other parts of the bridge was simplified as constant. Thus, the temperature gradient for steel bridges in Figure 5-14 was transformed to the simplified gradient shown in Figure 5-15 by equating the areas under the temperature curves for both figures.

128

Similarly, the temperature gradient for concrete bridges in Figure 5-14 was transformed to the simplified gradient shown in Figure 5-16. The temperature values for the simulations are summarized in Table 5-7.
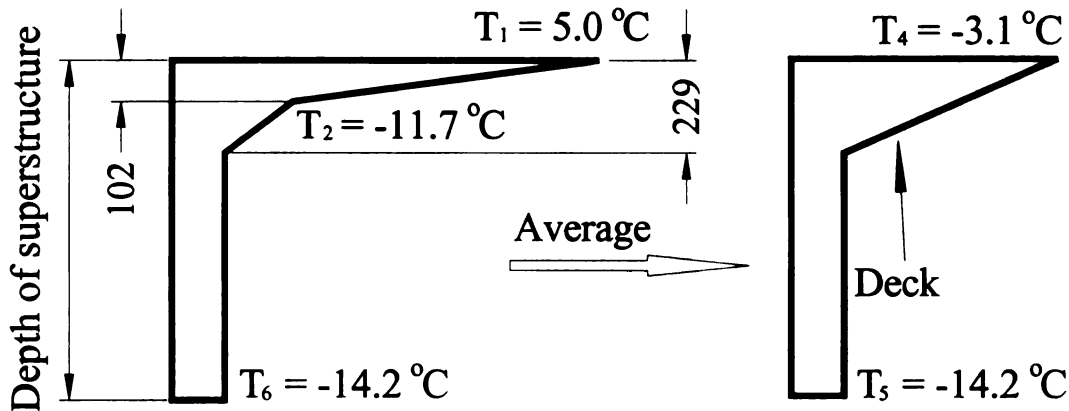
Figure 5-15 Simplification of temperature gradient for steel bridges (unit: mm)
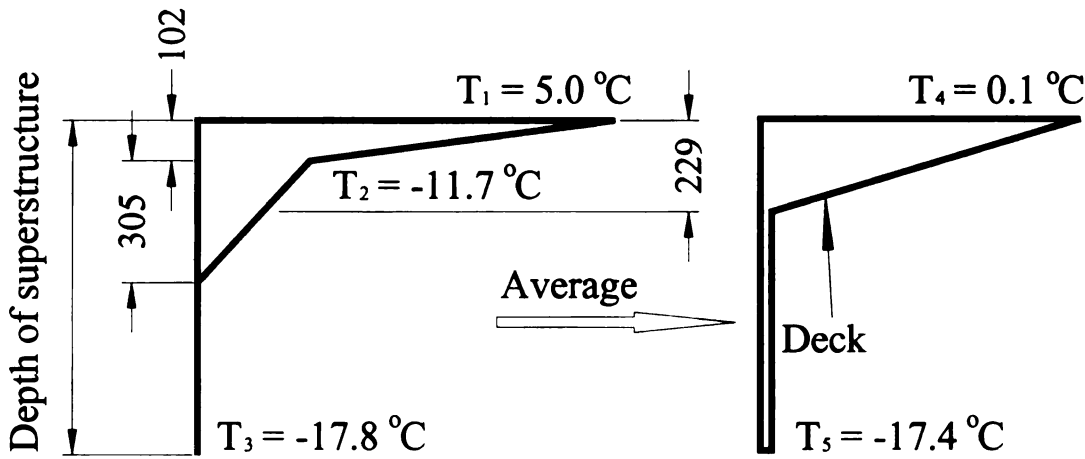
Figure 5-16 Simplification of temperature gradient for concrete bridges (unit: mm)

Table 5-7 Temperature values for linear temperature gradient in the deck

Structures (Members)		Construction (°C)	Winter (°C)	Summer (°C)
Steel Bridge	Top of the deck	15.6	-38.8	63.6
	Other members	15.6	-35.5	52.4
Concrete Bridge	Top of the deck	15.6	-23.2	44.6
	Other members	15.6	-17.9	27.0

5.5 Result Variables

Two responses were extracted from each simulation: the largest value of the maximum principal stress along the top of the abutment wall and the maximum horizontal strain from the elements in the front top corner of the abutment wall (Figure 5-5). Contour images of the principal tensile stresses on the abutment wall are shown in Figure 5-17. The location of the extracted maximum principal stress is the point where the girder is connected to the abutment wall (Figure 5-5). At this location, the model results are mesh sensitive. Thus, the maximum horizontal strain from the elements in the front top corner of the abutment wall was also extracted (Figure 5-5).

5.6 Result Interpretation and Parametric Analyses

Results from the FE simulations were plotted using skew angle as abscissa and result variables as ordinate. Most of the maximum principal stresses exceeded the tensile strength of the concrete by a large margin because the analyses assumed a linear elastic response. Extreme assumptions in the modeling process also contributed to the large stress values. For example, the pin-and-hanger assembly could still allow some

130

movement even though they were rusted, and the abutment wall could have slightly displacement and rotation. Also, the simulated damage-causing loads are conservatively high. Thus, interpretation focused on the variation trends of the resultant variables to the change of design parameters and damage scenarios.

(a) Top view of the abutment wall   (b) Amplified view
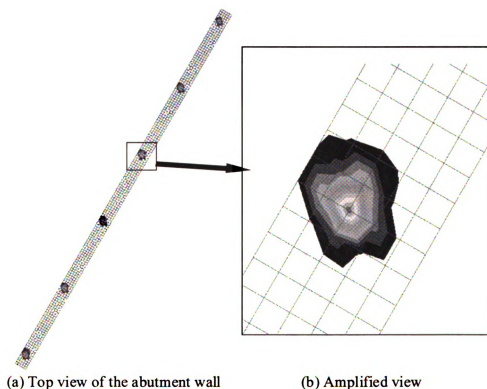
Figure 5-17 Principal tensile stresses in the abutment wall

5.6.1   Simple/cantilevered steel bridges

Figure 5-18 shows the distribution of maximum principal strain in a simple/cantilevered steel bridge model. The corresponding damage load is pavement pressure applied at the cross section of the deck on the left side of the bridge. It can be seen that the principal strains in the girders are largest at the region around the connection

points to the abutment wall (on the left). This indicates large forces transmitted to the abutment wall through bridge girder and connection bolts.
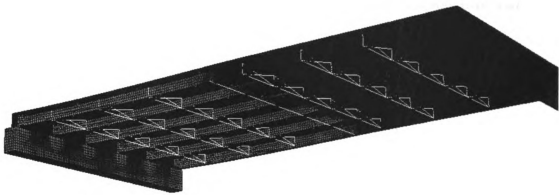
Figure 5-18 Maximum principal strain in a simple/cantilevered steel bridge model

Figure 5-19 shows the distribution of maximum principal strains on the face of the abutment wall. As expected, the positions of peak values are the connection points between the girder and the abutment wall. Comparing with Figure 1-4, the shape of strain contours are very similar to the shape of concrete spalling in the bridge abutment wall. The distribution of horizontal strain at a level 0.305 m bellow the top of bridge abutment wall is shown in Figure 5-20. The abscissa is the distance from left end of the abutment wall in meters; the ordinate is the horizontal strain. It can be observed that the horizontal strain reaches peak values at the positions where the girders connected with the abutment wall. This is to be expected as these are the locations of force transfer between these two elements.

Figure 5-19 Maximum principal strain on the surface of the abutment wall
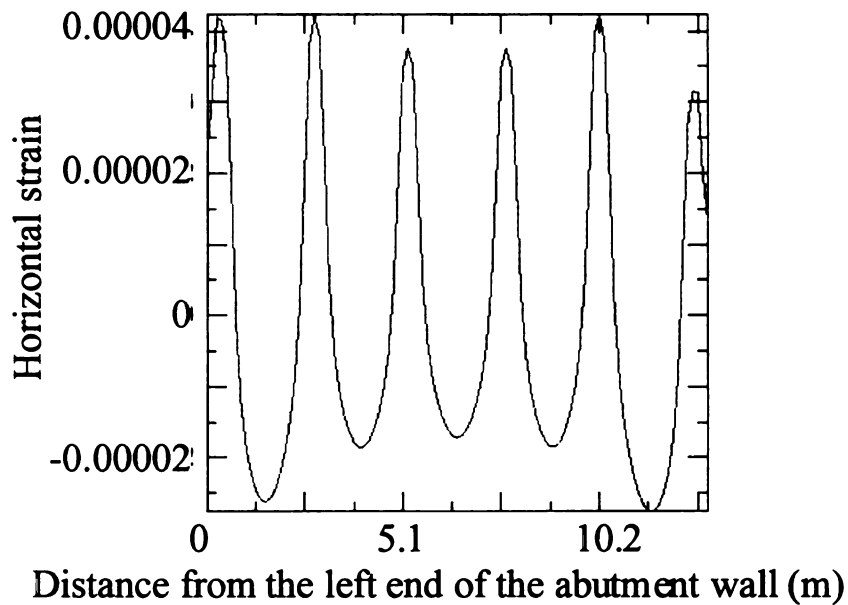
Figure 5-20 Horizontal strain at a level 0.305 m below the top of the abutment wall

For bridges subjected to pavement pressure, as shown in Figure 5-21, the maximum stress increases significantly with the increase of the skew angle. The maximum horizontal strain does not change much when the skew angle is between 0 and 30 degrees and increases significantly when the skew angle is larger than 30 degrees (Figure 5-22.)
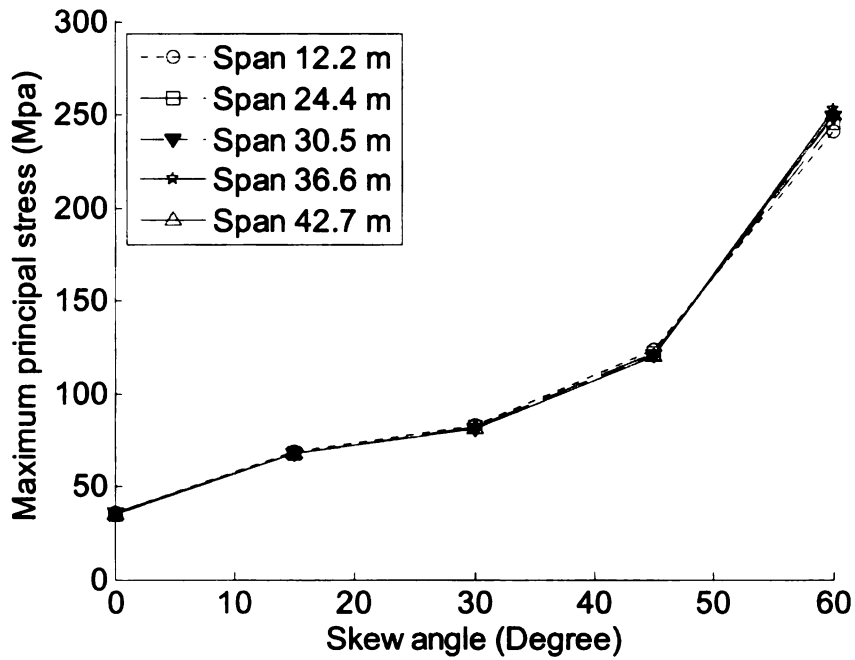
Figure 5-21 Maximum stress of bridges under pavement pressure (with free moving pin-and-hanger assembly, width = 17.8 m)
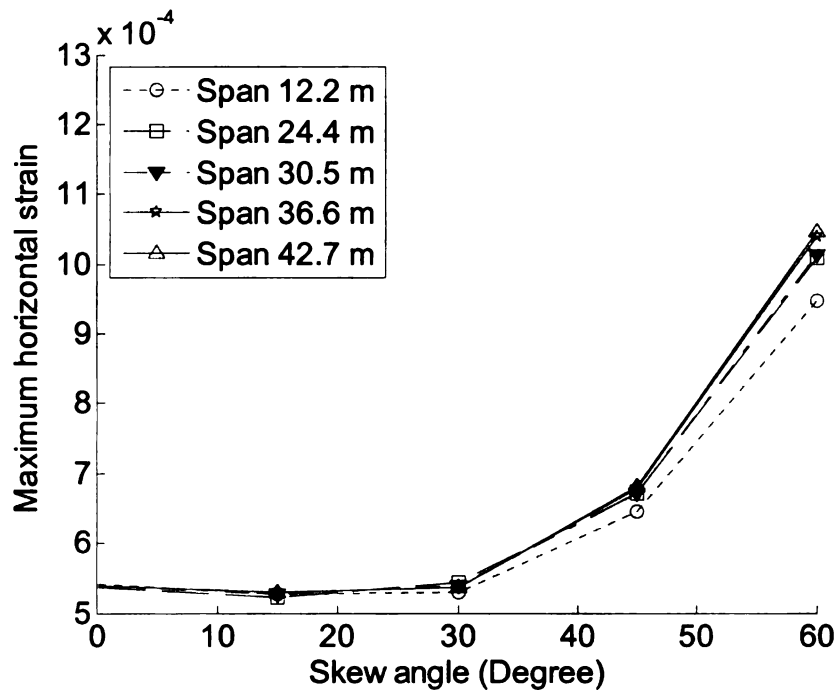
Figure 5-22 Maximum horizontal strain for bridges under pavement pressure (with free moving pin-and-hanger assembly, width = 17.8 m)

Bridges analyzed in Figure 5-21 and Figure 5-22 have free moving pin-and-hanger assembly. For comparison, analyses of same bridges with locked pin-and-hanger assembly are shown in Figure 5-23 and Figure 5-24. It can be observed that bridges with locked pin-and-hanger assembly have less demand on the abutment walls. For these bridges, a portion of pavement pressure can be transferred to girders in the adjacent span through locked pin-and-hanger. Thus, the locking of pin-and-hanger assemblies due to corrosion may actually alleviate the maximum demands on the wall. Span length and width of the bridge didn't have a significant effect on the maximum wall demands.
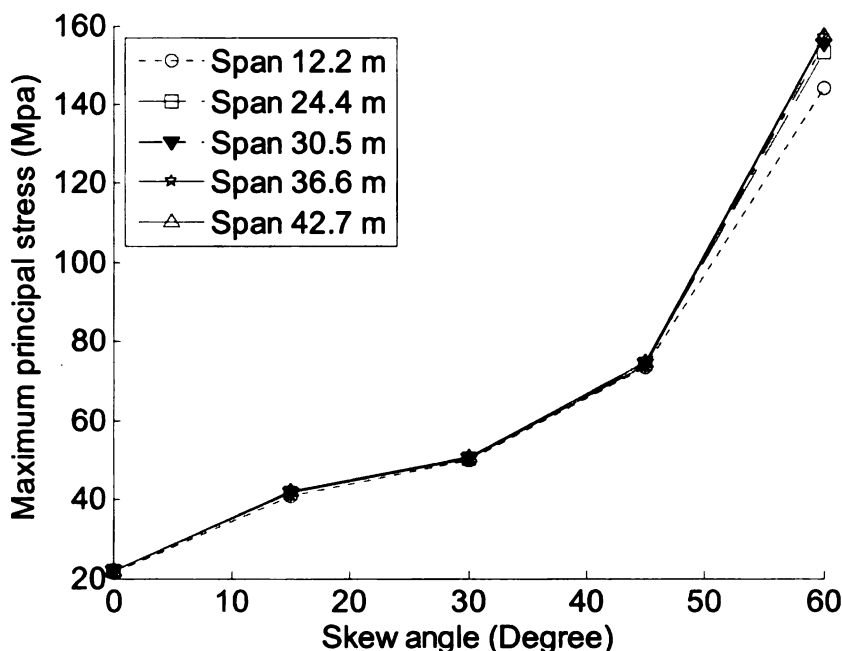
Figure 5-23 Maximum stress of bridges under pavement pressure (with locked pin-and-hanger assembly, width = 17.8 m)

For demands due to summer temperatures, the locking of pin-and-hanger assembly has a significant effect on the maximum stresses on the abutment wall, as shown in Figure 5-25 and Figure 5-26. The maximum stresses in the abutment wall for bridges with a locked pin-and-hanger were much larger than when the assembly is working

properly. When the pin-and-hanger is locked, both skew angle and span length have a significant influence on the maximum stress. Longer bridges and bridges with larger skew angles are subjected to larger stresses. The maximum horizontal strain demands follow similar trends. Horizontal strains increased with an increase of skew angle and span length. They also increased slightly with the increase of bridge width. Finally, result show that a locked of pin-and-hanger only increases the maximum horizontal strain by a moderate amount. Comparison of Figure 5-25 and Figure 5-26 also proved that when pin-and-hanger assemblies are locked, the temperature effects could be a significant contributor to the damage in the abutment wall.
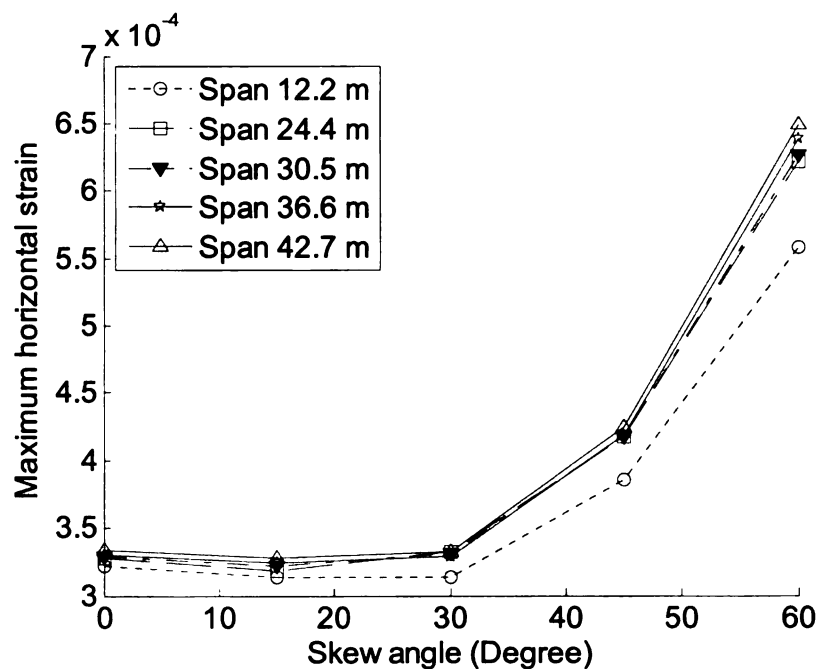
Figure 5-24 Maximum horizontal strain for bridges under pavement pressure (with locked pin-and-hanger assembly, width = 17.8 m)
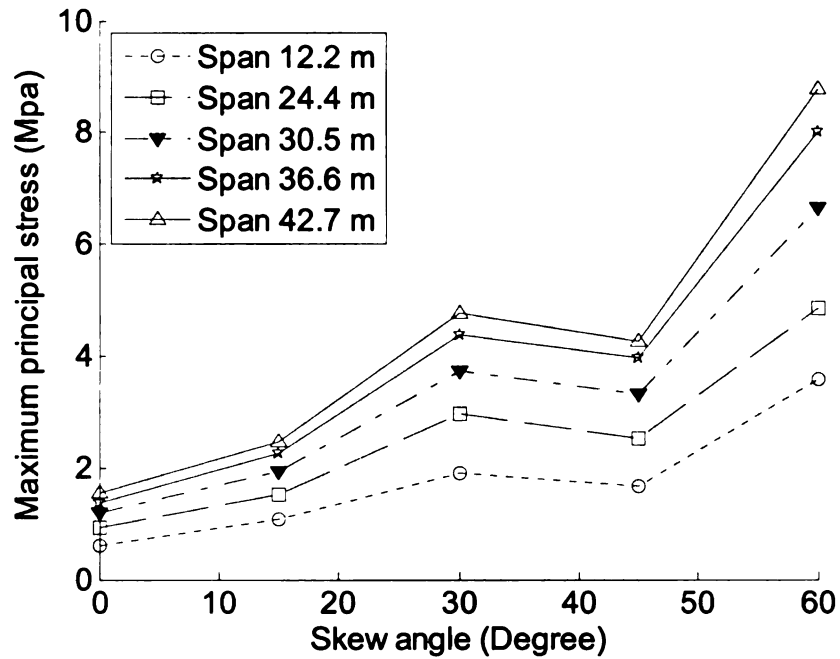
Figure 5-25 Maximum stress of bridges in summer (with free moving pin-and-hanger, width = 22.7 m)
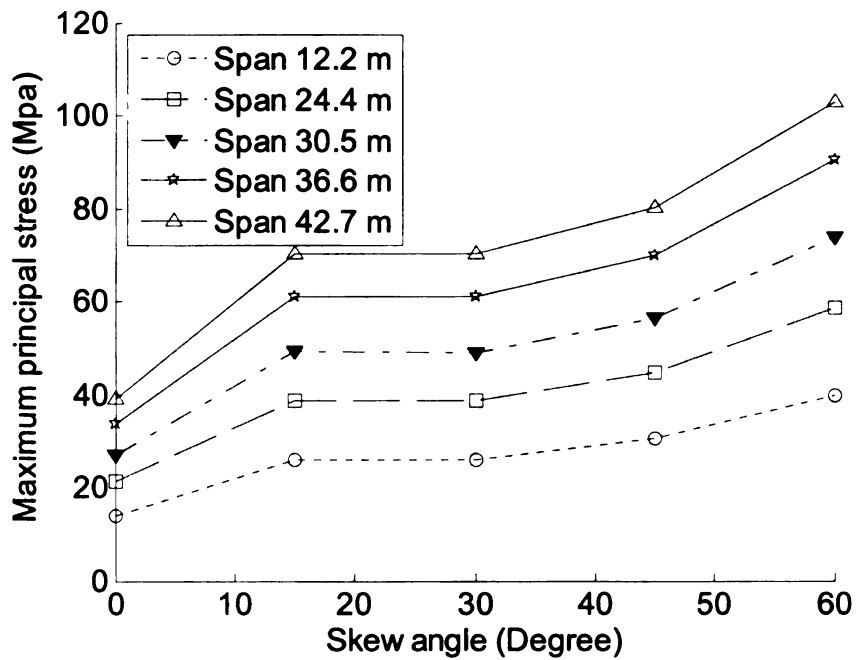
Figure 5-26 Maximum stress of bridges in summer (with locked pin-and-hanger, width = 22.7 m)

For bridges subjected to winter temperature variations, the trends of maximum stresses developed in the abutment wall are similar to those in summer, except that the values are negative. As shown in Figure 5-27 and Figure 5-28, when pin-and-hangers are in proper working condition, the influence of design parameters to maximum horizontal strains is trivial. When the pin-and-hangers are locked, bridges with longer spans tend to have less horizontal compressive strain in the abutment wall.
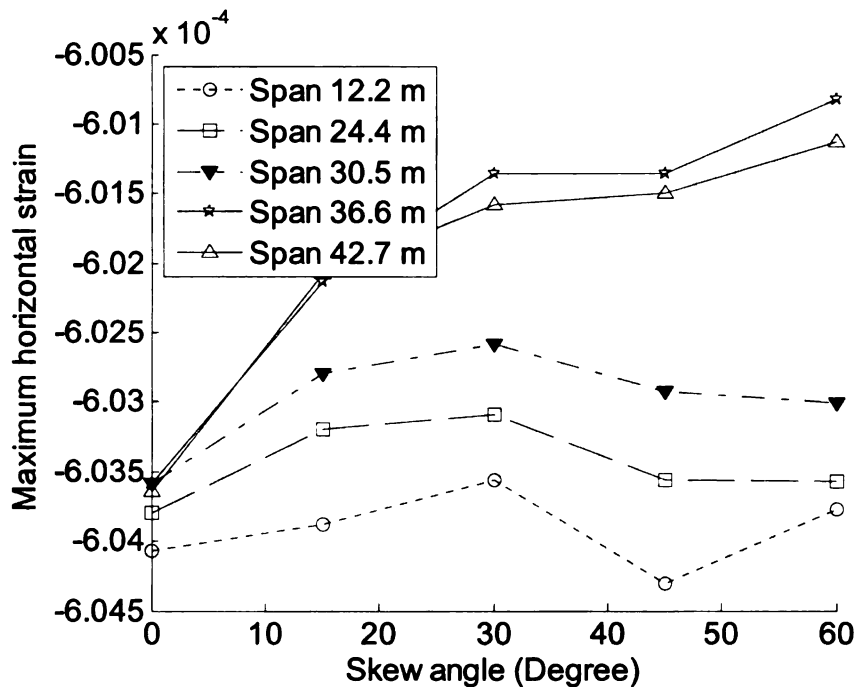
Figure 5-27 Maximum horizontal strain of bridges in winter (with free moving pin-and-hanger, with = 22.7 m)
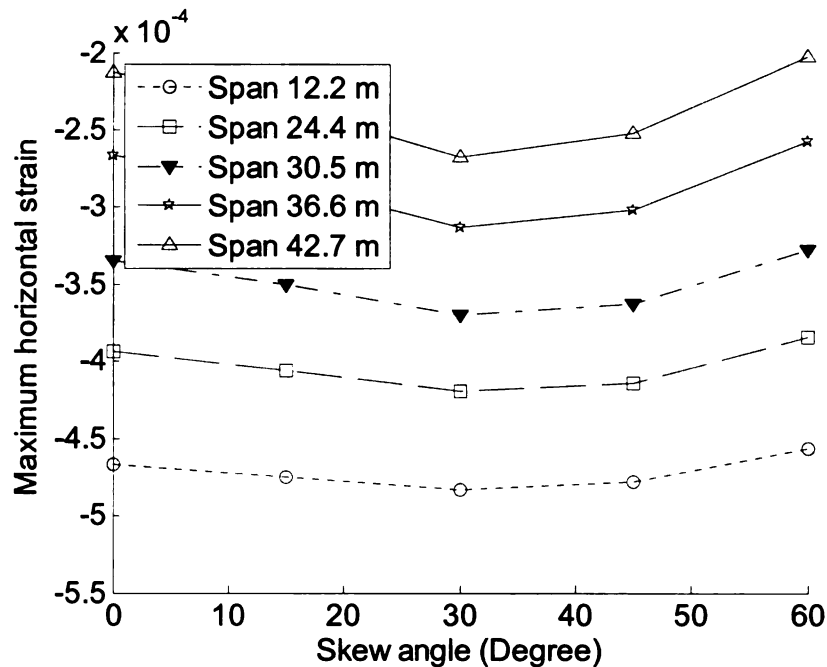
Figure 5-28 Maximum horizontal strain of bridges in winter (with locked pin-and-hanger, width = 22.7 m)

Comparing the effects of the three damage scenarios, the stresses generated by the pavement pressure were larger than those generated by the winter temperature field and the summer temperature field in that order. As mentioned at the beginning of Section 5.6, the absolute value of the resulting variables deviate from reality by a large margin due to the assumption of linear elastic response. Thus, the observation on the relative magnitudes of response caused by different damage scenarios should only be used as a reference.

5.6.2   Continuous steel bridges

The results of the finite element simulation for continuous steel bridges are summarized in this section. Plots and more details can be found in the final report to the research sponsor, MDOT [Burgueño and Li 2008].

For bridges with good pin-and-hanger assemblies subjected to pavement pressure, stresses in the abutment wall increased significantly with an increase of the skew angle. They also increased slightly with the increase of the deck width. The effect of span length on the abutment wall demand was trivial. For bridges under summer temperature load with locked pin-and-hanger, maximum abutment stresses increased with skew angle. The bridge width had trivial influence on the abutment wall demands. Generally, demands on the abutment wall increased with span length. For bridges under winter temperature loading with locked pin-and-hanger assemblies, variation trends for maximum demands were similar to those under summer temperature loads, although the magnitude of the horizontal strain was much smaller.

Comparing the effects of three damage scenarios, the maximum stresses generated by the pavement pressure were larger than those generated by summer and winter temperature effects. As mentioned before, these comparisons of magnitudes of response variables can only serve as a reference.

5.6.3 Prestressed concrete bridges

The results of the finite element simulation for prestressed concrete bridges are summarized in this section. Plots and more details can be found in the final report to the research sponsor, MDOT [Burgueño and Li 2008].

For bridges under pavement pressure, maximum stress in the abutment wall increased with skew angle. When the skew angle was less than 30°, the effect of skew on the maximum horizontal strain was trivial. When the skew angle was larger than 30°, the maximum horizontal strain increased significantly with the increase of skew angle. The

effects of span length and bridge width on the demands in the abutment walls were trivial. For bridges under summer temperature fields, the maximum principal stress and maximum horizontal strains increased with an increase in skew angle when up to a value of 30 degrees. In general, demands on the abutment wall increased slightly with the increase of span length. The effect of bridge width was trivial. The variation trends of abutment wall demands due to winter temperature loads were similar to those due to summer temperatures.

Since the bearing condition on one side of the bridge was pin connected and the other side allowing horizontal movement, the demands induced by pavement growth were much larger than those induced by temperature effects.

5.7 Discussion

The behaviors of highway bridges with three different structural types were simulated using finite element analyses. The structural types were: simple/cantilevered steel bridges, continuous steel bridges, and prestressed concrete bridges with I-girders. Each of these bridge systems was evaluated under three damage scenarios: pavement growth, summer temperature field, and winter temperature field. Four hundred and fifty simple/cantilevered steel bridges, 225 continuous steel bridges, and 108 prestressed concrete bridges were analyzed. A virtual database was created using these FE simulations and will be further exploited in the development of prediction models for structural damage in Section 7.5. It was observed through the FE simulations that:

- Stress demands in the abutment wall increased with an increase of skew angle. This pattern is more pronounced when the skew angle is larger than 30 degrees.

- For bridges under pavement pressure, the effect of span length is trivial. When considering summer or winter temperature fields, the effect of span length is moderate.

- Generally, the effect of bridge width to the stress demands in the abutment wall is trivial.

6 SOFT COMPUTING

6.1 Introduction

The discussion in Chapter 1 presented how the mechanism behind the development of structural damage is highly complicated. The deficiencies in an SISD make the work in developing damage prediction models even more difficult. In order to overcome the complexity and difficulties in the problem, soft computing was used as the main approach to develop predictive tools for the current research problem.

Soft computing is a collection of methodologies that permits the creation of prediction models by learning from data and mimicking human intelligence [Kecman 2001]. In comparison with hard computing (which is based on precise, definite, and rigorous data,) soft computing utilizes a tolerance for imprecise, uncertain, incomplete, and subjective data. The three principal types of soft computing are: neural networks, fuzzy logic and probabilistic reasoning [Zadeh 1994, Mathworks 2007b].

An artificial neural network is a network composed of one or more layers of computing units connected by synaptic weights. It can "learn" knowledge from the environment (data) and store the learned knowledge in synaptic weights for future use, such as a prediction [Aleksander and Morton 1990]. An ANN has a high capacity for nonlinear input-output mapping and is robust to faulty, incomplete or imprecise data. The application of four types of neural networks: multilayer perceptrons (MLP), radial basis function (RBF), support vector machine (SVM), and supervised self-organizing map (SSOM) were evaluated for the problem in this research. Considering the subjectivity in manual inspections, a fuzzy neural network (FNN) was developed to combine the

advantages of fuzzy logic and artificial neural networks and overcome the difficulties in the SISD.

6.2   Multilayer Perceptron Network

A multilayer perceptron (MLP) model is a network composed of several layers of neurons. Each neuron is a computation unit, which, given an input value, calculates an output value through an activation function. The multilayer perceptron model is then composed of neurons assumed to be organized in layers, each consisting of one or more neurons. An input vector enters the MLP through an input layer, which is followed by one or several hidden layers. The computation result is given through an output layer. The output of the previous layer contributes to the input of the next layer after being modified by synaptic weights. A typical structure of an MLP ANN is shown in Figure 6-1.

The data set for developing an MLP model can be divided into two subsets: training data and test data. Training data are used in training of an MLP. Test data are used in evaluating the performance of the MLP. The relationship between input variables and output variables is stored in synaptic weights after training, such that a trained network can predict the output values from novel inputs. The training process consists of a series of iterations (epochs.) In each epoch, input vectors enter the MLP through input layer and information flows to the output layer in a forward manner. Then, synaptic weights are updated using a back propagation algorithm, which minimizes the sum of the squares of the error computed at the output layer (comparing the computed output to actual known data). Thus, the back propagation algorithm seeks global optimization of the network

[Haykin, 1999]. After the training process, an MLP can predict the output values given novel input vectors, which is called a generalization process.

If designed for the prediction of damage in bridge abutments, as shown in Figure 6-1, the input layer with p neurons would input p bridge design and service parameters and the output layer would have k neurons to represent k condition levels of the bridge abutment. Two hidden layers are shown in the model schematic of Figure 6-1.
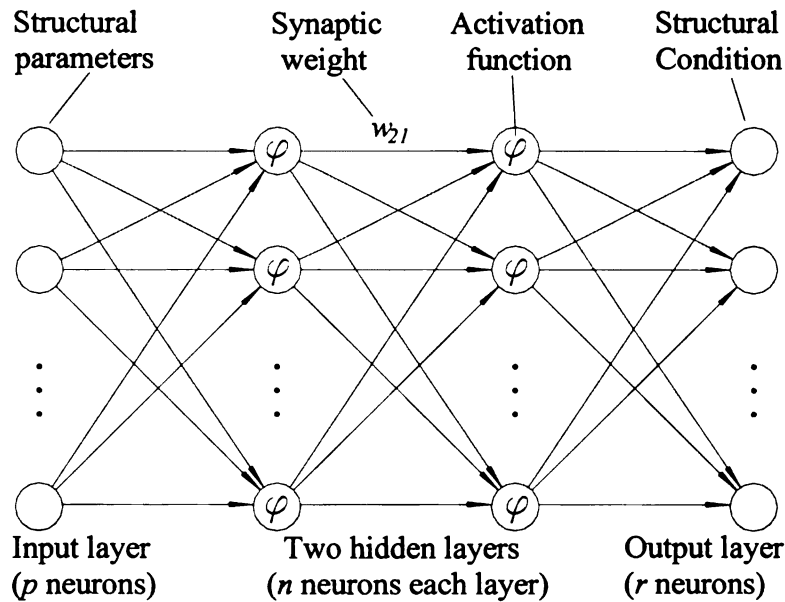
Figure 6-1 Diagram of MLP

A commonly used nonlinear activation function for individual neuron is the sigmoid function, as shown in equation (6-1) and Figure 6-2:

$$v_o(n) = \varphi(v_i(n)) = \frac{1}{1 + e^{-av_i(n)}}$$

(6-1)

where $v_o(n)$ is the output value of a neuron in nth training iteration; $v_i(n)$ is the input value of a neuron in nth training iteration; and a is a constant that modifies the shape of the sigmoid curve. The value of $v_i(n)$ can be calculated using equation (6-2):

$$v_i(n) = \sum_{j=1}^{m} w_{ij} x_j + b_i \qquad (6\text{-}2)$$

where m is the number of neurons in the previous layer, w_{i1}, w_{i2}, ... , w_{im} are synaptic weights connect the neuron with neurons in previous layers, x_1, x_2, ..., x_m are inputs applied to the neuron (which are outputs of the neurons in the previous layer,) and b_i is a bias applied to the neuron.
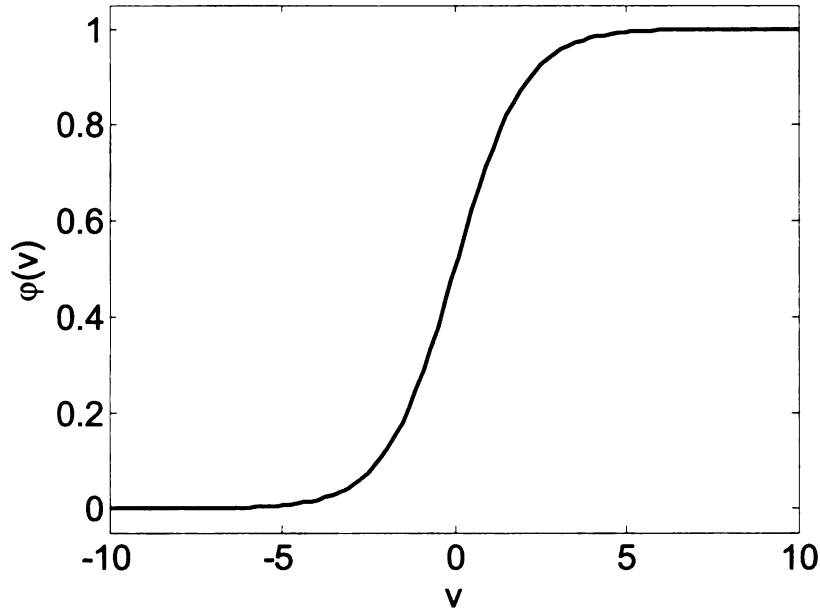
Figure 6-2 Sigmoid activation function ($a = 1$)

The error at the ith output neuron, $e_i(n)$, after the nth iteration is calculated using equation (6-3):

$$e_i(n) = d_i - y_i(n) \qquad \qquad (6\text{-}3)$$

where d_i is the target value for the neuron and $y_i(n)$ is the output of the neuron after nth iteration. The sums of squares of the error at the output layer after the nth iteration can be calculated using equation (6-4):

$$\varepsilon(n) = \frac{1}{2}\sum_{i=1}^{r} e_i^2(n) \qquad \qquad (6\text{-}4)$$

After the nth iteration, the weights of a network are adjusted in a back propagation process according to equation (6-5); where $w_{ij}(n)$ and $w_{ij}(n+1)$ are the jth weights in the ith layer in the nth and $(n+1)$th iterations, respectively; and η is the learning rate of the network [Ramuhalli 2005].

$$w_{ij}(n+1) = w_{ij}(n) - \eta \frac{\partial \varepsilon(n)}{\partial w_{ij}(n)} \qquad \qquad (6\text{-}5)$$

Several factors are important for good generalization of an MLP network:

- Architecture of the network, such as the number of hidden layers (n_l), and the number of neurons in each hidden layer (n).

- Selection of input variables and preprocessing of the input data.

- Network parameters. A set of important MLP parameters are listed in Table 6-1.

- Danger of overfitting, which refers to a phenomenon that the MLP learns too much from the training data and memorizes them. When this happens, the MLP

extracts the specific feature (which might be noises) of the training data instead

of the underlying input-output relationship of the problem.

Table 6-1 Parameters of MLP

Parameter	Description
Activation function of neurons (φ)	A function through which the input value to a neuron is transferred to a output value.
Learning rate (η)	Changing rate of synaptic weights and biases during the back propagation process in the training of an MLP.
Number of epochs in training (n_e)	Number of calculation cycles including presenting the training vector to the network in a feed forward manner and calculating the new weights and biases in a back propagation process.
Mean square error (mse)	Average squared error between the network outputs and the target outputs at the output layer of a neural network.

It has been proved that an MLP network with one hidden layer and any continuous

sigmoidal nonlinear activation function for hidden nodes can approximate arbitrary

decision regions [Cybenko 1989, Hornik et al. 1989, 1990, White 1990]. Theoretically,

only MLP networks with one hidden layer need to be used. However, it might be difficult

to obtain the optimal scenario for the MLP with one hidden layer to approximate the

complicated nonlinear input-output relationship. So MLPs with one, two, and three layers

of hidden neurons were applied in searching for an optimal network structure.

Overfitting should be avoided because the paramount goal of a prediction model is to

make predictions for novel data instead of training data. In order to avoid overfitting and,

thus, improve the prediction power of the network, the number of epochs (n_e) during

training shall not be too large and the mean square error (mse) to stop the training process

148

shall not be too low. The specific values for maximum n_e and mse should be set considering the characteristics of the problem.

The Matlab® neural network toolbox [Mathworks 2007c] was used to develop the MLP ANN models. Matlab built in functions (*newff*, *sim*, etc.) were used for training and testing of the networks. Custom programs were developed for setup of the neural networks and preparation of the training and testing data.

6.3 Radial Basis Function Network

The radial basis function network is based on the basic idea of curve fitting, which is searching for a hyper surface in a multidimensional space that best fits the training data. The hyper surface is composed of the combination of a set of basis functions, as shown in equation (6-6). In equation (6-6), $F(x)$ is the target function, w_i is the weight for ith basis function, and φ is a basis function [Haykin 1999]. Gaussian functions are commonly used basis function for RBFs and were thus used in this research as shown in equation (6-7), where σ is the width of the basis function. Figure 6-3 shows a Gaussian function in a two-dimensional space. The parameters of the basis functions and their combination weights can be derived through the training process. Two important parameters in RBF networks are the number of basis functions (N) and the width of the basis functions (σ). The diagram of RBF in a three-dimensional space is shown in Figure 6-4. The value the output variable can be calculated from the hyper surface given new input values. This approach is called an "exact" RBF.

$$F(x) = \sum_{i=1}^{n} w_i \varphi \left(\left\| x - x_i \right\| \right) \tag{6-6}$$

$$\varphi(r) = \exp\left(-\frac{r^2}{2\sigma^2}\right), \qquad \sigma > 0, \quad r \in \Re \qquad\qquad (6\text{-}7)$$

An "exact" RBF is susceptible to overfitting because the number of basis functions (N) might be much larger than the underlining dimension of the function $F(x)$. This problem can be solved by using regularization theory to develop a generalized RBF network, as shown in equations (6-8) and (6-9):
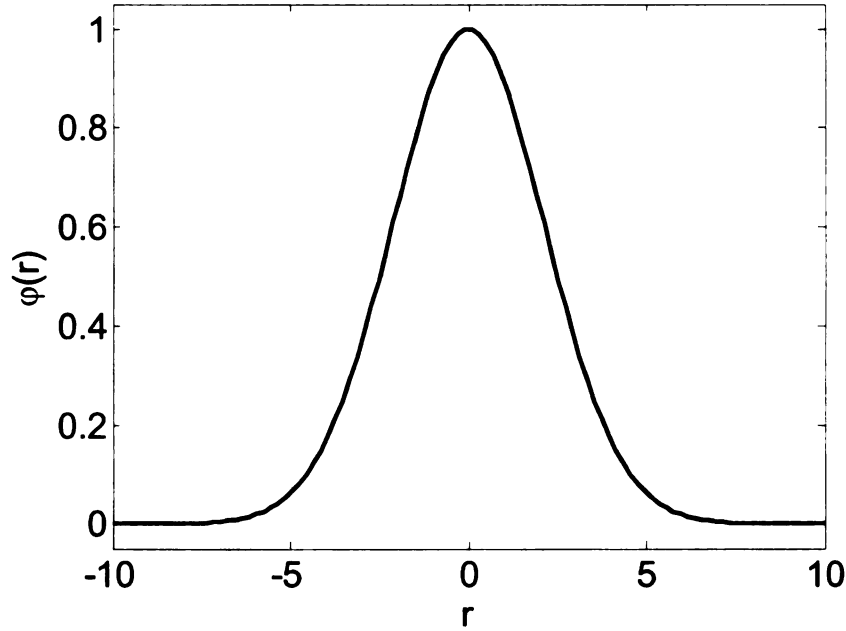
Figure 6-3 Gaussian function in two-dimensional space

$$F^*(x) = \sum_{i=1}^{m} w_i G\left(\left\| x - t_i \right\|\right) \qquad\qquad (6\text{-}8)$$

$$G = \begin{bmatrix} G(x_1, t_1) & G(x_1, t_2) & & G(x_1, t_m) \\ G(x_2, t_1) & G(x_2, t_2) & & G(x_2, t_m) \\ & & & \\ G(x_N, t_1) & G(x_N, t_2) & & G(x_N, t_m) \end{bmatrix} \qquad\qquad (6\text{-}9)$$

150
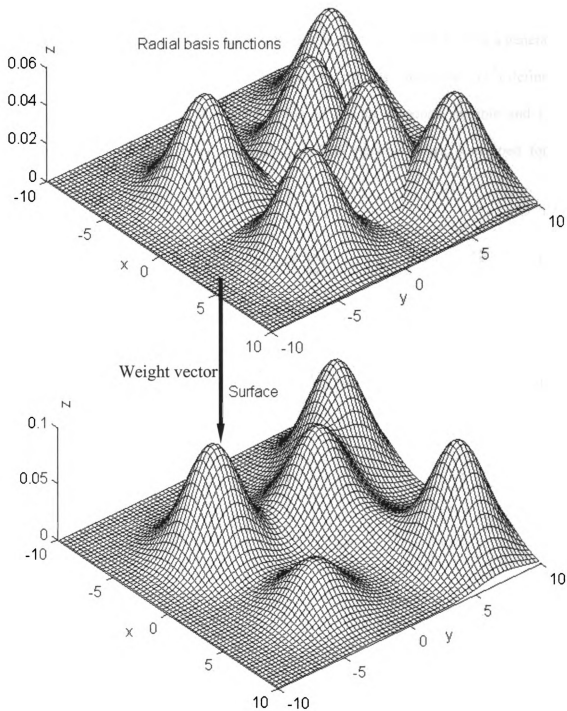
Figure 6-4 Diagram of RBF

where $F^*(x)$ is an approximated solution and t_i is the center of ith basis function. The number of basis functions is thus reduced from N in an "exact" RBF to m in a generalized RBF. Equation (6-8) can be solved by minimizing the cost functional $\xi(F^*)$ defined by equation (6-10), where d_i is the target value of the ith response variable and λ is a constant. Custom programs for a generalized RBF network were developed for this research.

$$\xi(F^*) = \sum_{i=1}^{N}\left(d_i - \sum_{j=1}^{m} w_i G\left(\left\|x_i - t_i\right\|\right)\right)^2 + \lambda\left\|DF^*\right\|^2 \qquad (6\text{-}10)$$

$$\left\|DF^*\right\|^2 = w^T G_0 w \qquad (6\text{-}11)$$

$$w = \begin{bmatrix} w_1 \\ w_2 \\ \vdots \\ w_m \end{bmatrix} \qquad (6\text{-}12)$$

$$G_0 = \begin{bmatrix} G(t_1,t_1) & G(t_1,t_2) & G(t_1,t_m) \\ G(t_2,t_1) & G(t_2,t_2) & G(t_2,t_m) \\ & & \\ G(t_m,t_1) & G(t_m,t_2) & G(t_m,t_m) \end{bmatrix} \qquad (6\text{-}13)$$

6.4 Support Vector Machine

Support vector machine (SVM) has become an important technique in soft computing in recent years. The SVM is related to statistical learning theory [Vapnik 1999]. The concept is that a series of separation boundaries might be able to separate two different classes of data in a hyper space. The basis of the SVM is to search for the decision boundary that maximizes the marginal distance between the boundary and the closest points in each data class that it separates (Figure 6-5 [Law 2006]). In Figure 6-5, sub-optimal decision boundaries (dashed lines) separate circles from squares (i.e., two data classes) for the training data. However, compared to the optimal (max-margin) decision boundary, sub-optimal boundaries provide a better chance for the test patterns to fall on the other side of the boundary and thus be misclassified. Nonetheless, sub-optimal decision boundaries can not be expected to have a good generalization performance.
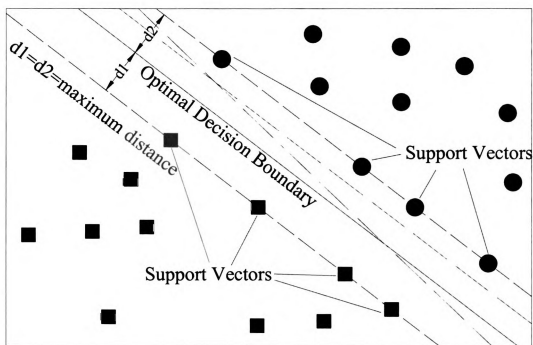
Figure 6-5 Optimal decision boundary decided by SVM

Equation (6-14) defines a decision surface to separate two classes; where w is a weight vector, x is a data vector, and b is a bias. The decision rules are described in equations (6-15) and (6-16). Data vectors that are closest to the decision boundary are support vectors, as shown in Figure 6-5. The search for the optimal decision boundary can then be transformed to a mathematical optimization problem.

$$w^T x + b = 0 \tag{6-14}$$

$$w^T x + b \geq 0 \qquad for \quad d_i = +1 \tag{6-15}$$

$$w^T x + b < 0 \qquad for \quad d_i = -1 \tag{6-16}$$

Most real world problems will not be linearly separable; however, the non-linearly separable vectors x_i might be linearly separable after being transformed to vectors $\varphi(x_i)$ in a higher dimensional space (Figure 6-6.) The notation "$\varphi(\cdot)$" represents the nonlinear transformation from input space to a higher dimensional feature space. This transformation is facilitated through the application of a "Kernel Trick". The "Kernel Trick" calculates the inner product of input vectors in a feature space instead of mapping input vectors to a feature space explicitly, as shown in equation (6-17). The use of a kernel function saves the calculation of transforming $\varphi(\cdot)$ for each vector explicitly and thus reduces the calculation load of an SVM.
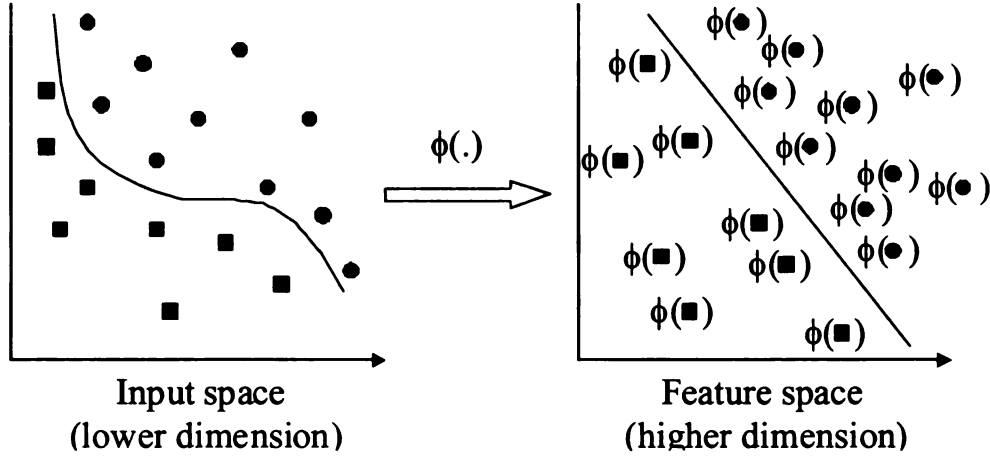
Figure 6-6 Transformation of feature space [Law 2006]

$$K(X, X_i) = \varphi^T(x)\varphi(x_i)$$

(6-17)

There are two main approaches to design an SVM for a general multi-class classification problem where the number of classes is greater than two. One is to construct and combine several binary classifiers, and the other is to consider all data in one optimization formulation. The formulation to solve multi-class SVM problems in one step has variables proportional to the number of classes. Therefore, for multi-class SVM methods, either several binary classifiers have to be constructed or a larger optimization problem is needed [Hsu and Lin 2002]. The two methods based on constructing and combining several binary SVM classifiers are:

A) One-against-all method: this method establishes k SVM models where k equals the number of classes. Each SVM is trained separately. In the training of the ith SVM, all of the training data in the ith class were labeled as positive and training data in other classes were labeled as negative [Hsu and Lin 2002]. In the training stage, the input data is put

155

into each of the k models. A weight w is defined for each model and k decision functions are obtained. In the testing stage the test vector will be classified to the class i if the ith SVM model yield the maximum of decision functions.

B) One-against-one method [Hsu and Lin 2002, Knerr et al. 1990]: this method constructs $k(k-1)/2$ classifiers and each classifier is trained on data from two classes. Using training data from the ith and the jth classes, the binary problem is solved such that data in the ith class falls on one side of the decision hyper plane and data in the jth class falls on the other side. The input data are applied to each of the $k(k-1)/2$ classifiers. If it is decided by one single SVM that the input vector x belongs to the ith class the count for the ith class is increased by one. Otherwise, the count for the jth class is increased by one. After counting the predictions from all the single SVMs the class with the largest count is then the predicted class. The voting approach described above is also called the "MaxWins" strategy. In the case that two classes have identical votes, the one with the lower class index is selected.

A freely distributed SVM toolbox [Gunn 1997] with a radial basis function as a kernel function was used as a single SVM classifier for this research. The one-against-one method was used to solve the multi-class classification problem based on a series of single SVM classifiers. Two important parameters are the width of the radial basis function d, and trade off parameter c between the error and the separation margin. Custom programs for constructing multi-classes classification models from single SVM classifiers were programmed for this research.

6.5 Supervised Self-Organizing Map

The development of self-organizing map (SOM) networks was motivated by the structure and function of the human brain in which neurons of different regions are responsible for different tasks: vision, hearing, smelling, etc. Different neurons in the SOM identify features of data in different classes. Neurons in the map usually lay on a one or two-dimensional lattice. After initializing the synaptic weights the formation of an SOM can be finished in three steps, which are: competition, cooperation, and adaptation [Haykin 1999, Kohonen 1990].

In the competition process, the index $i(x)$ identifies the neuron for input vector x and is calculated using equation (6-18):

$$i(x) = \arg \min_{j} \|x - w_j\|, \qquad j = 1, 2, \ldots, l \qquad (6\text{-}18)$$

where x is an input pattern, w_j is the synaptic weight vector for neuron j, and l is the number of neurons in the SOM. The winning neuron in the competition process defines the location of a topological neighborhood $(h_{j,i(x)})$ of the excited neurons using equation (6-19) through a cooperation process:

$$h_{j,i(x)} = \exp\left(\frac{d_{j,i}^2}{2\sigma^2}\right) \qquad (6\text{-}19)$$

where σ represents the effective width of the topological neighborhood, and $d_{j,i}$ represents the distance between the winning neuron i and the excited neuron j, as shown in (6-20).

$$d_{j,i}^2 = \|r_j - r_i\|^2 \qquad (6\text{-}20)$$

Finally, in the adaptation process, the weights of the neurons are updated using equation (6-21):

$$w_j(n+1) = w_j(n) + \eta(n)h_{j,i(x)}(n)(x - w_j(n))$$ (6-21)

where $w_j(n)$ and $w_j(n+1)$ are the weights of the jth neuron in the nth and the $(n+1)$th iterations, respectively; $\eta(n)$ is the learning rate in the nth iteration. After training, an SOM is organized in a way that the feature of the training patterns are captured and stored in the synaptic weight vectors. Two important parameters for an SOM are the number of rows and columns in the original lattice (n_r, n_c).

A self-organizing map is a kind of unsupervised learning network by nature. By providing proper supervised training it can also be transformed into a supervised learning network. Several steps are needed to achieve this:

- Create and train an ordinary SOM. The topology of the map and its weight vectors will represent the features of the training data. Each neuron in the map will win certain number of training vectors in a way that the weight vector of this neuron represents their common features.

- Count the number of training vectors that each neuron has won. The class of training vectors that is most populous among all won by a neuron is assigned to that neuron.

- In testing there will be a single winning neuron for each test vector and the class of the winning neuron will be assigned to it as the predicted value.

6.6 Evaluation of ANN Models for Abutment Distress Problem

None of the ANN model is inherently superior to the other without knowing the nature of the problem [Duda et al. 2001]. Four ANN models were applied to the bridge abutment problem and their fitness in solving the problem was evaluated. These four ANN models were introduced in previous sections: MLP, RBF, SVM, and SSOM.

6.6.1 Input variables and structure of the ANN models

The selection of a proper set of input variables is a key issue in building a good predictive model. The nature of a complex problem typically cannot be captured with only a few input variables. At the same time, redundant variables will cause overfitting, non convergence, and high computational costs. Thus, it is necessary to identify the variables that significantly contribute to the conditions of structures. Processes based on three different rationales were combined in the selection of prediction variables: knowledge-based evaluation (i.e., the subjective selection of variables based on principles of structural engineering,) statistical analyses (Section 3.4.1.1,) and trial and error.

Incorporating the statistical analyses, the knowledge of bridge engineering, and trial and error, input variables for ANNs were decided to be: length, deck width, skew, Ageinsp, ADTT, Matdiff, Apprsurstif. Abut_Rating was designated as the response variable. The first six variables are quantitative and they were normalized before input to network models. ApprSur_type is a qualitative variable with four major classes, bituminous, bituminous concrete, unknown, and concrete. It was transformed to three indicator variables: v1, v2, and v3. "v1" takes 1 if the approach surface is bituminous, 0 otherwise. Similarly, "v2" takes 1 if the approach surface is bituminous concrete, 0

otherwise; "v3" takes 1 if the approach surface is unknown, 0 otherwise. Two fifth of the records in the NBI manual inspection database were randomly selected as the training data for the MLP networks and the rest were used as testing data. For RBF, SVM, and SSOM networks, a quarter of the records in the data set were randomly selected as training data and the rest were used as testing data.

Proper setting of an ANN structure is one of the key issues to build a good prediction model. Rules of thumb have been developed for the different ANN models and no rigorous theoretical procedure was available at the time of this research. Parameters for the ANNs were thus determined by the combination of rules of thumb and trial and error. It was impossible to test every possible parameter combinations since multiple parameters existed for each ANN with infinite possible values for each parameter. Thus, the approach used in this study was as follows: for parameters x and y, k values that spread over their ranges, respectively, were selected and build ANN models for each of k^2 combinations between $[x_1, x_2, ...x_k]$ and $[y_1, y_2, ...y_k]$ were built. Model parameters with minimum testing error would be the center of next trial (x_i, y_j). In a similar procedure, k values that spread over $[x_{i-1}, x_{i+1}]$ and $[y_{j-1}, y_{j+1}]$, respectively, were selected and find the refinement of the optimal combination was found. This search process was refined until a satisfactory testing error was reached. While this approach is susceptible to a local minimum effect, it was a practical way to solve the problem due to the lack of a rigorously theoretical method.

6.6.2 Evaluation of ANN models

For the MLP ANN models, a network with 2 hidden layers, 130 neurons in each hidden layer and a learning rate $\eta = 0.05$ had the best performance. For the best model, $n_e = 10,000$, and $mse = 0.05$, and a sigmoid function was used as the activation function. Predictions from the trained MLP ANN are tabulated in the confusion matrix shown in Table 6-2 together with the manual inspection (i.e., true) values. A confusion matrix [Kohavi and Provost 1998] contains information about actual and predicted classifications and can thus be used as a measure of the model performance [Silva et al. 2004]. In Table 6-2 the columns are the predicted values and the rows are the manual inspection (or true) value. The numbers in the cells with row and column numbers between 0 and 9 are the numbers of observations that fall into those categories. Accordingly, the diagonal elements (darker gray cells) are the number of correct predictions. Thus, cells far from the diagonal imply that the predictions are away from the actual response. The row labeled correct ratio (CR) gives the ratio of the number of correct predictions to the number of all instances for that given level of response (given in the "True Sum" row). Subjectivity in the rating of structural members is well recognized and a margin of error of ±1 has been found to be representative [Phares et al. 2001]. Thus, an acceptable prediction band width can be defined within the confusion matrix by considering a prediction acceptable if it is within ±1 of the true response value. The expanded band width in the confusion matrix is shown by a lighter gray shade along the main diagonal in Table 6-2. Considering all records that fall within the acceptable bandwidth, an acceptable ratio (AR) can be used as another criterion to evaluate the performance of the network. Additionally, a distress identification ratio (DIR) was

161

defined as the number of inspection cases whose inspection (or true) value is less than 5 and was predicted to be less than 5. The DIR is calculated by summing the top left 5×5 square sub-matrix of Table 6-2 and dividing by the sum of the first half of the row "True Sum."

The RBF network with parameters $N = 3$ and $\sigma = 290$ had the best performance. For the SVM networks, the best performance was obtained when its parameters were $d = 4$ and $c = 50$. The SSOM with parameters $n_r = 16$ and $n_c = 19$ had the optimal performance. The confusion matrices for the RBF, SVM, and SSOM predictions are shown in Table 6-3, Table 6-4, and Table 6-5, respectively.

Table 6-2 Confusion matrix of abutment rating prediction using an MLP ANN

True Predicted	0	1	2	3	4	5	6	7	8	9
0	3	0	0	0	0	0	0	2	2	0
1	0	0	0	0	0	0	0	0	0	0
2	0	0	5	0	1	5	8	2	2	0
3	0	0	2	23	22	17	61	112	32	0
4	0	0	0	6	71	20	127	185	36	0
5	1	0	0	2	22	162	557	632	78	0
6	0	0	2	0	1	20	516	442	35	0
7	0	0	0	9	29	78	1251	5226	807	2
8	1	0	0	0	1	1	37	273	272	1
9	0	0	0	0	1	0	7	14	3	2
True Sum	5	0	9	40	148	303	2564	6888	1267	5
Correct ratio	60.0%	N/A	55.6%	57.5%	48.0%	53.5%	20.1%	75.9%	21.5%	40.0%
Acceptible ratio	60.0%	N/A	77.8%	72.5%	77.7%	66.7%	90.6%	86.3%	85.4%	60.0%

Table 6-3 Confusion matrix of abutment rating prediction using an RBF ANN

Predicted \ True	0	1	2	3	4	5	6	7	8	9
0	0	0	0	0	0	0	0	0	0	0
1	0	0	0	0	0	0	0	4	0	0
2	0	0	0	0	0	0	2	2	0	0
3	0	0	0	0	0	0	0	0	0	0
4	0	0	0	0	3	10	25	17	0	0
5	0	0	4	4	0	13	38	64	13	0
6	2	0	33	179	216	787	3179	9214	979	8
7	0	0	0	0	0	0	0	0	0	0
8	0	0	0	0	0	0	0	0	0	0
9	0	0	0	0	0	0	0	0	0	0
True Sum	2	0	37	183	219	810	3244	9301	992	8
Correct ratio	0.0%	N/A	0.0%	0.0%	1.4%	1.6%	98.0%	0.0%	0.0%	0.0%
Acceptable ratio	0.0%	N/A	0.0%	0.0%	1.4%	100.0%	99.2%	99.1%	0.0%	0.0%

Table 6-4 Confusion matrix of abutment rating prediction using an SVM ANN

Predicted \ True	0	1	2	3	4	5	6	7	8	9
0	1	0	0	0	0	0	1	16	0	0
1	0	0	0	0	0	0	0	0	0	0
2	0	0	29	0	0	1	2	12	0	0
3	0	0	8	112	13	15	41	114	6	0
4	0	0	0	24	143	64	134	350	14	0
5	0	0	0	6	27	508	554	988	46	1
6	0	0	0	16	5	111	1598	1781	81	0
7	0	0	0	14	25	82	618	4374	170	0
8	1	0	2	6	5	29	283	1637	671	1
9	0	0	0	0	0	0	12	23	4	5
True Sum	2	0	39	178	218	810	3243	9295	992	7
Correct ratio	50.0%	N/A	74.4%	62.9%	65.6%	62.7%	49.3%	47.1%	67.6%	71.4%
Acceptible ratio	50.0%	N/A	94.9%	76.4%	83.9%	84.3%	85.4%	83.8%	85.2%	85.7%

Table 6-5 Confusion matrix of abutment rating prediction using an SSOM ANN

Predicted \ True	0	1	2	3	4	5	6	7	8	9
0	0	0	0	0	0	6	15	78	2	0
1	0	0	0	0	0	0	0	0	0	0
2	0	0	7	4	2	7	36	74	8	0
3	0	0	7	56	18	35	173	364	29	0
4	0	0	2	40	112	142	474	973	83	1
5	0	0	16	32	33	318	645	1456	108	0
6	0	0	4	10	16	130	897	1604	119	1
7	1	0	0	24	27	94	616	3193	252	1
8	1	0	0	14	9	77	379	1544	389	4
9	0	0	0	0	0	1	9	15	2	0
True Sum	2	0	36	180	217	810	3244	9301	992	7
Correct ratio	0.0%	N/A	19.4%	31.1%	51.6%	39.3%	27.7%	34.3%	39.2%	0.0%
Acceptible ratio	0.0%	N/A	38.9%	55.6%	75.1%	72.8%	66.5%	68.2%	64.8%	57.1%

The performance of the best prediction models (MLP, RBF, SVM, and SSOM) are compared in Figure 6-7. The MLP and SVM showed better performance among the four. Performance of the RBF network is not considered good because of a low DIR value, even though it had the highest AR value.
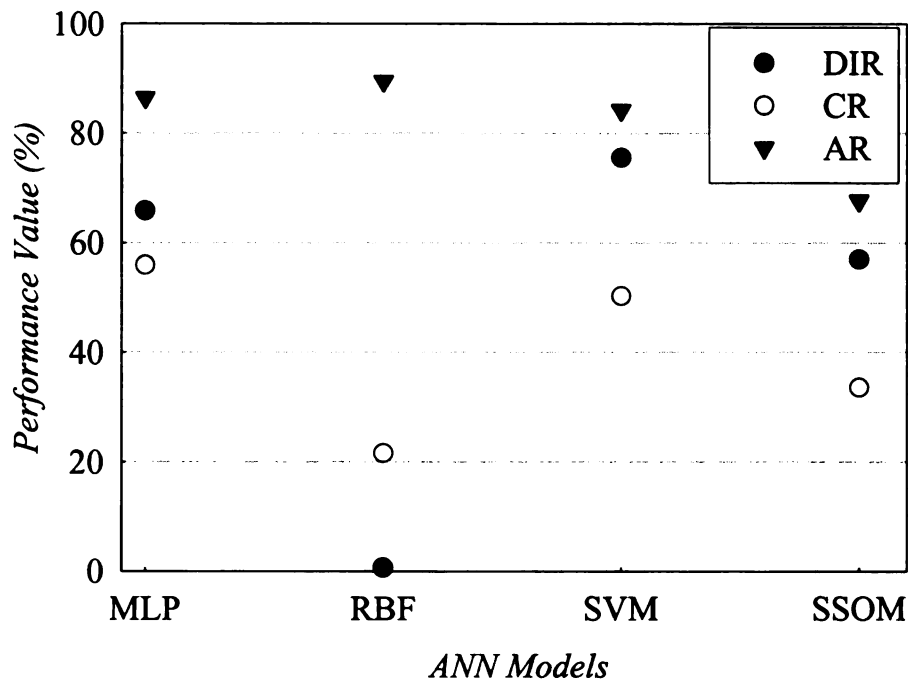
Figure 6-7 Performance of ANN models

6.6.3 Deterioration curves for highway bridge abutment walls

Since the national bridge inspection (NBI) program was created not very long ago [Hartle et al. 1991], inspection records for each bridge in the database only covers a short life span, as shown in Figure 6-8. It is thus very difficult, if not impossible, to find the life cycle trend of abutment condition from these inspection records. However, ANN models can extract and combine useful information to generate a deterioration curve for the abutment wall throughout the life cycle of a highway bridge.
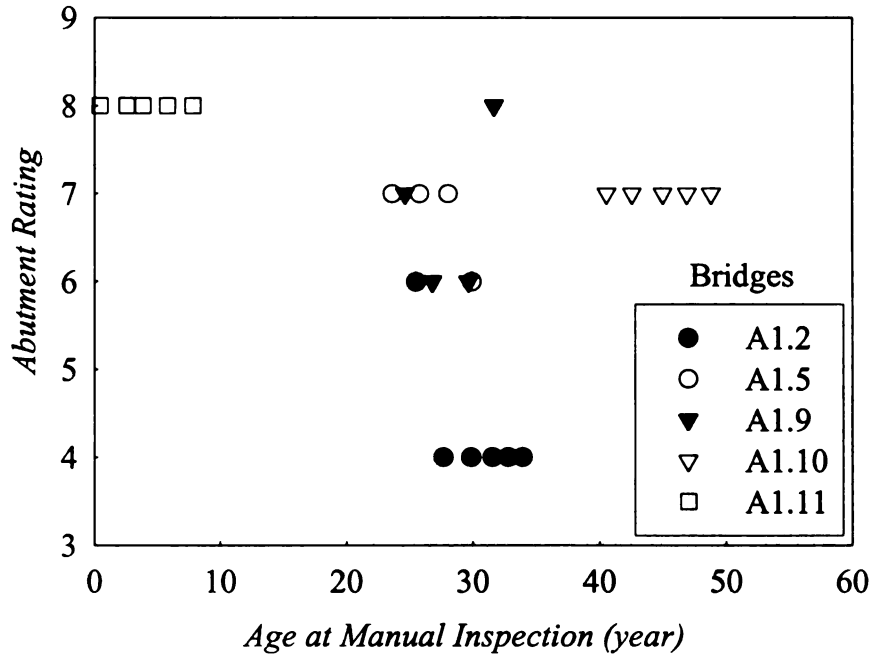
Figure 6-8 Scatter plot of abutment rating vs. age at manual inspection

The MLP and the SVM network models were applied to retrieve and predict the conditions of the abutment walls of a simple/cantilever steel bridge in the State of Michigan (bridge A1.5). The deterioration curves for this bridge are shown in Figure 6-9. The abutment ratings predicted by the ANN models are shown by the stepwise lines. The stepwise shape follows from the integer 0 to 9 rating scale. Data points corresponding to the manual ratings currently available in the database for this bridge are also shown as dotted-connected triangles. Confidence bands for the deterioration curves are also shown in the figure as dashed curves. The width of the stepwise confidence band is two times the standard deviation of each of the predicted values. The center of the band is biased from the predicted value to account for the asymmetrical deviation of the model. The amount of bias is decided by the ratio of those manual ratings above the predicted value to those below it. Therefore, both the width and bias of the confidence band change with

the predicted value. Since abutment condition is predicted to degrade gradually, the stepwise confidence bands were smoothed to curves through the Lowess method using a first-degree polynomial. Since ANN models are non-parametric models, the confidence levels for the confidence bands are difficult to derive through statistical methods. However, the confidence level can be obtained through testing results (summarized in Table 6-2 and Table 6-4.) The confidence levels of the deterioration curves in Figure 6-9 are shown in Table 6-6.
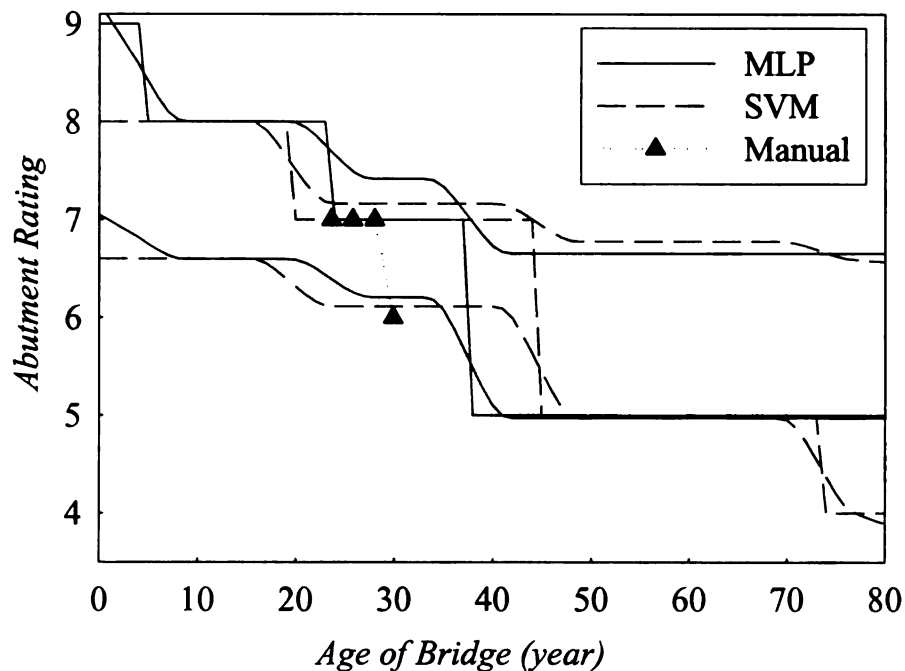
Figure 6-9 Abutment deterioration curve for bridge A1.5

Table 6-6 Confidence level for the confidence bands of deterioration curves

Predicted value	0	2	3	4	5	6	7	8	9
MLP(%)	100	47.8	23.0	49.0	49.4	94.3	70.6	93.0	70.4
SVM(%)	5.6	72.7	58.6	46.8	49.9	94.1	82.8	87.6	20.5

It should also be noted that not all of the deterioration curves have the same shape as seen in Figure 6-9. Development of different deterioration curves has shown that for some bridges abutment deterioration was predicted to occur earlier than others and/or degrade at different rates. There are also some deterioration curves that show abnormal behavior and their validity is thus suspected. Further discussion about this issue is given in Section 7.4.3.

6.7 Fuzzy Neural Network Model

An artificial neural network can map complicated input-output relationship and fuzzy sets can account for the subjectivity in manual inspections using vague decision boundaries. By combining them, a fuzzy-neural network was developed to predict structural condition using design and operation parameters. In the training phase, integer structural ratings were transformed to membership values of fuzzy sets. In the testing phase, predicted membership values were back transformed to integer structural ratings through another neural network. Samples that can be used in training the back transform neural network were limited. Duplications and noise vectors were utilized to improve the generalization capacity.

A fuzzy set (FS) is a collection of members whose relationship with the set is defined by a membership function. The key feature of a fuzzy set is its continuous and gradual boundary, contrary to the rigorous and sharp boundary of an ordinary set. This feature is close to the thinking and decision making process of a human being [Zadeh 1965]. It thus enables an FS to address uncertainties in a database [Yao 1980]. ANN and FS can be combined to develop a fuzzy-neural network models [Jain and Martin 1999, Pal and

Mitra 1999] to map a nonlinear relationship using a data set with uncertainty and subjectivity.

6.7.1 Fuzzy Sets

Fuzzy sets are often defined by linguistic variables [Zadeh 1975a, 1975b, 1975c, 1994]. The membership function value of a linguistic variable means the degree to which the output belongs to that linguistic variable. The membership function value is in the range of [0, 1], where "1" means the highest degree of membership and "0" means lowest degree. Thus, a membership function enables an FS to account for the imprecision or subjectivity exists in real world problems.

FS is a suitable tool for damage assessment of structures considering the subjectivity of manual inspections and the large variance in structural ratings. Transforming discrete integer ratings to continuous membership values of linguistic variables, such as *"damaged"*, *"poor"*, *"moderate"*, *"good"*, and *"excellent"*, can reflect the thinking process of structure inspectors better than discrete integer ratings. It is thus more reasonable to use these linguistic variables as the output variable of an ANN.

A Gaussian function was used as the membership function of the FS as shown in Figure 6-10. The activation function used in the ANN was a sigmoid function, it is most effective when the input values are distributed in the range [-1, 1]. Values of membership functions were thus transformed to the [-1, 1] range by multiplying them by 2 and subtracting 1, as shown in Figure 6-11.
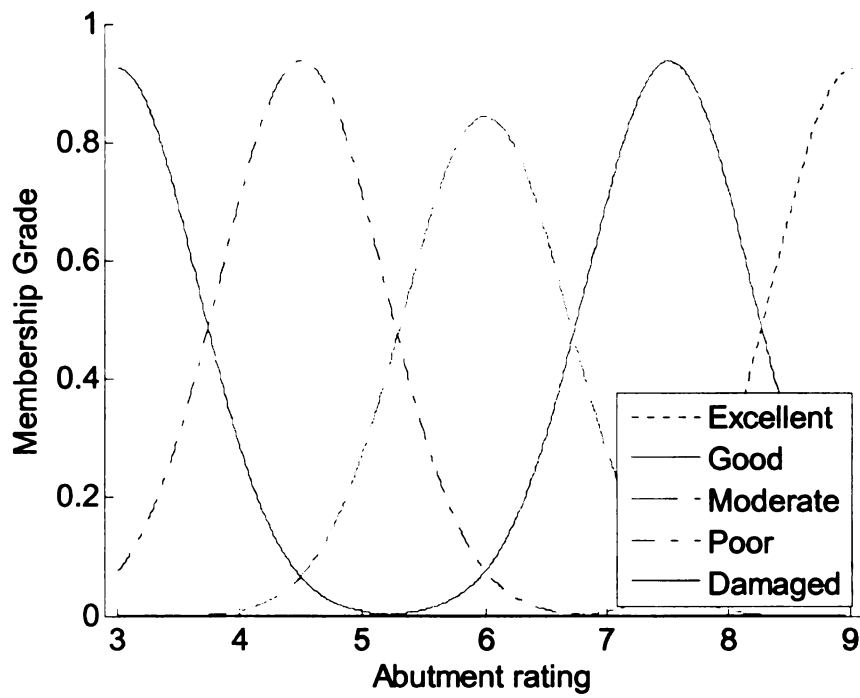
Figure 6-10 Membership function of fuzzy sets
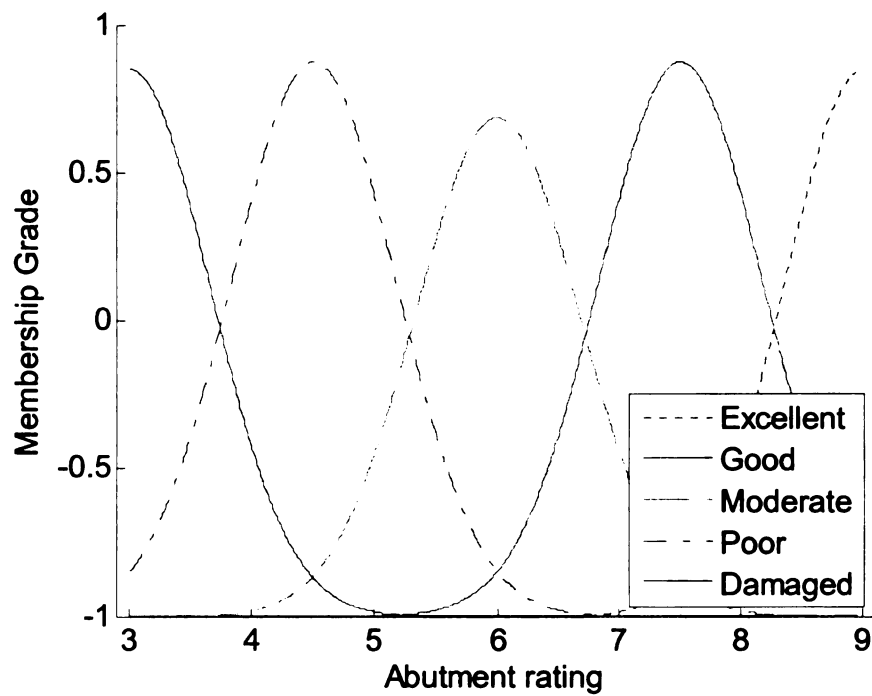
Figure 6-11 Membership function of fuzzy sets after modification for ANN

6.7.2   Fuzzy-Neural Network

An FNN can be developed by incorporating a fuzzy output processing module into a conventional neural network, as shown in Figure 6-12. The ANN in an FNN will use the membership values of linguistic variables as outputs. A fuzzy output transform module includes two transformation processes. One process is to transform "vague" structural rating into "linguistic" variables to serve as output variables in the training of an MLP ANN. The other process is to transform the "linguistic" output of the MLP ANN back to the form of structural ratings that directly indicate conditions of structures in the prediction phase. Another MLP ANN model needs to be developed for this back transformation.

The structure of the ANN is illustrated in Figure 6-12. The parameter values for the best performance were: $p=13$, $n=145$, and $k=5$. One third of the records in each abutment rating category were selected and combined as test data. The remaining records were used as training data. If the number of remaining records in any category was larger than 1500, those extra records were excluded from the training data to provide some level of balance. In the training of the neural network, the mean square error and the maximum number of epochs to stop were set at 0.05 and 30000, respectively.
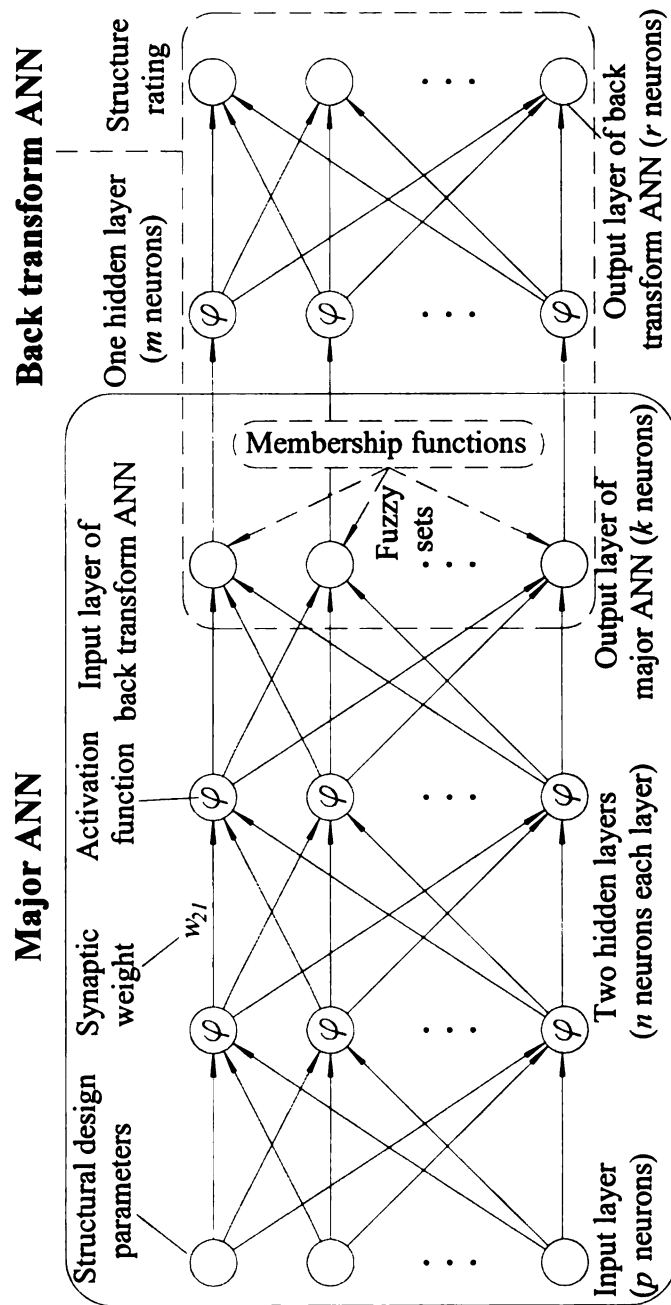
Figure 6-12 Schematic of an FNN model

174

6.7.3 Back transforming scheme

Sparseness of the training points was a major difficulty in the development of a neural network to transform membership values of linguistic variables back to structural ratings. For instance, seven integral structural ratings were transformed to five linguistic variables in the training of the neural network. Thus, only seven known points (seven integral ratings) were available in the 5-dimensional space (five linguistic variables) in the training of the back transform ANN. A neural network can not be properly trained using such sparse training data. By duplicating each training point and adding a random noise vector to each of the duplications, the seven known points would be expanded to seven clusters of points; and thus cover the space better and improve the generalization of the back transforming ANN. The magnitude of the random noise to reach the optimal generalization depends on the distance of the training points, the structure of the neural networks, etc. The ratings that showed structural damage were duplicated more than the other ratings to improve the probability of identifying structural damage after being processed by the fuzzy transform module.

The structure of the back transformation MLP ANN had 1 hidden layer (see Figure 6-12,) and its parameters were $k = 5$, $m = 100$, and $r = 7$. In the training of the back transformation module, 9400 vectors were included in the training data set. For abutment ratings of 3 and 4 there were 4200 vectors for each. For ratings of 5 to 9 there were 200 vectors for each of them. The components in the random vector were random values in the range of [-0.1, 0.1]. The mean square error and the maximum number of epochs to stop training were set at 0.02 and 1000, respectively.

6.7.4 Results

In addition to the DIR performance metric a false alarm ratio (FAR) was used as an indicator to evaluate the performance of prediction models. FAR is defined as the ratio of "good structures" identified as damaged to all "good structures." The DIR and FAR were calculated using Equations (6-22) and (6-23), respectively:

$$DIR = \frac{n_{id}}{n_d} \times 100\% \tag{6-22}$$

$$FAR = \frac{n_{fd}}{n_g} \times 100\% \tag{6-23}$$

where n_d is the number of records in which the *abutment rating* from the manual inspection was "3" or "4," among the n_d records, n_{id} is the number of records in which the predicted rating was also "3" or "4," n_g is the number of records in which the *abutment rating* from the manual inspection was greater than "5" among n_g records, and n_{fd} is the number of records in which the predicted rating was "3" or "4."

The DIR and FAR of the fuzzy neural network were 82.31 % and 14.61 %, respectively. Compared to the DIR and FAR of a conventional MLP ANN, which are 65.84 % and 2.65 %, respectively (Section 6.6), the FNN model showed a 16.47 % improvement of DIR at the cost of an 11.96 % increase in the FAR. The confusion matrix of the fuzzy neural network is shown in Table 6-7. It can be seen from Table 6-7 that the FNN model can identify damage in bridge abutments with satisfactory accuracy.

Table 6-7 Confusion matrix of an FNN

Predicted \ True	3	4	5	6	7	8	9	Sum
3	110	34	46	60	150	11	0	411
4	52	218	235	191	319	45	2	1062
5	0	0	0	0	0	0	0	0
6	18	50	213	877	1134	170	8	2470
7	2	13	77	216	1604	319	11	2242
8	0	2	3	6	100	81	7	199
9	1	3	0	2	3	7	2	42
True Sum	183	320	574	1352	3310	633	30	6426
Correct ratio	60.11%	68.13%	0.00%	64.87%	48.46%	12.80%	6.67%	45.00%
Acceptible ratio	88.52%	78.75%	78.05%	80.84%	85.74%	64.30%	30.00%	81.06%

It should also be pointed out that the model could not give a prediction for the rating "5". This might be caused by the noise vectors added for training of the back transformation model. It can also be noticed that most of the test patterns with manual inspection rating "5" were predicted as "4" or "6." The deviation is considered acceptable given the large variance in the manual inspection data. Table 6-7 is presented in a manner slightly different from Table 6-2 to Table 6-5 because it was found through field inspection that the bridges with abutment rating less than 3 were closed and thus not in normal operation. Thus, those inspection records were deleted from the database in the later stages of the study.

6.7.5   Bridge abutment deterioration curve

The FNN model was applied to predict the abutment condition of one prestressed concrete bridge in the State of Michigan. Its abutment deterioration curve is shown in Figure 6-13. A confidence band was evaluated through the confusion matrix of the prediction model (Table 6-7). The confidence level was 82.3 % for the case that abutment damage exists and 81.4 % for a 75-year life span for the bridge.

It should also be noted that not all the deterioration curves are in the exactly same shape as Figure 6-13. The abutment walls of some bridges deteriorate at earlier times, some are predicted to degrade faster, and some of them show abnormal (and suspect) trends due to the improper prediction of the model or the inherent complexities of the structural inventory database. Figure 6-14 shows the deterioration curve developed using the FNN for the bridge shown in Figure 6-9 (bridge A1.5) for comparison. Compared with predictions of the MLP and SVM (Figure 6-9,) the prediction of the FNN (Figure

6-14) is more precise in matching the manual inspections. However, the deterioration trend developed by the FNN is not as reasonable as those of the MLP and SVM. Figure 6-9 is the one selected among several bridges for which the MLP and SVM developed deterioration curves that show reasonable trends. For the FNN, the bridge was defined for comparison, so the above comparisons can not be generalized without further and more comprehensive comparisons and evaluations. There are also some deterioration curves exemplify unreasonable deterioration trends. Further discussion about this issue can be referred to section 7.4.3.
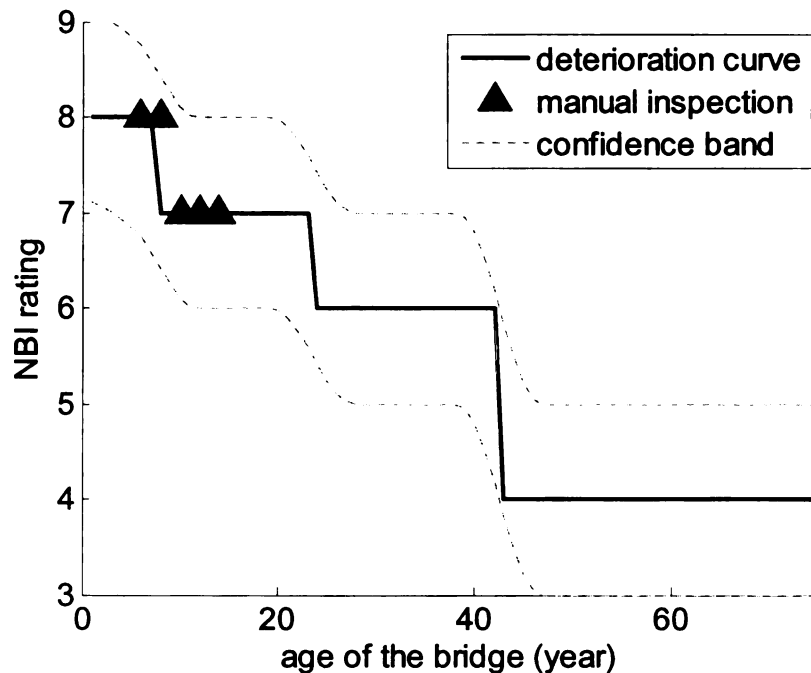
Figure 6-13 Abutment deterioration curve of a prestressed concrete bridge
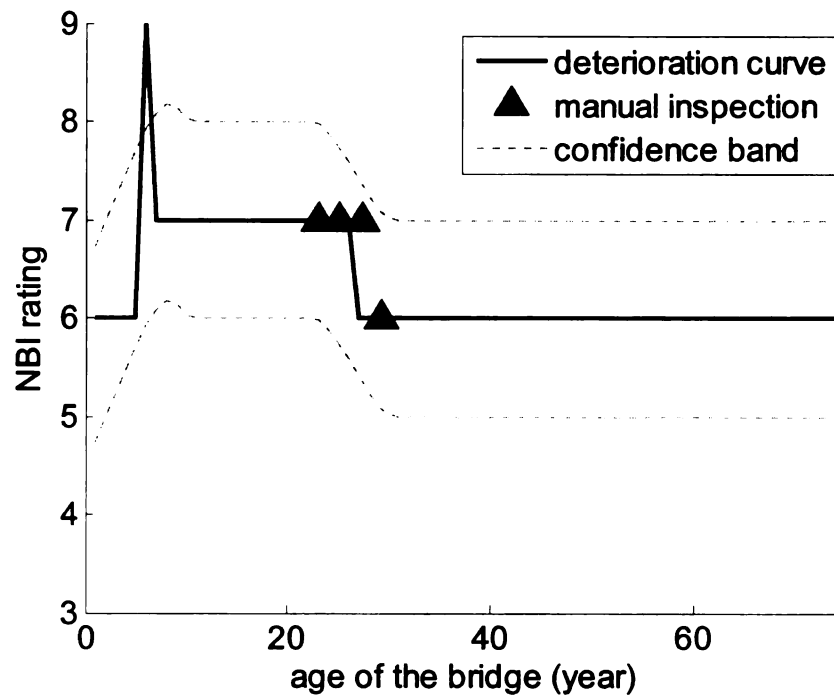
Figure 6-14 Deterioration curve developed by an FNN for the bridge in Figure 6-9

6.8 Discussion

Four major types of neural network models were developed for the present research problem to predict the condition of highway bridge abutment walls based on the NBI database. These four neural network models were: multilayer perceptron (MLP), which is based on recursive learning; radial basis function network (RBF), which is based on curve fitting; support vector machine (SVM), which is based on optimization of a decision boundary; and supervised self-organizing map (SSOM), which is based on feature extraction and feature mapping.

Since the primary goal for developing the ANN models was to predict abutment distress, SVM seemed to be the optimal ANN model since it had the highest ratio of damage identification (DIR). The MLP model also had good performance as it had the

second highest DIR indicator with high acceptable ratio (AR) and correct ratio (CR) at the same time. The SSOM model was inferior to the MLP model for all three performance indicators. The RBF model did not seem to perform well for this problem because its DIR was too low. Thus, it couldn't identify abutment distress even though its acceptable ratio was the highest among the four. For the problem of abutment damage identification and prediction the SVM and MLP models were identified as the suitable ones to build degradation prediction models.

A fuzzy neural network was also developed to identify damage in bridge abutment to account for the subjectivity in the manual inspections. A fuzzy transform module was designed to alleviate the negative effect of subjectivity by using linguistic variables and membership functions instead of integer structural ratings. A Gaussian function was used as the membership function of the fuzzy sets. In the training of the back transform network of the fuzzy transform module, the sparseness of the training data set was alleviated by duplicating the training data and adding noise to the duplications. The accuracy in identifying structural damage was improved by focusing on damage patterns in the training of back transform network. An FNN model was used to predict structural damage in abutment walls and the DIR of the FNN model reached 82.31 %, which exceeded the conventional network by 16.47 %.

7 ENSEMBLE OF NEURAL NETWORKS AND COMBINATION OF DATABASES

7.1 Introduction

ANN models have shown reasonable performance in predicting damage in abutment walls of highway bridges as presented in Section 6.6. However, those models can hardly be further improved considering the complexity of the problem and the difficulties with the database. In this chapter, an ensemble of networks (ENN) was explored to develop a damage prediction model with improved accuracy. An ensemble of neural networks is a set of individually trained neural networks from which predictions for novel inputs are obtained through the combination of individual predictions by certain voting schemes [Opitz and Maclin 1999]. The concept of an ensemble of neural networks follows from the principle of "divide and conquer," which means that a complicated task can be decomposed into a series of simpler tasks and the solution to the complicated problem can be arrived at by combining the solution of the simpler problems [Haykin 1999]. The accuracy of an ensemble of neural network is expected to be improved by combining the knowledge learned by each individual neural network, even though those individual networks are trained on subsets of data and do not have the optimal performance for the complete problem. A diagram for the concept of an ensemble of neural networks is shown in Figure 7-1.
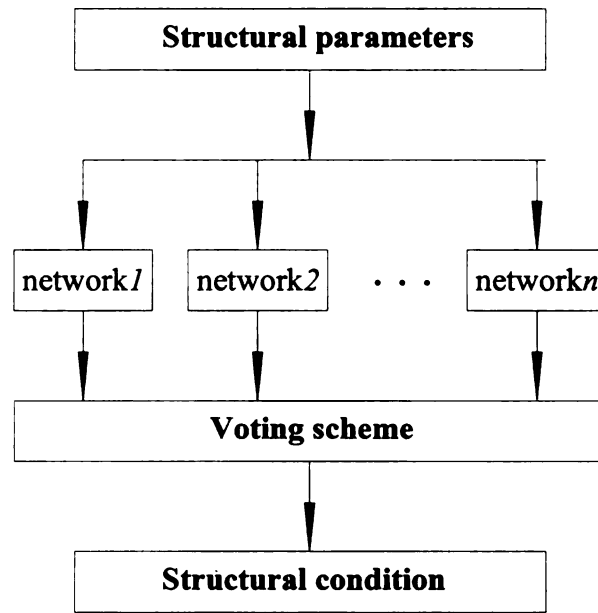
Figure 7-1 Diagram of ensemble of MLPs

The motivations for using an ensemble of neural networks (ENN) in this research are:

- An individual neural network is susceptible to be trapped into local minima and to overfitting. Combining the predictions of individual neural networks, the performance of an ENN will not be influenced when a few of the individual networks are trapped into different local minimal.

- An individual neural network might misrepresent part of the training data. Since different network might misrepresent different features of the data, the negative effects of the misrepresented data can be minimized by combining individual neural networks to help each other.

- The source of the damage in the abutment walls for the present research problem is highly scattered, including mechanical processes, environmental factors, traffic conditions, weather conditions, construction qualities, corrosion, etc. It is thus

very difficult for a single neural network to capture all these factors from the training data.

- A novel data organization scheme applied in an ensemble of neural network can help to overcome the unbalance in the manual inspection database.

- An ensemble of neural network provides the opportunity to combine the evidential database with a virtual database to improve the accuracy of the prediction model.

Theoretically, an ENN can overcome the bias/variance dilemma [Duda et al. 2001, Haykin 1999] of an ANN and thus improve the performance of the prediction model. The bias/variance dilemma refers to the interdependence of the bias and the variance of a neural network. Bias refers to the accuracy of a neural network. A neural network with large bias will produce a wrong prediction. Variance refers to the precision of a neural network. A network with a large variance can not be reliable even though its bias might be small. Given a certain amount of training data the bias of a neural network can not be reduced significantly without the increase of the variance, and vice versa. The error of a neural network can be expressed using equation (7-1):

$$E\big(F(x) - E[D|X = x]\big)^2 = B\big(F(x)\big) + V\big(F(x)\big) \qquad \text{(7-1)}$$

where $F(x)$ is the input-output function mapped by the neural network; the bias $B(F(x))$ is calculated using equation (7-2); and the variance $V(F(x))$ is calculated using equation (7-3).

$$B\big(F(x)\big) = \big(E(F(x)) - E[D|X = x]\big)^2 \qquad \text{(7-2)}$$

$$V(F(x)) = E(F(x) - E[F(x)])^2 \qquad (7-3)$$

It has been proved that the prediction made by summarizing the predictions of individual neural networks in an ensemble will not reduce the bias of the function *F(x)* [Haykin 1999]. However, it would help to reduce the variance of the function *F(x)* and thus, improve the performance of the prediction model.

In this research, MLPs with a back propagation algorithm (see Section 6.2) were used to compose an ensemble for two reasons: first, an MLP is good at mapping nonlinear input-output relationships as discussed in section 6.2; and second, an individual MLP is vulnerable to local minima, which means that the searching for synaptic weights might stop at a point corresponding to a suboptimal generalization of rules hidden in the training data. The performance of an ENN is expected to be better when the errors of the individual neural networks in the ensemble are more independent [Hansen et al. 1992, Sharkey 1999]. Kolen and Pollack [1990] demonstrated that the accuracy of an MLP using back propagation algorithm was sensitive to the initial conditions. The effects of variation in initial conditions to the generalization of the network were not likely to be as significant as the variation of the training data sets [Sharkey 1999]. In this research, both the training data sets and the initial synaptic weights were different for the different MLPs in the ensemble.

The Matlab® [Mathworks 2007c] neural network toolbox was used to develop the individual MLP ANN models. Matlab's built-in functions were used in training and testing of the dividual MLP networks. Customer programs were developed to setup the

structure of each MLP, organize the training data sets, compose the ensemble of neural networks, and realize the different voting schemes. A stand-alone executable program "SbNet" were developed based on the prediction model using an ensemble of neural networks. Such a program can predict bridge abutment condition and life-time degradation curves given design parameters or an MDOT bridge identification number.

In the following three sections of this chapter, the data organization, voting schemes, and the results of their application in an ensemble of neural networks for the example problem are presented. Then, the combination of databases into an ensemble of neural networks and the development of a program for the example problem is provided.

7.2 Data Organization

The principal motive for devising a novel data organization scheme is to overcome the unbalanced distribution of structural inspection records in the database, which is a challenging issue for an individual network. Two major approaches to organize data sets are *bagging* [Breiman 1996, Duda et al. 2001, Sharkey 1999] and *boosting* [Duda et al. 2001, Schapire 1990]. Bagging is a procedure to produce multiple training sub-sets by randomly drawing samples from the original training set with replacement. Boosting is a procedure to produce multiple training sub-sets in a manner that the subsequent selection is focused on the samples that are not recognized well by the classifiers training on the previous training sub-sets. Compared with boosting, bagging has been proven to be more resilient to noise [Opitz and Maclin 1999, Quinlan 1996], which is also a major difficulty in using a structural inventory system database. Bagging is effective in making full use of

small data sets; and Breiman [1996a, 1996b] proved that bagging can improve the accuracy of unstable prediction models, such as neural networks.

In this research, the concept of bagging was applied after modification-bagging within each structural condition to alleviate the difficulty of rare damage records. Each network in the ensemble was trained by a different data set. Each data set contained the same number of records (n_i) for each structural condition and these n_i records were randomly selected from each category with replacement. As a result, the training set for each individual network was balanced and different from each other and the errors of these networks had some degree of independence. The procedure of bagging within categories is schematically shown in Figure 7-2.
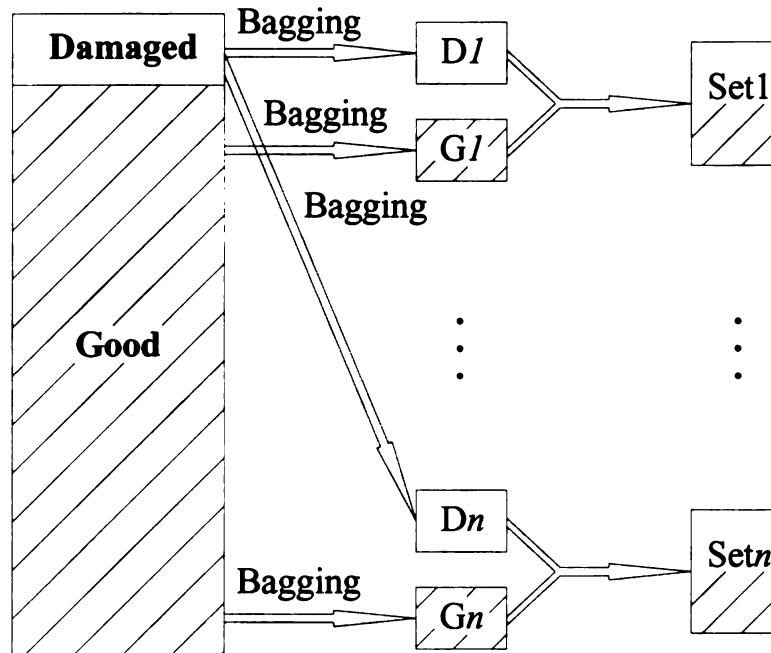
Figure 7-2 A novel data organization scheme: bagging with categories

Neural networks ensemble can be trained through parallel computing since bagging within category enabled each individual neural network to be trained and tested independently. Parallel computation can significantly improve the efficiency in developing the ensemble since the training of each individual neural network is time-consuming.

7.3 Voting Scheme

Voting scheme refers to the way to combine the individual answers of the neural networks to reach a final prediction by the ensemble. The voting schemes applied in this research were:

(a) **Plurality Voting:** The final prediction of the ensemble is the one that receives more "votes" from individual networks than other possible predictions [Hansen and Salamon 1990].

(b) **Modified Majority Voting:** In a majority voting scheme, the final prediction of the ensemble is the one that receives more than half of the votes from individual networks [Hansen and Salamon 1990, Zhou et. al. 2002]. In this research, a modified majority voting scheme was applied. If no structural condition obtains more than half of the votes, the prediction will be the worst structural condition that receives more than a quarter of the votes. If no structural condition obtains more than a quarter of the votes, the prediction will be the worst structural condition that receives more than the average number of votes for each structural condition.

(c)Weight Voting: The predictions of individual networks are modified by weights before being combined to reach the final prediction. The weights can be determined through different methods, considering either the training error of individual networks or their potential to make good predictions in the applications [Guo and Luh 2004, Marwala 2000]. In this study, weights are assigned to neural networks in the ensemble based on the mean square error from their training phase. As such, a larger training mean square error results in a lower weight for that neural network. The votes are multiplied by the corresponding weights before added to the collection boxes.

(d) Subjectivity Voting: This voting scheme takes into account the subjectivity of the manual inspection ratings. When an individual network "decides" that the structural rating is x, the voting scheme recognizes that there is a possibility that the actual rating is $x+1$ or $x-1$, and with a smaller possibility for $x+2$ or $x-2$. For the example problem, as shown in Figure 7-3, when a network in the ensemble predicts "7", the count for "7" will be increased by 0.7. Counts for "5," "6," "8," and "9" will be increased by 0.02, 0.08, 0.16, 0.04, respectively, based on the subjective bias trend in the manual inspection of bridges [FHWA 2001].

(e) Evaluation Voting: Instead of combining the predictions of some individual neural networks, the evaluation voting scheme takes into account the values of all output neurons of the networks in the ensemble. For output neurons that represent the same structural condition in different neural networks, their values were summed to obtain a probability value for that structural condition. The structural condition that has the highest probability value will be the prediction of the ensemble.
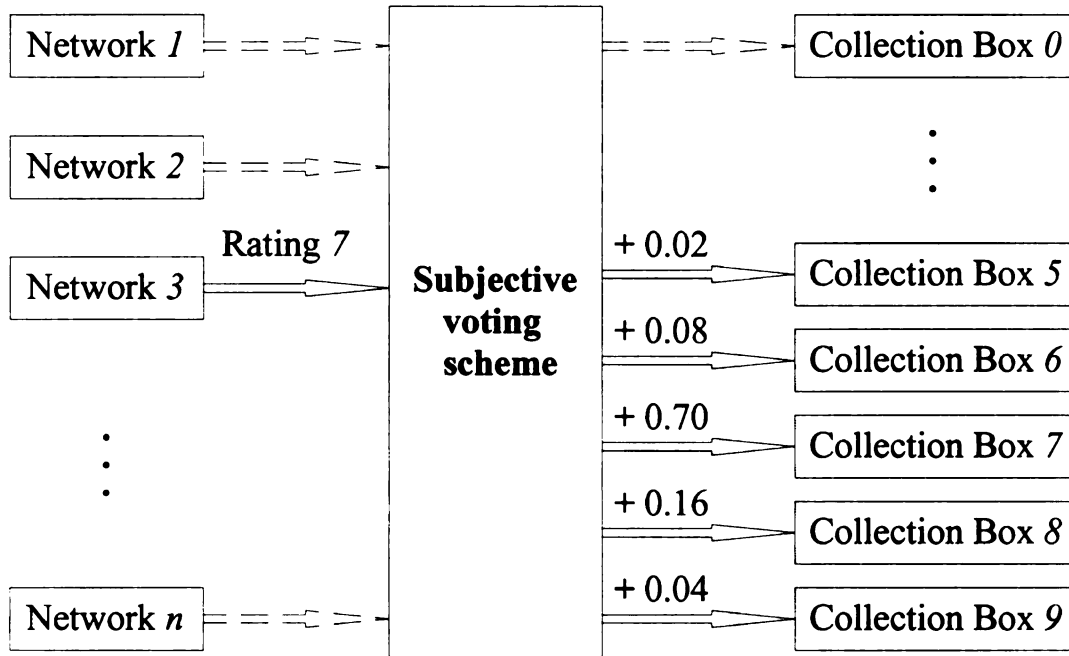
Figure 7-3 Example of subjectivity voting scheme

7.4 Results

7.4.1 Ensemble and network structure

The structure of each individual neural network can be referred to Figure 6-1. The parameter values were: $p = 13$, $n = 50$ and $r = 8$. One third of the records in each abutment rating category were selected and combined as test data and the remaining records were used as training data. Only 59 records showed an abutment rating of "9" in the training data. Thus, all of them were used in the composition of training sets for the individual neural networks. For records with other abutment rating values, 200 were selected from each rating category through a bagging procedure to be combined to form one individual training data set. In the training of individual networks, the mean square error and the maximum number of epochs to stop were set at 0.15 and 10000,

respectively. A neural network was excluded from the ensemble when its mean square error from the training phase was greater than 0.25.

7.4.2 Evaluation of Voting Schemes

For the example research problem, weight w_i for the ith network in the weight voting scheme was calculated with equation (7-4):

$$w_i = \sqrt{2.5 - 10 \times mse_i} \qquad (7-4)$$

where mse_i is the mean square error of the ith network in the training phase. The report from the Federal Highway Administration [2001] noted that there was a tendency to assign a rating lower than it should be for structural members with good condition; and that, similarly, there was a tendency to assign a rating higher than it should be for structural members with poor condition. The collection scheme for the subjective voting considering these tendencies is shown in Table 7-1. The values in the individual cells of the table mean that when the network predicts the rating noted in the row title, the collection box in the noted column title will be increased by that value.

The damage identification ratio (DIR) and false alarm ratio (FAR) values (see Sections 6.6.2 and 6.7.4) versus the number of neural networks in the ensembles for different voting schemes are plotted in Figure 7-4 and Figure 7-5, respectively. From these figures it can be seen that the performance of the ensemble of neural networks improves with the increase of numbers of networks in each ensemble up to a size of approximately 50 to 60. No significant improvement is observed after the number of networks in the ensemble exceeds 60.

Table 7-1 Collection algorithm for subjective voting

Prediction	Collection box						
	3	4	5	6	7	8	9
3	0.9	0.08	0.02				
4	0.15	0.8	0.04	0.01			
5	0.04	0.16	0.7	0.08	0.02		
6		0.04	0.16	0.6	0.16	0.04	
7			0.02	0.08	0.7	0.16	0.04
8				0.01	0.04	0.8	0.15
9					0.02	0.08	0.9

The solid squares in Figure 7-4 show the highest DIR of all the 500 individual neural networks trained in this simulation. It can be seen from Figure 7-4 that the ensemble of neural networks outperformed the best individual neural network by a large margin even though most of the neural networks in the ensemble are not as good as the best neural network. Similarly, the solid squares in Figure 7-5 represent the lowest FAR of all the 500 individual neural networks in the simulation. It can be seen from Figure 7-5 that the ensembles of neural networks with evaluation voting, plurality voting, and weight voting schemes have a lower FAR than the best individual neural network. The ensembles of neural networks with modified majority voting and subjectivity voting present FARs that are 3 % to 4 % higher than the best individual neural network. The increase in the FAR is acceptable for engineering applications.
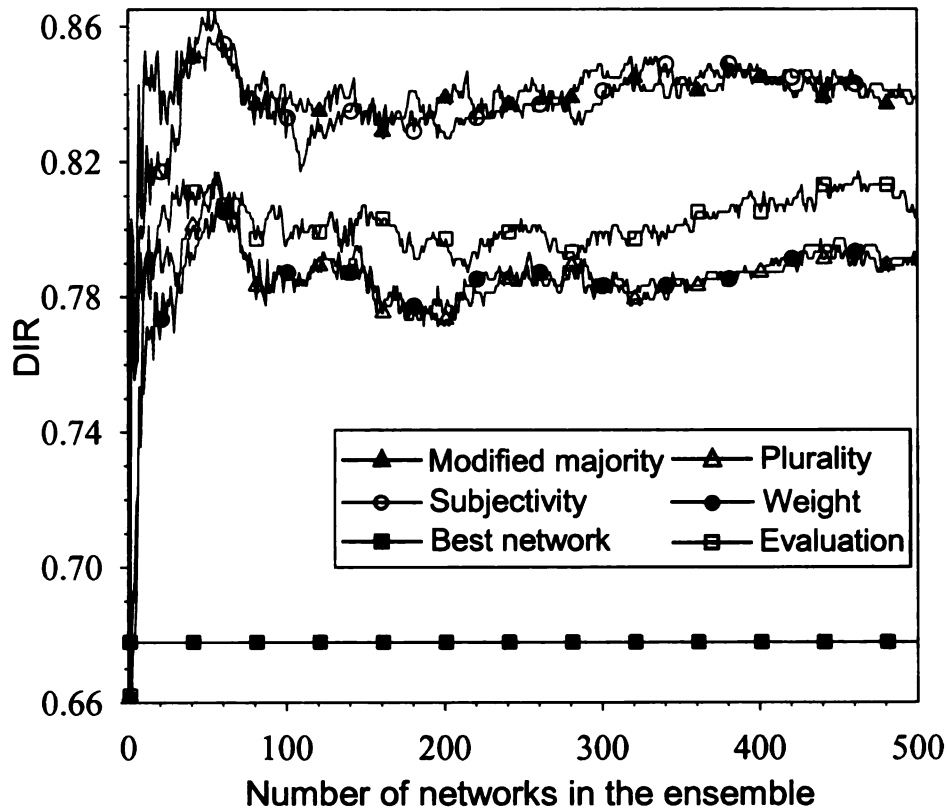
Figure 7-4 DIR versus number of networks in an ensemble of neural networks

Because failure to identify a damaged structure will have a more serious impact than identifying a good structure as damaged, the philosophy in developing a structural damage prediction model should be to increase the DIR as much as possible without raising the FAR too much. In this study, the indicator to evaluate the prediction models was the difference between the DIR and half of the FAR values. The performance of the best ensemble of neural networks using different voting schemes is shown in Table 7-2. It can be seen from Table 7-2 that the modified majority voting scheme led to the highest DIR, followed by the subjectivity voting scheme. The evaluation voting scheme had the lowest FAR and a decent DIR, outperforming both the weight and plurality voting schemes for both indicators.
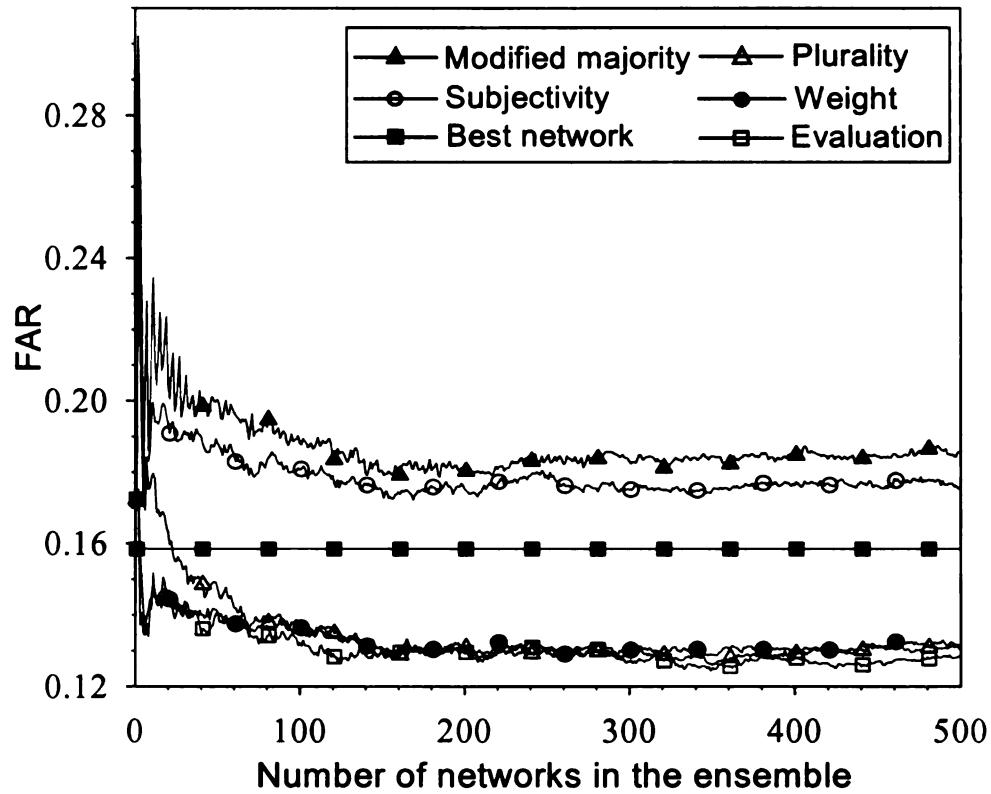
Figure 7-5 FAR versus number of networks in an ensemble of neural networks

Table 7-2 Evaluation of different voting schemes

Voting scheme	Number of networks for best performance	DIR	FIR	Indicator
majority	51	86.48%	19.89%	0.7654
Subjectivity	58	85.88%	18.78%	0.7650
Evaluation	463	81.71%	12.77%	0.7532
Plurality	56	81.51%	14.54%	0.7424
Weight	59	81.11%	13.90%	0.7416

7.4.3 Bridge Abutment Deterioration Curves

To illustrate the use of the ANN ensembles in developing life-degradation curves, an ensemble of 51 networks using a modified majority voting scheme was applied to predict the abutment condition of an existing continuous steel bridge in the State of Michigan. The abutment deterioration curve for this bridge is shown in Figure 7-6. "CB" in the legend means the confidence band. A confidence band was evaluated through the confusion matrix of the prediction model, which is shown in Table 7-3. The confidence level was 91.33 % for the case when abutment damage existed. The confidence level was 74.54 % for 70 years life of the bridge.
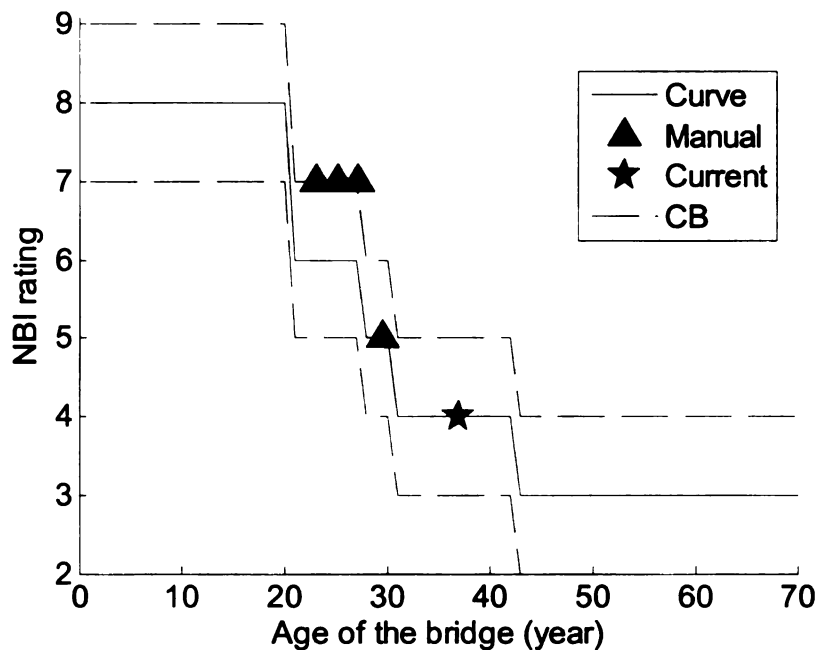
Figure 7-6 Abutment deterioration curve of a continuous steel bridge

Table 7-3 Confusion matrix of an ensemble of neural networks using modified majority voting

Predicted \ True	3	4	5	6	7	8	9	Sum
3	141	54	94	159	295	14	3	760
4	24	216	127	226	325	35	2	955
5	8	26	243	279	430	34	3	1023
6	7	11	60	470	556	55	2	1161
7	1	4	26	130	1064	106	4	1335
8	0	4	23	85	619	377	7	1115
9	2	5	1	3	21	12	9	42
True Sum	183	320	574	1352	3310	633	30	6391
Correct ratio	77.05%	67.50%	42.33%	34.76%	32.15%	59.56%	30.00%	39.43%
Acceptable ratio	90.16%	92.50%	74.91%	65.01%	67.64%	78.20%	53.33%	70.72%

In the development of Figure 7-6, the age span for the manual inspection rating is relatively short because manual inspections according to the NBI system started in Michigan in the early 1990s, as shown in Figure 6-8. This is another difficulty in the exploitation of the structural inventory system database for life-cycle prediction model as it is very difficult to extrapolate structural member degradation trends from such a short span of manual inspection records. Furthermore, a major part of the highway bridges in Michigan was built in the 1960s and 1970s. Thus, most of these age spans were concentrated within 30 years of life of bridges, with very few inspections records for very "young" or very "old" bridges. The ensemble of neural networks anneals the information from different structures to predict the conditions of each structure in the future and retrieve the historical path for the development of structural damage in bridge abutments.

It should also be noted that not all the deterioration curves have the same shape as shown in Figure 7-6. Figure 7-7 shows a deterioration curve with long flat range before major distress occurred. It can also be seen that the deterioration curve matches the manual inspection records well. It may be inferred that this bridge was well design and maintained and that no major environmental or operational factors caused its abutment wall to deteriorate seriously before 40 years of its service.
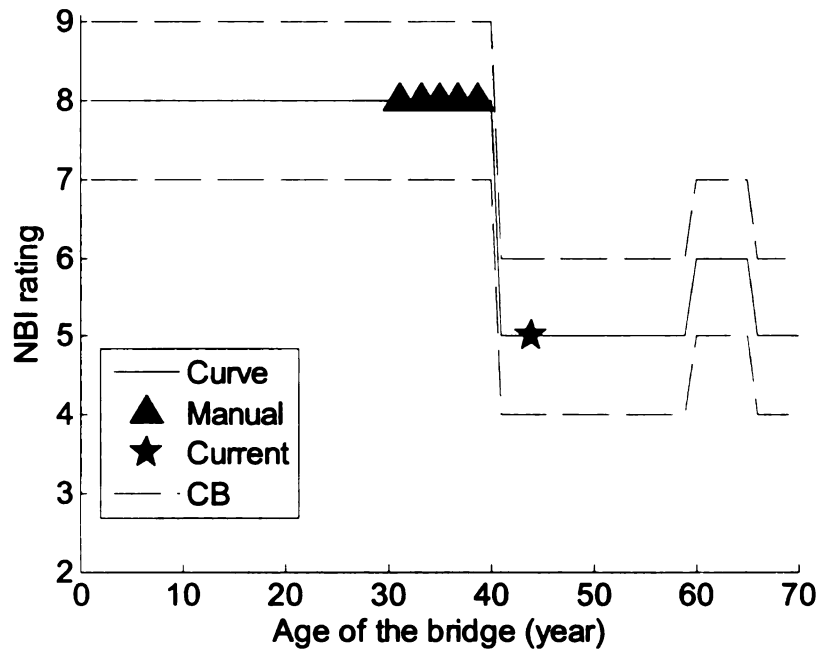
Figure 7-7 A deterioration curve with long flat range

Figure 7-8 shows a deterioration curve with a spike, or jump, in the middle. It can be seen from Figure 7-8 that the deterioration curve matches the manual inspection records well before the spike occurs. Probably, the spike point occurs because the ensemble of neural networks did not generalize that pattern well. The deterioration curve looks reasonable if the spike point is removed. Figure 7-8 and Figure 7-9 show situations in which current age of a bridge is smaller than its ages at inspection. This means that the bridge has been rebuilt in its service life. These rebuilt bridges add another difficulty in developing prediction models and lead to the occurrence of some unreasonable deterioration curves.
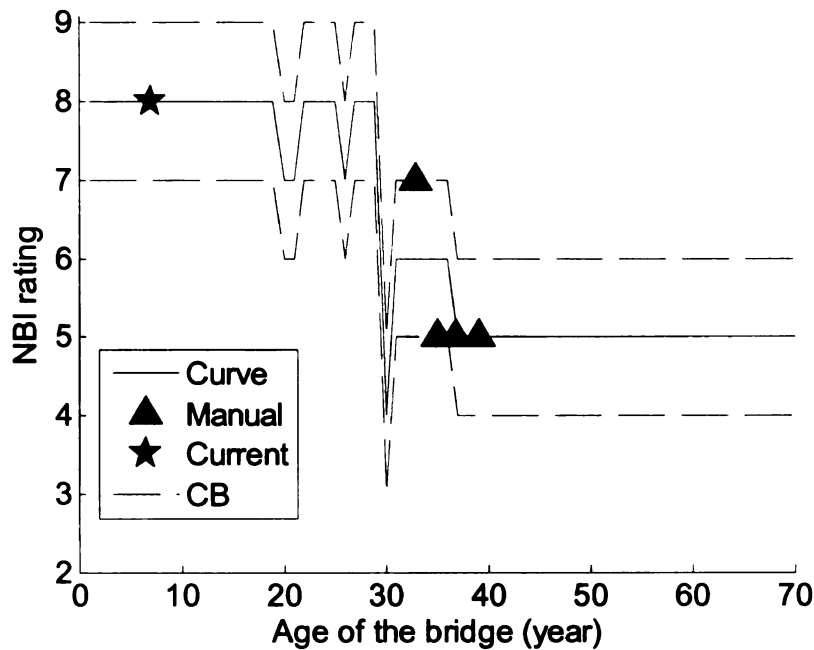
Figure 7-8 A deterioration curve with spike in the middle

Figure 7-9 shows a strange looking, and thus suspect, deterioration curve. The condition of the bridge abutment walls deteriorate dramatically after 20 years of their service. Then, after remaining in a poor condition for 23 years, the abutment walls of the bridge are restored back into fair condition. Two reasons might have caused this strange predictive curve. One is that the ENN does not generalize the patterns well enough and thus make a wrong prediction. Another is that highway bridges are continuously repaired and the abutment walls are restored to good condition after damage is observed. Unfortunately, the prediction model also incorporated the records of restored abutment walls into the prediction model, which may lead to the abnormal results.
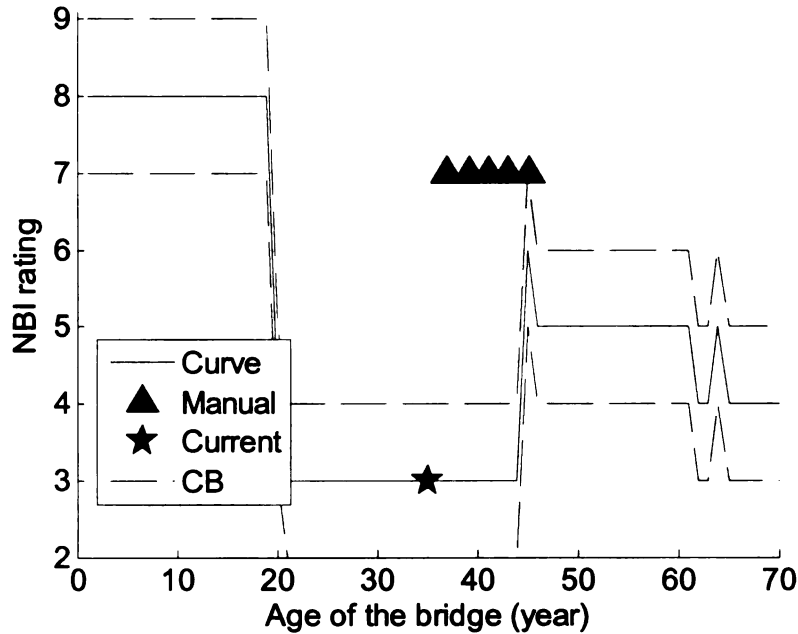
Figure 7-9 A deterioration curve shows increase of abutment rating

Figure 7-10 shows the deterioration curve developed using the ENN for the bridge shown in Figure 6-9 (bridge A1.5) for comparison. Compared with the MLP and SVM (Figure 6-9,) the ENN (Figure 7-10) predicts an earlier beginning of the significant deterioration (20 to 30 years versus about 40 years after the bridge was constructed) and a worse abutment condition in later life of the bridge (rating 4 versus rating 5.) It is also noticed that a few small spikes exist in Figure 7-10, which is acceptable for engineering applications especially considering the subjectivity and large variance of manual inspections. It should also be pointed out that the deterioration trend developed by the MLP and SVM (Figure 6-9) is the one selected among several bridges for which the MLP and SVM developed reasonable deterioration curves. For the ENN, the bridge was defined for comparison, it can be considered as its standard performance.

200
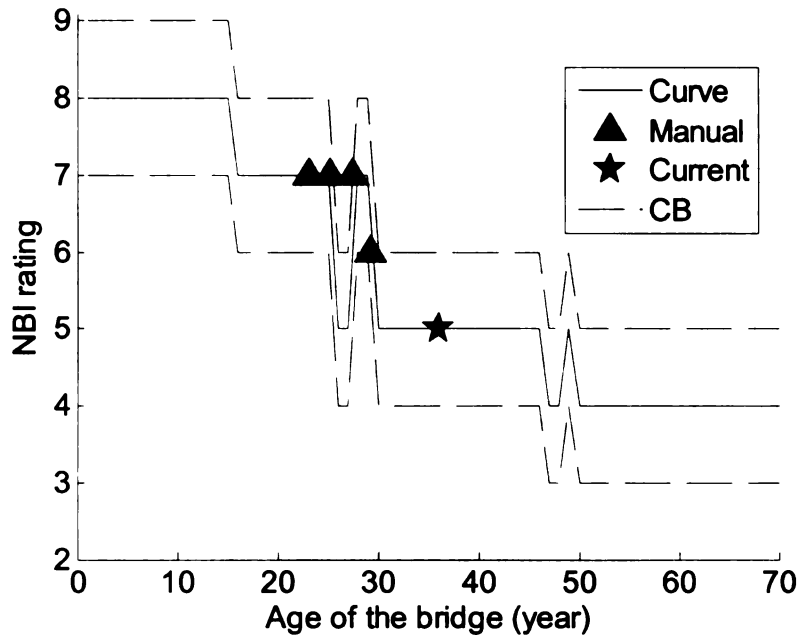
Figure 7-10 Deterioration curve developed by an FNN for the bridge in Figure 6-9

7.5 Combination of Databases for Soft Computing

7.5.1 Introduction

The nature of infrastructure damage is complex. Many factors interact with each other to cause the damage. Some of these factors are design parameters, some of them are environmental effects, and some of them are from influence of adjacent structures. Neither an evidential database nor a virtual database alone is sufficient to provide complete information for solving the problem. The evidential database records the behavior of the structure under all effects, but suffers from the subjectivity of manual inspection, incompleteness and imprecision. The virtual database has the advantages of providing accurate input-output relations for a series of structures, no matter if they exist in reality or not. At the same time, it has a diminished credibility and applicability due to the necessary simplification and assumptions in building models. In other words, a virtual

201

database can not exactly model the real structure or fully simulate all of the damage factors, and thus only contains partial information about the problem.

In this research, the evidential database and virtual database were combined to develop an ensemble of neural networks. ANN models based on evidential databases have been used to predict the performance indicator of aged aircraft with good accuracy [Shyur et al. 1996, Luxhoj et al. 1997]. ANN models based on simulated databases have been used for structural damage detection and localization based on the dynamic characteristics [Zhao et al. 1998, Fang et al.2005]. However, these two types of databases have not been used together to solve problems dealing with damage prediction of infrastructure and identification of potential causes of damage.

The major difficulty in the combination of evidential database and virtual database in this research is the large gap between explanatory and response variables of the evidential database and virtual database. The virtual database is based only on simulated behavior of the bridge from the perspective of mechanics and most of the explanatory variables are bridge design parameters (see Section 5.) On the other hand, the evidential database records the behavior of bridges through their service life including effects of all factors, such as mechanics, environmental factors, and human behavior. Its explanatory variables included not only design parameters, but also operation and environmental factors. The response variables of the virtual database are stresses and strains in the structure, whereas the response variables of the evidential database are subjective manual inspection ratings.

7.5.2 Concept and Methodology

The methodology for the combination of the evidential database and the virtual database is shown in Figure 7-11. An ensemble of neural networks based on the evidential database was trained in the same way as discussed in Section 7.4. The voting scheme was based on modified majority voting. It was observed that for about 33 % of the test vectors, over 50 % of members in the ensemble of networks reached agreement. For those 33 % of the test vectors, the DIR is as high as 94.24 % and the FAR is as low as 9.43 %. However, for those test vectors the votes were scattered (no more than 25 % of the members "agreed" on the same prediction,) the accuracy of the ensemble are low. As discussed in Section 7.5.1, the evidential database and virtual database were created from completely different sources. Thus, the chance that they share common weakness is low. Consequently, the concept behind this combination is to use the networks trained based on virtual database to help make predictions for those structures that were difficult for the ensemble of networks based on evidential database.

7.5.3 Networks trained on virtual database

One difficulty in the combination of databases was the gap between structural evaluation ratings in reality and the response variables derived from numerical simulation. The response variables in two databases must be the same so that they can help each other in making a prediction. For the bridge abutment damage example, as mentioned in Section 1.2, the response variable in the evidential database is the structural member rating in a scale of 0 to 9. This rating can not be simulated through FEA models. Instead, some variables such as maximum principal stress or maximum principal strain can be derived from FEA simulations.
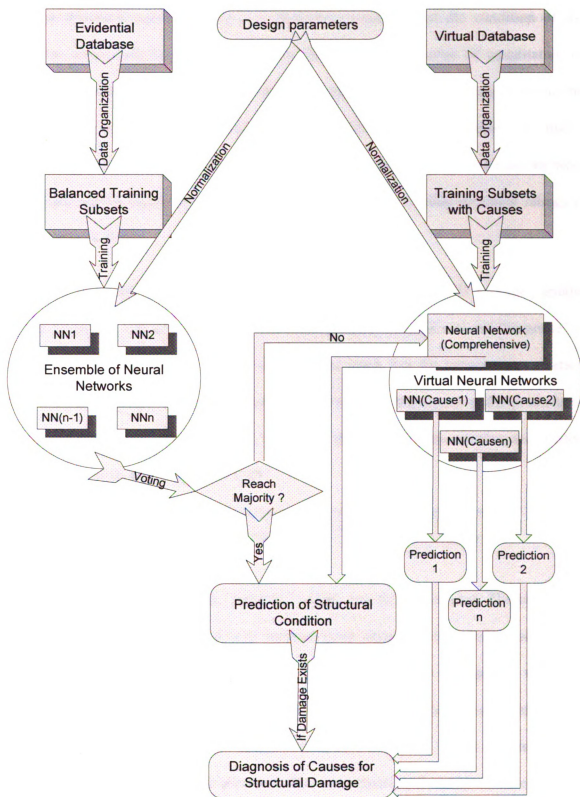
Figure 7-11 Scheme of database combination

The structural member rating is a qualitative evaluation of the condition of the structure which will be influenced by the interaction of a series of quantitative or qualitative variables, such as stresses, strains, temperatures, chemical components in the environment, and the quality of the construction. Thus, it was not feasible to find a relationship between structural member rating and FEA output. Some assumptions were thus made and an algorithm to transform the FEA output to virtual structural ratings is proposed as follows:

For each bridge in the simulation case matrices (see Section 5.3) a single variable called "response" was defined. For the pavement pressure damage scenario "response" is the product of the maximum stress and maximum strain. For the temperature variation scenario the "response" R_T is the square root of the sum of the square of the products of maximum stress, σ_{max}, and maximum horizontal strain, ε_{11}, in the summer and winter, respectively, as shown in equation (7-5).

$$R_T = \sqrt{\left(\sigma_{max}\varepsilon_{11max}\right)^2_{summer} + \left(\sigma_{max}\varepsilon_{11max}\right)^2_{winter}} \qquad (7\text{-}5)$$

The natural logarithm of the "response" values was then calculated. The reason for calculating the natural logarithm is to compact those extremely large values since they are induced by the elastic assumption in the FEA. Transformation of responses was done within each structural type so that they were not influenced by the deviation induced in the modeling approaches. At the completion of this step, two virtual databases were created: a database for pavement pressure effect and a database for temperature effects.

Combining and expanding the two data sets through weighted summation of the "response" by considering different pavement and temperature conditions, the weights for "bitumen," "mixed," "unknown," and "concrete" pavement were taken to be 0.1, 0.5, 0.5 and 1.0, respectively. The weights for temperature effects are taken to be 0.56 for bridges in a county with the smallest annual temperature difference in the State of Michigan and 1.0 for bridges in a county with the largest annual temperature difference. Weights for bridges in other counties were derived through linear interpolation according to their annual temperature differences. Each bridge in the case matrix was expanded to 32 bridges according to the combination of pavement and temperature conditions. For instance, when it has a concrete pavement and a low annual temperature difference, the comprehensive "response" R_C value will be calculated as:

$$R_C = 1.0 \times R_P + 0.25 \times R_T \qquad (7\text{-}6)$$

Three MLP networks were thus trained using virtual databases: a network based on the pavement pressure scenario, a network based on temperature effect scenario, and a network that combined those two effects. The parameters of the three networks are shown in Table 7-4. The response variables in the virtual databases were strains and stresses in the structure. They were transformed to virtual structural conditions by assigning a rating 3 for structures with largest response values in each structural type and a 9 for structures with lowest response values. The virtual structural conditions for other structures can be derived through linear interpolation.

206

Table 7-4 Parameters of networks based on virtual database

Network	Network parameters					
	n_l	n	n_e	mse	η	mo
Pavement pressure	1	40	2000	0.01	0.1	0.9
Temperature effect	2	40	2000	0.01	0.1	0.9
Combined effects	2	80	10000	0.01	0.1	0.9

7.5.4 Improvement in damage identification

The confusion matrix of the ensemble of networks with combined evidential and virtual databases is shown in Table 7-5. The DIR and FAR indices of the ensemble of networks with combined databases is 86.68 % and 20.02 %, respectively. A 0.2 % improvement of DIR at the cost of 0.13 % increase of FAR was achieved comparing to the best performed ensemble of 51 neural networks trained on the evidential database exclusively.

In order to further evaluate the improvement in prediction power by combining databases, the networks trained on virtual database was combined with an ensemble of 42 neural networks trained on the evidential database. The ensemble of neural networks based on combined databases had a DIR of 85.09 % and an FAR of 19.68 %. The DIR and FAR of the ensemble of neural networks based on the evidential database exclusively were 84.89 % and 19.76 %, respectively. Thus, the DIR was increased by 0.20 % and FAR was reduced by 0.08 %. Both performance indicators were thus improved by the combination of the databases.

207

Table 7-5 Confusion matrix for the ensemble of networks with combined databases

Predicted \ True	3	4	5	6	7	8	9	Sum
3	140	54	93	170	302	17	3	42
4	26	216	128	220	317	35	2	779
5	8	26	243	275	429	31	3	944
6	7	11	60	469	558	55	2	1015
7	0	4	26	130	1064	106	4	1162
8	0	4	23	85	619	377	7	1334
9	2	5	1	3	21	12	9	1115
True Sum	183	320	574	1352	3310	633	30	6391
Correct ratio	76.50%	67.50%	42.33%	34.69%	32.15%	59.56%	30.00%	39.40%
Acceptible ratio	90.71%	92.50%	75.09%	64.64%	67.70%	78.20%	53.33%	70.71%

7.5.5 Diagnosis of possible causes for structural damage

The ensemble of neural network based on combined databases could also be applied to diagnose the possible causes of structural damage, as shown in Figure 7-11. Given the design parameters of a bridge, the networks trained on pavement pressure scenario and temperature effects scenario would give two predictions. In case the ensemble of neural networks based on combined databases predicts that the structure is in poor condition, the predictions of two networks trained on damage causes can be checked and evaluated. A prediction closer to the damage condition could signify that the cause has a larger contribution to the damage of the structure, as shown in equations (7-7) and (7-8).

$$C_{pav} = \frac{R_T + 2 - R_{EC}}{R_T + R_P + 4 - 2 \times R_{EC}} \times 100\% \qquad (7\text{-}7)$$

$$C_{tem} = \frac{R_P + 2 - R_{EC}}{R_T + R_P + 4 - 2 \times R_{EC}} \times 100\% \qquad (7\text{-}8)$$

where C_{pav} is the contribution of pavement pressure; C_{tem} is the contribution of temperature; R_{EC} is the prediction given by the ensemble of neural networks based on combined databases. As an example, the length, width and skew angle of a simple/cantilever steel bridge are 40.8 m, 27.3 m, and 12°, respectively. The approach pavement of the bridge is concrete. The ensemble of neural networks based on combined databases predicted its abutment rating as "3." The pavement pressure network and temperature effect network predicted its rating as "5" and "4," respectively. Thus, the

system could predict that the contribution of the pavement pressure to the damage is 43 % and the contribution of temperature effect is 57 %.

7.6 Software Development: Bridge Abutment Damage Diagnosis (SbNet)

A program, Bridge Abutment Damage Diagnosis (SbNet), was developed for MDOT engineers to predict the condition of bridge abutment walls given design parameters. SbNet is a stand-along executable program compiled from matlab codes of pre-trained ensemble of networks as described in Sections 7.1, 7.2, 7.3, and 7.4. After the analysis and evaluation of stepwise deterioration curves derived using soft computing models, it was found that most of them can be approximated by logistic curves. In SbNet, the deterioration curves were fitted to logistic curves using equation (7-9) through Matlab's curve fitting toolbox [Mathworks 2007a]. SbNet can make predictions either using design parameters for bridges in design or using MDOT's Bridge ID for existing bridges. The output of SbNet includes: bridge deterioration curve based on actual integer values or on smoothed logistic curves, predictions saved in txt files, and the bridge abutment rating given the age of the bridge or current abutment rating if it is an existing MDOT highway bridge. One of the deterioration curves of a bridge abutment wall is shown in Figure 7-12. It is a simple/cantilevered steel bridge. The SbNet User's Manual can be found in the final report to the research sponsor, MDOT [Burgueño and Li 2008].

$$f(x) = a \cdot \frac{1 + m \cdot \exp\left(\dfrac{b - x}{t}\right)}{1 + n \cdot \exp\left(\dfrac{b - x}{t}\right)} \tag{7-9}$$
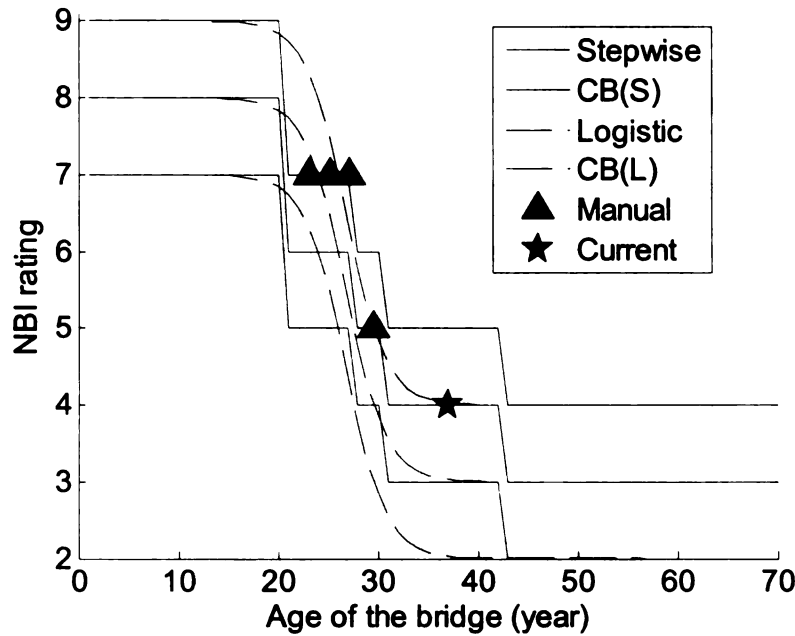
Figure 7-12 Deterioration curve shown in Figure 7-6 with smoothed curve

7.7 Discussion

An ensemble of neural networks with a novel data organizing scheme was applied to improve the identification of damage in abutment walls of highway bridges. The unbalance of structural inspection databases was overcome by organizing the training data using bagging within each structural condition. Several new voting schemes were devised; with modified majority voting, subjective voting, and evaluation voting schemes showing good performance. The damage identification ratio of an ensemble of networks reached 81 % to 86 %, which exceeded the performance of the best individual networks in the ensemble by 13 % to 18 %. An ensemble of networks obtained optimal or close to optimal performance when 50 to 60 neural networks were included in the ensemble. An ensemble of neural networks was the optimal prediction model derived through this research for predicting conditions of abutment walls of highway bridges.

Previous research [Freund and Schapire 1996, Quinlan 1996, Opitz and Maclin 1999] has shown that most of the improvement in performance of an ensemble is achieved with the first few (10 to 25) additional classifiers (i.e., neural networks). For the structural damage prediction problem a similar behavior was seen except that considerably more networks were needed to achieve most of the improvement. The reason for this difference was the characteristics of the present problem of structural damage prediction and the corresponding structural inventory database. In order to obtain a balanced training data set a small part of the records with good structural condition were selected in each round of bagging. Consequently, more networks were needed to "learn" most of the knowledge from the records with good structural conditions. Combination of the evidential database and a virtual database from FE simulations improved the performance of the ensemble of networks. However, the improvement was not significant because of the significant differences between the evidential database and virtual database for the example problem.

A stand-alone program named SbNet was developed to help MDOT engineers in the maintenance of existing bridges and in the design of new ones. It was based on a well-trained ensemble of neural networks and is able to predict bridge abutment condition given design parameters or MDOT bridge ID. SbNet can be a promising diagnostic tool so that maintenance and repairs can be more efficiently managed with reliable prediction of future structural condition and the deterioration trend. The software could also be used as a predictive tool for new designs to evaluate and compare the life-time performance of the abutment walls for different bridge design options.

8 FUTURE RESEARCH AND CONCLUSION

Conclusions from the presented research work are given in this chapter. Three promising future research directions are also proposed: predicting structural damage for other structures, improving the combination of databases, and online updating of soft computing models.

8.1 Further Research

Developing damage prediction models for other structures, improving the combination of databases, and online updating of soft computing models are three promising directions in future research.

8.1.1 Prediction models for other structures

The concept and methodologies developed in this research can be easily applied to predict damage in other structural component in civil infrastructures. The soft computing procedures can be upgraded to a model that can evaluate the condition of a structure holistically. Another computation model could be developed to evaluate the condition and reliability of the structure based on the condition of all the individual structural components. The knowledge of structural engineering needs to be incorporated in this computation model, such as load path, importance of individual structural members, and failure mechanism of the structure.

8.1.2 Improved combination of databases

The concept and methodology of database combination is a promising direction to improve the power of soft computing in damage identification for civil infrastructure. In

this research, the prediction power did not improve significantly through the combination of evidential database and virtual database due to the limitation of the databases. However, the combination model can be improved through two approaches in future research:

- Improve the accuracy of finite element simulations. Even though there will always be simplification in the finite element simulation. A better approximation to the real-world problem can be reached through developing nonlinear structural models that consider geometric nonlinearity and material nonlinearities.

- Create a dynamic database through online instrumentation of a series of typical structures. The dynamic database should have the same explanatory variables with the evidential database and the same response variables as the virtual database. Such a more representative and precise dynamic database can provide new information for the computing model and improve the combination of the evidential database and virtual database.

8.1.3 Prediction model with online updating capacity

The prediction power of soft computing models can be improved continuously if the neural networks can be retrained with updated evidential and dynamic databases. The online updating of soft computing models can include a procedure to screen, normalize, and organize the raw inspection and instrumentation data to fit in the databases and a procedure to train and test the soft computing models, as shown in Figure 8-1. The concept of parallel computing based on high performance computer servers can be implemented to improve the online training and testing of a prediction model.
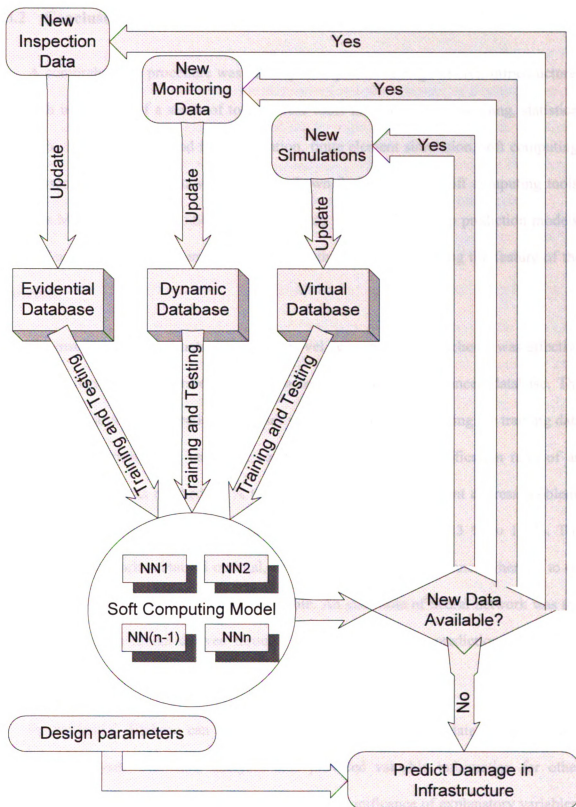
Figure 8-1 Online update scheme for soft computing model

8.2 Conclusions

A comprehensive procedure was developed to predict damage in civil infrastructures through integration of a series of tools. These tools included data processing, statistical analysis, field inspection and instrumentation, finite element simulation, soft computing, and ensembles of neural networks. It was shown that a series of soft computing tools, such as MLP, RBF, SVM, SSOM, and FNN; can be used to develop prediction models, even if none of them is inherently better than others without knowing the feature of the problem.

An ensemble of neural networks with a novel data organization scheme was effective to predict damage in structures based on a complicated and unbalanced database. The unbalance of structure inspection databases was overcome by organizing the training data using bagging within each structural condition. The damage identification ratio of an ensemble of networks reached 81 % to 86 % for the bridge abutment distress problem, which exceeded the best individual networks in the ensemble by 13 % to 18 %. The ensemble of networks obtained optimal, or close to optimal performance when 50 to 60 neural networks were included in the ensemble. An ensemble of neural network was the optimal prediction model derived through this research for the prediction of highway bridge abutment condition.

An evidential database can be developed from SISD through data processing and statistical analyses. Statistical analyses also provided valuable information for other analyses and simulations, such as evaluation of the significance of explanatory variables, revealing the common features of the structures that were susceptible to structural

damage, and the development of case matrices for finite element analyses. A virtual database can be developed through finite element analyses. Such a virtual database can reveal the relationship between design parameters and the behavior of a structure and it can be combined with the evidential database to improve prediction models developed through an ensemble of neural networks. Additional information about the behavior of structures can be collected through field inspections and instrumented monitoring.

The comprehensive procedure developed in this research can predict damage in structures and evaluate the potential causes of damage. With the identification of potential causes of structural damage and the accurate prediction of the structural condition, the human resources and funding in maintenance and repair of civil infrastructures can be deployed more efficiently.

REFERENCES

AASHTO (2007). AASHTO LRFD Bridge Design Specifications.

ABAQUS, Inc (2006). ABAQUS/Analysis User's Manual-version 6.6.1.

American Institute of Steel Construction (AISC 2006). Steel Construction Manual.

Askeland, D. R., Ksslinger, F. and Wolf, R. V. (1987, Nov 15) Investigation of Bridge Pin Failure. Report to Missouri Highway and Transportation Commission.

Aleksander, I. and Morton, H. (1990). An Introduction to Neural Computing. London: Chapman and Hall.

ASCE. (2005). Report Card for America's Infrastructure. http://www.asce.org/ reportcard/2005/ index2005.cfm.

Ayyub, B. M. and McCuen, R. H. (1997). Probability, Statistics & Reliability for Engineers. NY, Boca Raton: CRC Press

Bishop C. (1995). Neural networks for pattern recognition. Oxford:Oxford University Press.

Blake, C. L. and Merz, C. Z. (1998). UCI Repository of Machine Learning Databases. http://www.ics.uci.edu/mlearn/MLRepository.html. Irvine, CA: Department of Information and Computer Science, University of California-Irvine.

Breiman, L. (1996a). Heuristics of instability in model selection. Annals of Statistics: 24(6), 2350-2383.

Breiman, L. (1996b). Bagging Predictors. Machine Learning: 24, 123-140.

Briaud, J. L., Maher, S. F. and James, R. W. (1997, May). Bump at the End of the Bridge. Civil Engineering: 67(5), 68-69.

Burgueño, R. and Li, Z. (2008). Identification of Causes and Development of Strategies for Relieving Structural Distress in Bridge Abutments, Final Report for Michigan Department of Transportation.

Burke, M. P. (1998). Pavement pressure generation: neglected aspect of jointed pavement behavior. Transportation Research Record: 1627, 22-28.

Burke, M. P. (2004, January). Reducing Bridge Damage Caused by Pavement Forces. Concrete International, 53-57.

Carpenter, G. A., Grossberg, S., Markuzon, N., Reynolds, J. H. and Rosen, D. B. (1992, September). Fuzzy ARTMAP: A Neural Network Architecture for Incremental Supervised Learning of Analog Multidimensional Maps. IEEE Transactions on Neural Networks: 3(5), 698-713.

Cattan, J. and Mohammadi, J. (1997). Analysis of bridge condition rating data using neural networks. Microcomputers in Civil Engineering: 12(6), 419-429.

Chan, L.S., Gilman, G. A. and Dun, O.J. (1976). Alternative Approaches to Missing Values in Discriminant Analysis. Journal of the American Statistical Association: 71(365), 842–844.

Chen, C. H. (2005). Structural identification from field measurement data using a neural network. Smart Mater. Struct: 14, S104–S115.

Chen, R. and Yu, J. (2007). An Improved Bagging Neural Network Ensemble Algorithm And Its Application. Third International Conference on Natural Computation: 5, 730-734.

Cybenko, C. (1989). Approximations by superposition of sigmoid functions. Mathematics of Control Signals and Systems: 2, 303-314.

Dixon, J. K. (1979, October) Pattern Recognition with Partly Missing Data. IEEE Transactions on Systems, Man and Cybernetics: SMC-9(10), 617-621.

Dreiseitl, S. and Ohno-Machado, L. (2002). Logistic Regression and Artificial Neural Network Classification Models: A Methodology Review. Journal of Biomedical Informatics:35, 352-359.

Duda, R. O., Hart, P. E. & Stork, D. G. (2001), Pattern Classification 2nd editionn. John Wiley & Sons.

Elewa, M.A. (2004, May). Effect of Secondary Structural Components on the Serviceability of Steel Girder Bridges. Ph.D. Dissertation. East Lansing, MI: Department of Civil and Environmental Engineering, Michigan State University.

Fang, X., Luo, H. and Tang, J. (2005). Damage of structures detection using neural network with learning rate improvement. Computers and Structures: 83, 2150–2161.

Federal Highway Administration (FHWA 2001). Reliability of Visual Inspection for Highway Bridges, Volume 1: Final Report.

Freund, Y. and Schapire, R. (1996). Experiments with a new boosting algorithm. Processings of the Thirteenth International Conference on Machine Learning, 148-156.

Fu, J.Y., Liang, S.G. and Li, Q.S. (2007). Prediction of wind-induced pressures on a large gymnasium roof using artificial neural networks. Computers and Structures: 85, 179-192.

Granger, E., Rubin, M. A., Grossberg, S. and Lavoie, P. (2000). Classification of Incomplete Data Using the Fuzzy ARTMAP Neural Network. IEEE International Joint Conference on Neural Networks Proceedings: 6, 35-40.

Graybill, F. A. and Iyer, H. K. (1994). Regression Analysis–Concepts and Applications., Belmont, CA: Dux-bury Press.

Gunn, S. R. (1997). Support Vector Machines for Classification and Regression. Technical Report University of Southampton, Image Speech and Intelligent Systems Research Group.

Guo, J. J. & Luh, P. B. (2004). Improveing Market Clearing Price Prediction by Using a Committee Machine of Neural Networks. IEEE Transactions on Power Systems. 19(4), 1867-1876.

Haldar, A. and Mahadevan, S. (2000). Probability, Reliability and Statistical Methods in Engineering Design. NY: John Wiley & Sons, Inc.

Hansen, L. K., Liisberg, C. and Salamon, P. (1992). Ensemble Method for Handwritten Digit Recognition. Proceedings of the IEEE-SP Workshop on Neural Networks for Signal Processing. 333-342.

Hansen, L. K. and Salamon, P. (1990). Neural Network Ensembles. IEEE Transactions on PatternAnalysis and Machine Intelligence. 12(10), 993-1001.

Hartle, R. A., Amrhein, W. J., Wilson, K. E. and Baughman, D. R. (1991). Bridge inspector's training manual 90, Federal Highway Administration. Washington, D.C: U. S. Department of Transportation.

Hastie, T., Tibshirani, R. and Friedman, J. (2001) The elements of statistical learning: data mining, inference, and prediction. New York: Springer.

Hornik, K., Stinchcombe, M. and White, H. (1989). Multilayer Feedforward Networks Are Universal Approximators. Neural Networks: 2, 359-366.

Housner, G. W. and Vreeland, T. J. (1965). Analysis of Stress and Deformation. NY: Macmillan Company.

Huang, C. S., Hung, S. L., Wen, C. M. and Tu, T. T. (2003). A Neural Network Approach for Structural Identification and Diagnosis of a Building from Seismic Response Data. Earthquake Engineering and Structural Dynamics: 32, 187–206.

Hornik, K., Stinchcombe, M. and White, H. (1990). Universal approximation of an unknown mapping and its derivatives using multilayer feedforward networks. Neural Networks: 3(5), 551-560.

Hsu, C. W. and Lin, C. J. (2002). A comparison of methods for multi-class support vector machines. IEEE Transactions on Neural Networks: 13(2), 415–425.

Haykin, S. (1999). Neural Networks: A comprehensive foundation 2nd Edition. Upper Saddle River, NJ: Prentice Hall.

Jain, L. C. and Martin N. M. (1999). Fusion of neural networks, fuzzy sets, and genetic algorithms: industrial applications. CRC Press.

Juszczak, P and Duin, R. P. W. (2004). Combining One-Class Classifiers to Classify Missing Data. Multiple Classifier Systems, Proceedings: 3077, 92-101.

Juang, C. H., Ni, S. H. & Lu, P. C. (1999). Training Artificial Neural Networks with the Aid of Fuzzy Sets. Computer-Aided Civil and Infrastructure Engineering: 14, 407-415.

Kecman, V. (2001). Learning and Soft Computing: Support Vector Machines. Neural Networks, and Fuzzy Logic Models. Cambridge, MA: MIT Press.

Knerr, S., Personnaz, L. and Dreyfus, D. (1990). Single-layer learning revisited: A stepwise procedure for building and training a neural network. Neurocomputing: Algorithms, Architectures and Applications NY: Springer-Verlag.

Kohavi, R. and Provost, F. (1998). Glossary of Terms. Machine Learning. 30, 271-274.

Kohonen, T. (1990). The self-organizing map. Proceedings of the Institute of Electrical and Electronics Engineers: 78, 1464-1480.

Kolen, J. F. and Pollack, J. B. (1990). Back Propagation is Sensitive to Initial Conditions. Technical Report TR 90-JK-BPSIC.

Kutner, M. H., Nachtsheim C. J., Neter J. & Li, W. (2005). Applied Linear Statistical Models, 5th edn. New York: McGraw-Hill/Irwin.

Land Jr., W. H., McKee, D., Velazquez, R., Wong, L., Lo, J. Y. and Anderson, F. (2003). Application of support vector machines to breast cancer screening using mammogram and clinical history data. Proceedings of SPIE - The International Society for Optical Engineering. 5032 I, 546-556.

Law, M. (2006). A Simple Introduction to Support Vector Machines. Lecture for CSE 802. East Lansing, MI: Department of Computer Science and Engineering, Michigan State University.

Lee, J., Yi, J. D., Kim, J. D., and Yun, C. B. (2004). Health Monitoring Method Using Committee of Neural Networks Advances in Nondestructive Evaluation. 1983-1988.

Lim, C. P., leong, J. H. and Kuan M. M. (2005). A Hybrid Neural Network System for Pattern Classification Tasks with Missing Features. IEEE Transactions on Pattern Analysis and Machine Intelligence: 27(4), 648-653.

Little, R.J.A. and Rubin, D.B. (2002). Statistical Analysis with Missing Data. 2nd edition. Wiley-Interscience.

Long, J. H., Olson, S. M., Stark, T. D. and Samara, E. A. (1998). Differential Movement at Embankment-Bridge Structure Interface in Illinois. Transportation Research Record: 1633, 53-60.

Luxhoj, J. T., Williams, T. P. and Shyur, H.-J. (1997). Comparison of regression and neural network models for prediction of inspection profiles for aging aircraft. IIE Transactions (Institute of Industrial Engineers). 29(2), 91-101.

Marwala, T. (2000, January). Damage Identification Using Committee of Neural Networks. Journal of Engineering Mechanics, 43-50.

Mathworks Inc. (2007a).Curve Fitting User's Guide.

Mathworks Inc. (2007b). Fuzzy Logic Toolbox 2 User's Guide.

Mathworks Inc. (2007c). Neural Network User's Guide.

MDOT (2001). Bridge Design Guides. Lansing, MI.

MDOT (2003), Michigan Structure Inventory and Appraisal Coding Guide. Lansing, MI.

Mitra, S., and Hayashi, Y. (2000). Neuro-fuzzy rule generation: survey in soft computing framework. IEEE Transactions on Neural Networks: 11(3): 748-768.

Montgomery, D. C., Peck, E. A. & Vining, G. (2006), Introduction to Linear Regression Analysis 4th edition. John Wiley & Sons;

Myers R. H., Montgomery D. C. and Vining, G. G. (2002), Generalized Linear Models With Applications in Engineering and the Science. John Wiley & Sons.

Myers, J., Nanni, A., Stone, D., Vellore, S.G., and Earney, T.P. (2001) Precast I-Girder Crack-ing: Causes and Design Details. Technical Report No. RDT 01-008/RI 97-021, University of Missouri-Colombia/University of Missouri-Rolla,

Opitz, D. and Maclin, R. (1999). Popular Ensemble Methods: An Empirical Study. Journal of Artificial Intelligence Research: 11, 169-198.

Pal, S. K. and Mitra, S. (1992). Multilayer Perceptron, Fuzzy Sets, and Classification. IEEE Transactions on Neural Networks: 3(5), 683-697.

Pal, S. K. and Mitra, S. (1999). Neuro-fuzzy pattern recognition methods in soft computing. NY: John Wiley & Sons.

Pande A. and Abdel-Aty M. (2005, September). Identification of Rear-end Crash Patterns on Instrumented Freeways: A Data Mining Approach. Proceedings of the 8th International. IEEE Conference on Intelligent Transportation Systems. Vienna, Austria, 13-16.

Parasuraman, K., Elshorbagy, A. and Si, B. C. (2006). Estimating saturated hydraulic conductivity in spatially variable fields using neural network ensembles. Soil Science Society of America Journal: 70(6), 1851-1859.

Park, S, Yun, C. B., Roh, Y. and Lee, J. J. (2006). PZT-based active damage detection techniques for steel bridge components. Smart Materials and Structures: 15, 957–966.

Phares B. M., Rolander, D. D., Graybeal, B. A. and Washer, G. A. (2001). Reliability of Visual Bridge Inspection. Public Roads: March/April, 22-29.

Pleune, T. T. and Chopra, O. K. (2000). Using artificial neural networks to predict the fatigue life of carbon and low-alloy steels. Nuclear Engineering and Design: 197(1-2), 1-12.

Quinlan, J. R. (1996). Bagging, boosting, and c4.5. Proceedings of the Thirteenth National Conference on Artificial Intelligence, 725-730.

Ramuhalli, P. (2005). Course Notes for ECE 885 Artificial Neural Networks. East Lansing, MI: Michigan State University.

Rice, J. A. (1995). Mathematical Statistics and Data Analysis. Belmont, CA: Duxbury Press.

Richards, A. M. (1979). Measurement Of Stress In Concrete Pavements. Transportation Research Record: 713, 9-15.

Roberts, C. A. and Attoh-Okine, N. O. (1998, September). Comparative analysis of two artificial neural networks using pavement performance prediction. Computer-Aided Civil and Infrastructure Engineering: 13(5), 339-348.

SAS Institute Inc (2004). SAS 9.1 Documentation.

Schapire, R. (1990). The Strength of weak learnability. Machine Learning: 5(2), 197-227.

Sharkey, A. J. C. (editor, 1999). Combining Artificial Neural Nets: Ensemble and Modular Multi-Net Systems. London: Springer.

Shober, S. F. (1997). Great Unsealing: A Perspective on PCC Joint Sealing. Transportation Research Record: 1597, 22-30.

Shyur, H.J., Luxhoj, J. T. and Williams, T. P. (1996). Using neural networks to predict component inspection requirements for aging aircraft. Computers & Industrial Engineering: 30(2), 257-267.

Silva, A., Cortez, P., Santos, M.F., Gomes, L., and Neves, J. (2004). Multiple organ failure diagnosis using adverse events and neural networks. Proceedings of the 6th International Conference on Enterprise Information Systems. 401-408.

Smith, K. D., Snyder, M. B., Darter, M. I., Reiter, M. J. and Hall, K. T. (1987). Pressure Relief and Other Joint Rehabilitation Techniques. FHWA, U. S. Department of Transportation.

Sohn, S. Y. and Lee S. H. (2003). Data fusion, ensemble and clustering to improve the classification accuracy for the severity of road traffic accidents in Korea. Safety Science: 41, 1–14.

Song, H., Zhong, L. and Han, B. (2005). Damage of structures detection by integrating independent component analysis and support vector machine. Advanced Data Mining and Applications: First International Conference, Proceedings. 670-677.

SPSS Inc. (2004). SPSS® 13.0 Base User's Guide.

Snedecor, G. W. and Cochran, W. G. (1989). Statistical Methods, 8th Edition. Iowa State University Press/AMES.

Sybase Inc. (2004). Getting Started InforMaker.

Taha, M. M. and Lucero, J. (2005). Damage identification for structural health monitoring using fuzzy pattern recognition. Engineering Structure: 27, 1774-83.

Taylor, J. S. & Cristianini, N. (2004). Kernel Methods for Pattern Analysis, Cambridge University Press.

Vapnik, V. N. (1999). The Nature of Statistical Learning Theory, 2nd edn. Springer.

Wagstaff, K. L. and Laidler V. G. (2005). Making the Most of Missing Values: Object Clustering with Partial Data in Astronomy. Astronomical Data Analysis Software and System XIV: 347, 172-176.

Weisberg, S. (2005). Applied Linear Regression, 3rd edition. John Wiley & Sons.

White, H. (1990). Connectionist Nonparametric Regression: Multilayer Feedforward Networks Can Learn Arbitrary Mappings. Neural Networks: 3(5), 535-549.

224

Xiao, Y. D., Clauset, A., Harris, R., Bayram, E., Santago, P. and Schmitt, J. D. (2005). Supervised Self-Organizing Maps in Drug Discovery. 1. Robust Behavior with Overdetermined Data Sets. Journal of Chemical Information and Modeling: 45(6), 1749-1758.

Yang, S. and Browne, A. (2004). Neural Network Ensembles: Combining Multiple Models for Enhanced Performance Using a Multistage Approach. Expert Systems: 21(5), 279-288.

Yao J. T. P. (1980, August). Damage Assessment of Existing Structures. Journal of the Engineering Mechanics Division, 785-799.

Yu, L., Wang, S. and Lai, K. K. (2008 February). Credit risk assessment with a multistage neural network ensemble learning approach. Expert Systems with Applications: 34(2), 1434-1444.

Yun, C. B., Lee, J. W., Kim., J. D. and Min, K. W. (2003). Damage Estimation Method Using Committee of Neural Networks. Proceedings of SPIE - The International Society for Optical Engineering: 5047, 263-274.

Zadeh, L. A. (1965). Fuzzy Sets. Information and Control: 8, 338-353.

Zadeh, L. A. (1975a). Linguistic Variable and Its Application to Approximate Reasoning. Information Sciences: 8(4), 199-249.

Zadeh, L. A. (1975b). Linguistic Variable and Its Application to Approximate Reasoning. Information Sciences: 8(4), 301-357.

Zadeh, L. A. (1975c). Linguistic Variable and Its Application to Approximate Reasoning. Information Sciences: 9(1), 43-80.

Zadeh, L. A. (1994). Fuzzy Logic, Neural Networks, and Soft Computing. Fuzzy Systems, 77-84.

Zhao, J., Ivan, J. N. and DeWolf, J. T. (1998). Damage of structures detection using artificial neural networks. Journal of Infrastructure Systems: 4(3), 93-101.

Zhou, Z., Jiang, Y., Yang, Y. and Chen, S. (2002). Lung Cancer Cell Identification Based onArtificial Neural Network Ensembles. Artificial Intelligence in Medicine: 24, 25-36.